6th International Mass Spectrometry School

Fundamentals, advances, instrumentation and applications

School Program

Book of Abstracts

Cagliari (Italy), September 17-22, 2023

https://www.spettrometriadimassa.it/imss2023

TABLE OF CONTENTS

WELCOME FROM THE CHAIR AND THE SCIENTIFIC AND ORGANIZING COMMITTEES OF THE 6th IMSS

On behalf of the Division of Mass Spectrometry (DSM) of the Italian Chemical Society, we would like to welcome you to the 6th International Mass Spectrometry School (IMSS) 2023 in Cagliari, Sardinia, Italy.

The International Mass Spectrometry Foundation started this educational activity, aimed to enforce, promote and diffuse the culture of mass spectrometry, in 2013 with the first edition of this school held in Siena (Italy).
After ten years, moving in Europe and out of Europe (Siena (Italy), Natal (Brazil), Dubrovnik (Croatia), Sitges (Spain) and Belfast (Ireland)) the school comes back to Italy in the town of Cagliari, in the magnificent island of Sardinia to celebrate its 10th anniversary.
Many students attended the various editions of IMSS and each completely fulfilled its aims: give a good education, establish and favorite students-tutors and students- students interactions, high level tutors, informal and friendly atmosphere, great social events.

We think that also IMSS 2023 will be a useful occasion to enjoy science, learn or refresh principles and main applications of mass spectrometry with a look at the future, networking among participants and with tutors, enjoy ideas, suggestions by students, taste delicious food, experience the real local life in Cagliari, a very nice and lovely town in South Sardinia!

The city has a heritage of great importance, it's a green, small, clean and safe city with a Mediterranean climate. The international airport, very close to downtown, connects Cagliari to many towns in Europe.

We do wish IMSS 2023 will be an important experience for young scientists, not only from a scientific and cultural standpoint, but also for relationships, networking, talks, social events in the special atmosphere of Cagliari and Sardinia.
With the support of everybody, we do hope that IMSS 2023 will be a successful, amazing and unforgettable school!!

Gianluca Giorgi (IMSS 2023 chair) and

the IMSS 2023 scientific and organizing committees

WELCOME FROM THE IMSF PRESIDENT

It gives me great pleasure to invite you to join us at the 6th International Mass Spectrometry School in Cagliari, Sardinia for the 17-22 September 2023. Returning to Italy for the 10th anniversary of this flagship IMSF activity offers a unique opportunity to advance your MS knowledge.
Education is at the heart of the professional development the IMSF aims to stimulate. Come to Cagliari to learn from and connect with mass spectrometrists across the globe.
The exciting program of lectures and workshops covers the breadth of mass spectrometry, from fundamentals to applications. Interlaced with collaborative problem solving sessions and outstanding networking opportunities for all delegates, students and tutors alike it is one of the highlights of the 2023 mass spectrometry calendar

Ron M.A. Heeren (IMSF President)

IMSF EXECUTIVE COMMITTEE, IMSF NATIONAL AFFILIATES

Executive Committee

Ron M. A. Heeren	President	The Netherlands
Stephen Blanksby	Vice President	Australia
John Langley	Past President	UK
Maarten Altelaar	Treasurer	The Netherlands
Martina Marchetti-Deschmann	Secretary	Austria
Diego Cobice	Educational Officer	Ireland
Gavin Reid	Vice-President (Conference) Chair IMSC 2024	Australia
Gianluca Giorgi	Vice-President (Education) Chair IMSS 2023	Italy
Julia Chamot-Rooke	Region A Repres. (Europe/Africa)	France
Yu Xia	Region B Repres. (Asia/Oceania)	China
Vicki Wysocki	Region C Repres. (North America)	USA
Rosa Erra-Balsells	Region D Representative (Central and South America)	Argentina

National Affiliates

- *Argentina – Rosa Erra Balsells*
- *Australia/New Zealand – Tara Pukala*
- *Austria – Günter Allmaier*
- *Belgium – Jeff Rozenski*
- *Brazil – Marcos Eberlin*
- *Canada – Derek Wilson*
- *Czech Republic – Jan Preisler*
- *Denmark – Steen Pontoppidan*
- *Finland – Olli Laine*
- *France – Isabelle Fournier*
- *Germany – Thorsten Benter*
- *Greece – Despina Tsipi*
- *Hong Kong – Andy Siu*
- *Hungary – Karoly Vekey*
- *India – Rajesh Kumar Vatsa*
- *Ireland – Mike Kinsella*
- *Israel – Yariv Brotman*
- *Italy – Gianluca Giorgi*
- *Japan – Michisato Toyoda*
- *Korea – Byungjoo Kim*
- *Malaysia - Low Teck Yew*
- *The Netherlands – Anouk Rijs*
- *Norway – Leon Reubsaet*
- *Peoples Rep. of China – Yuanjiang Pan*
- *Poland – Katarzyna Pawlak*
- *Portugal – Maria Helena Florencio*
- *Romania – Zaharie Moldovan*
- *Russia – Albert Lebedev*
- *Singapore – Lin Qingsong*
- *Slovenia – Helena Prosen*
- *South Africa – Egmont Rohwer*
- *Spain – Estaban Abad*
- *Sweden – Jonas Bergquist*
- *Switzerland – Yury Tsybin*
- *Taiwan – Yi-Sheng Wang*
- *United Kingdom – Neil Oldham*
- *United States of America – Julia Laskin*
- *Ukraine – Marina Kosevich*

INTERNATIONAL MASS SPECTROMETRY SCHOOLS

1st IMSS – Siena, Italy	*2013*
2nd IMSS – Natal, Brazil	*2015*
3rd IMSS – Dubrovnik, Croatia	*2017*
4th IMSS – Sitges, Spain	*2019*
5th IMSS – Belfast, Ireland	*2022*

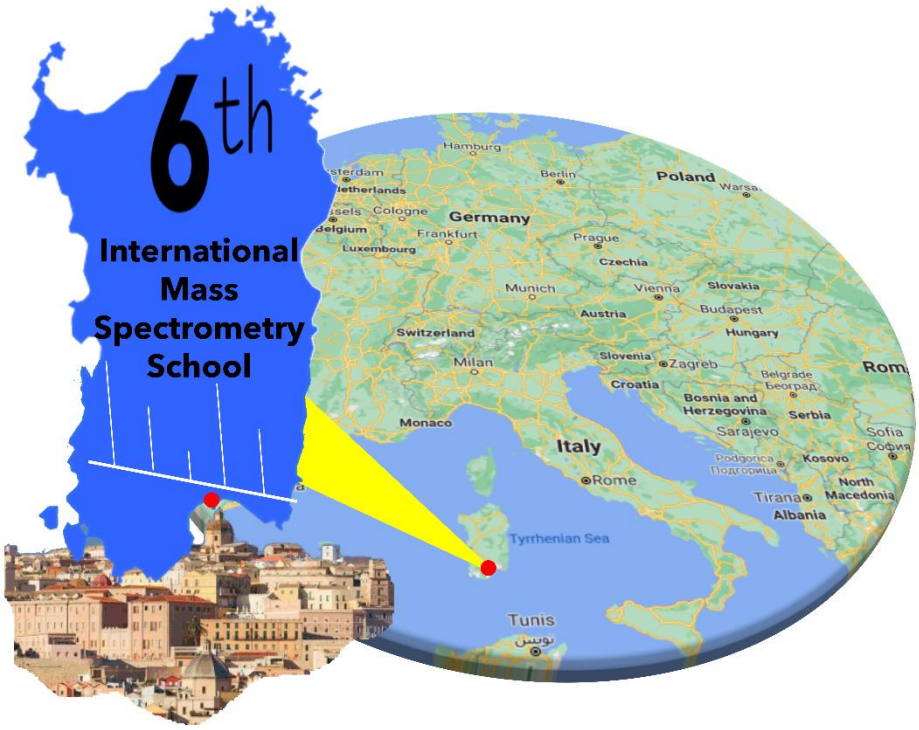

6th IMSS SCIENTIFIC COMMITTEE

Gianluca Giorgi
Univ. of Siena

Cecilia Bergamini
ARPAE, Bologna

Giuliana Bianco
Univ. of Basilicata

Donatella Caruso
Univ. of Milano

Riccardo Flamini
CREA-VE, Conegliano

Roberta Galarini
IZSUM, Perugia

Fulvio Magni
Univ. of Milano Bicocca

Luciano Navarini
Illycaffè, Trieste

6th IMSS ORGANIZING COMMITTEE

Michela Begala
Univ. of Cagliari

Pierluigi Caboni
Univ. of Cagliari

Luigi Atzori
Univ. of Cagliari

Tiziana Cabras
Univ. of Cagliari

Giovanna Lucia Delogu
Univ. of Cagliari

Giorgia Sarais
Univ. of Cagliari

Carlo Tuberoso
Univ. of Cagliari

Pietro Urgeghe
Univ. of Sassari

6th IMSS TUTORS

Carlos Afonso	Université de Rouen	France
Giuliana Bianco	Univ. of Basilicata	Italy
Pierluigi Caboni	University of Cagliari	Italy
Diego Cobice	Ulster University	Ireland
Chiara Cordero	Univ. of Torino	Italy
Valérie Gabelica	Université de Bordeaux	France
Pascal Gerbaux	University of Mons	Belgium
Gianluca Giorgi	University of Siena	Italy
Ron M. A. Heeren	Maastricht University	The Netherlands
Giancarlo la Marca	University of Florence	Italy
John Langley	University of Southampton	UK
Martina Marchetti-Deschmann	Technischen Universität Wien	Austria
Giuseppe Paglia	University of Milano Bicocca	Italy
Michele Suman	Barilla, Parma	Italy
Vicki Wysocki	Ohio State University	USA

ECTS CREDITS

The 6th IMSS will give ECTS credits to students who passed the examination test.

According to the Italian rules, 1 ECTS credit = 25 working hours, a participant could be eligible for 1.5 ECTS credits.

The ECTS credits will be reported in the final Certificate of Attendance with the Exam outcome together with the actual number of the working hours, so to facilitate conversions in different countries.

NICO NIBBERING TRAVEL AWARDS

The International Mass Spectrometry Foundation established the Nico Nibbering Travel Awards to support students participation in the 6th IMSS.

Prof. Nibbering was a passionate advocate for young scientists and supported the education and career-development of mass spectrometrists from many countries around the world through his mentorship and the delivery of education and workshop programs.

The Nico Nibbering Student Travel Awards serve to honor his many contributions to international mass spectrometry and build on his legacy of supporting young scientists in this field.

BEST ORAL AWARDS

to be assigned to two young researchers under 35 years of age presenting an oral communication.
Each award consists of a certificate and an expenses contribution.

BEST POSTER AWARD

to be assigned to a young researcher under 35 years of age presenting a poster communication.
The award consists of a certificate and a 2024 online subscription to JMS.

BEST MS SOLVER AWARD

to be assigned to the Best MS Solver.
The award consists of a certificate and a gift.

PATRONAGES

REGIONE AUTÒNOMA DE SARDIGNA
REGIONE AUTONOMA DELLA SARDEGNA

Agris
Agentzia pro sa chirca in agricultura
Agenzia regionale per la ricerca in agricoltura
REGIONE AUTÒNOMA DE SARDIGNA
REGIONE AUTONOMA DELLA SARDEGNA

Arpas
Agentzia regionale
pro s'amparu de s'ambiente de Sardigna
Agenzia regionale
per la protezione dell'ambiente della Sardegna
REGIONE AUTÒNOMA DE SARDIGNA
REGIONE AUTONOMA DELLA SARDEGNA

Università degli Studi di Cagliari

con il patrocinio
uniss
UNIVERSITÀ DEGLI STUDI DI SASSARI

SARDIGNA CHIRCAS
SARDEGNA RICERCHE

ISTITUTO
ZOOPROFILATTICO
SPERIMENTALE
DELLA SARDEGNA
"G. Pegreffi"

EuChemS
European Chemical Society

IUPAC
INTERNATIONAL UNION OF
PURE AND APPLIED CHEMISTRY

MEDIA PARTNERS

chemistry
an Open Access Journal by MDPI

[iito]

molecules
an Open Access Journal by MDPI

SPONSORS

Agilent
Trusted Answers

BRUKER

Chimica Sarda

BODANCHIMICA s.r.l.
REAGENTI - VETRERIE - STRUMENTAZIONE - ARREDI DA LABORATORIO - CERTIFICAZIONI LAT ACCREDIA
PRODOTTI: SETTORE ALIMENTARE, APISTICO, COSMETICO, ERBORISTICO, ENOLOGICO, MICOLOGICO E AFFINI
ACQUA DISTILLATA E ULTRAPURA - GHIACCIO SECCO

GRUPPO CHIMECO
Servizi Tecnici per l'Industria

GM.Solution S.r.L

100th SAPIO GRUPPO
Breathing the future

GENERAL INFORMATION

The IMSS 2023 is held in Cagliari, the most important city of Sardinia located in its Southern part.
The city has a soul consisting of a millenary history, culture, nature, beach tourism, charmed by the views of Castello, the ramparts and the Roman remains, the Sardinian sea, as well as by the dynamism of a surprisingly lively city.

School venue
The IMSS 2023 venue is

Hotel Regina Margherita ****

viale Regina Margherita 44, Cagliari

VISIT SARDINIA

Discover Sardinia, its landscapes, amazing beaches, delicious food & wines

SARDEGNA Turismo

https://www.sardegnaturismo.it/en

SOCIAL EVENTS

SUNDAY *Sept. 17*	*h. 8:30 p.m.* ***Welcome cocktail at TERRAPIENO CLUB HOUSE*** *Viale Regina Elena 14, Cagliari*
MONDAY *Sept. 18*	*h. 6:00 p.m.* ***Urban trekking in Cagliari****: discover the beautiful and sneaking corners of the town.* *Guided tour*
TUESDAY *Sept. 19*	*h. 7:30 p.m.* ***Dinner & live music at CAPOLINEA BEACH POETTO*** *Lungomare Poetto – Cagliari*
WEDNESDAY *Sept. 20*	*h. 2:15 p.m.* ***All to the beach!!*** *Enjoy the magnificence of sand and sea of the Sardinia beaches.* *Travel by bus*
THURSDAY *Sept. 21*	*h. 8:00 p.m.* ***Social dinner at AQUILA CLUB*** *Calata dei Trinitari – Cagliari*

PROGRAM

Sunday, September 17

17:30	Registration	
18:15	Opening session	
18:45	Mass spectrometry. Where is it from? Where it is and where is it going?	J. Langley
20:00	*End of session*	
20:30	*Welcome cocktail*	

Monday, September 18

Ionization techniques: volatile molecules

8:30	Mass spectrometry: an introduction	J. Langley
9:30	Ionization of volatile molecules: electron ionization (EI), chemical ionization (CI). Fragmentation processes, energetics (Part 1)	G. Giorgi
10:15	*Coffee break & poster session*	
11:00	Ionization of volatile molecules: electron ionization (EI), chemical ionization (CI). Fragmentation processes, energetics (Part 2)	G. Giorgi
12:00	Study of complex mixtures of volatile molecules: GC, fast GC, GC×GC	C. Cordero
13:15	*Buffet lunch*	

Ionization techniques: polar molecules

14:30	Soft ionization techniques: ESI, DESI, APCI. Ambient mass spectrometry. Mechanisms of ion production	C. Afonso
16:00	*Coffee break & poster session*	
16:30	Study of complex mixtures of polar molecules: HPLC, UHPLC, LC x LC	J. Langley
18:00	*End of session*	
18:00	*Urban trekking* in Cagliari: discover the beautiful and sneaking corners of the town ..... Guided tour	

Tuesday, September 19

MALDI. Analyzers (I)

8:30	Matrix-assisted laser desorption ionization, MALDI-2. Mechanisms of ion production	R.M.A. Heeren
9:30	Analyzers (I). Ion separation in space: beam instruments: sectors, quadrupole, time-of-flight	M. Marchetti-Deschmann
10:30	*Coffee break & poster session*	

Analyzers (II). High resolution, accurate mass measurements

11:00	Analyzers (II). Ion separation in time: ion traps, FT-ICR, Orbitrap	C. Afonso
12:00	High resolution mass spectrometry, accurate mass measurements. Examples and applications	G. Bianco
13:00	*Buffet lunch*	

Tandem mass spectrometry

14:30	Tandem Mass Spectrometry (MS/MS) and MS^n: ion activation	P. Gerbaux
16:30	*Coffee break & poster session*	
17:15	Tandem Mass Spectrometry (MS/MS) and MS^n: ion dissociation	P. Gerbaux
18:30	*End of session*	
19:30	*Poetto beach*: dinner and live music!	

Wednesday, September 20

Fragmentation/decomposition reactions. Artificial intelligence in MS. Proteomics

8:30	Examples of fragmentation/decomposition reactions	D. Cobice
10:00	*Coffee break & poster session*	
10:30	Artificial intelligence in MS	C. Cordero
11:45	Bottom-up, top-down, and complex-down proteomics	V. Wysocki
13:00	*Buffet lunch*	
14:15	*All to the beach!* Travel by bus Enjoy the magnificence of sand and sea of the Sardinia beaches	
19:00	*Go back to Cagliari*	

Thursday, September 21

MS Imaging, ion mobility

8:30	Imaging mass spectrometry	R.M.A. Heeren
9:45	Ion mobility	V. Gabelica
11:00	*Coffee break & poster session*	

Do it by yourself !

11:30	Exercises on MS, HRMS and MS/MS interpretation, mechanisms, ... Award for the best MS solver!	D. Cobice, V. Gabelica, G. Giorgi
13:00	*Buffet lunch*	

Short orals. Workshop. Problem solving. MS in lipidomics & metabolomics

14:20 Short orals by students:

OR1 P1 **Decoding the key aroma compounds of cocoa using mass spectrometry**

Amandine André, Elodie Gillich, Lisa Ullrich, Irene Chetschik

ZHAW Zürich University of Applied Sciences, School of Life Sciences and Facility Management, ILGI Institute of Food and Beverage Innovation, Research Group Food Chemistry, Wädenswil, Switzerland

OR2 P10 **MALDI 1 & 2 MS imaging of lipid double-bond positional isomers using off-line ozonolysis**

D. Bezdeková,[1] J. Preisler,[1] M. Hendrych,[2] K. Dreisewerd,[3] A. Bednařík [1]

[1] Chemistry Department, Faculty of Natural Sciences, Masaryk University, Czech Republic

[2] First Pathological Department, St. Anne's University Hospital Brno, Czech Republic

[3] Institute of Hygiene and Interdisciplinary Center for Clinical Research (IZKF), University of Münster, Germany

OR3 P13 **The quest for the unambiguous identification of ß-naphthol and triarylcarbonium colorants by MeV-SIMS - Procedures for mass calibration & data evaluation**

Teodora Raicu,[1] Matea Krmpotić,[2] Zdravko Siketić,[2] Iva Bogdanović-Radović,[2] Dubravka Jembrih-Simbürger [1]

[1] Institute for Natural Sciences and Technology in the Arts (INTK), Academy of Fine Arts Vienna, Vienna, Austria

[2] Ruđer Bošković Institute, Zagreb, Croatia

OR4 P15 **Structural characterization of mobility-selected ions: combining TIMS with IR ion spectroscopy on an FT-ICR MS platform**

Lara van Tetering, Kas Houthuijs, Jelle Schuurman, Jonathan Martens, Giel Berden, Jos Oomens

FELIX Laboratory, Institute for Molecules and Materials, Radboud University, Nijmegen, Netherlands

OR5 P26 **Leveraging LC-TIMS-QTOFMS for addressing analytical challenges in chemical exposome studies**

Konstantina S. Diamanti,[1] Dimitrios E. Damalas,[1] Georgios O. Gkotsis,[1] Eleni I. Panagopoulou,[1] Maria-Christina Nika,[1] Carsten Baessmann,[2] Bob Galvin,[2] Nikolaos S. Thomaidis [1]

[1] Laboratory of Analytical Chemistry, Department of Chemistry, National and Kapodistrian University of Athens, Panepistimiopolis Zografou, Athens, Greece
[2] Bruker Daltonics GmbH & Co. KG, Bremen, Germany

OR6 P28 **Saliva peptidome profiling in glioblastoma multiforme brain tumour by HPLC-MS top-down platform**

Alexandra Muntiu,[1] Diana Valeria Rossetti,[2] Federica Vincenzoni,[1,3] Irene Messana,[2] Massimo Castagnola,[4] Giuseppe La Rocca,[3,5] Alessandro Olivi,[3,5] Andrea Urbani,[1,3] Giovanni Sabatino,[3,5] Claudia Desiderio [2]

[1] Dipartimento di Scienze Biotecnologiche di Base, Cliniche Intensivologiche e Perioperatorie, Università Cattolica del Sacro Cuore, Rome, Italy
[2] Istituto di Scienze e Tecnologie Chimiche “Giulio Natta”, Consiglio Nazionale delle Ricerche, Rome, Italy
[3] Fondazione Policlinico Universitario A. Gemelli IRCCS, Università Cattolica del Sacro Cuore, Rome, Italy
[4] Centro Europeo di Ricerca sul Cervello-IRCCS Fondaz. Santa Lucia, Rome, Italy
[5] Institute of Neurosurgery, Fondazione Policlinico Universitario A. Gemelli IRCCS, Catholic University, Rome, Italy

---

OR7 P32 **Metabolomics applied to discover prognostic markers in human heart transplantation**

E.C. Montatixe Fonseca,[1] M.C. Mimmi,[3] A. Corazza,[4] M. Belliato,[2] C. Pellegrini,[1] S. Pelenghi [1]

[1] Cardiac Surgery Unit 1, IRCCS San Matteo Hospital Foundation, Pavia, Italy
[2] Anesthesiology and Intensive Care Unit 2, IRCCS San Matteo Hospital Foundation, Pavia, Italy
[3] Department of Molecular Medicine, University of Pavia, Italy
[4] Department of Medical Area, University of Udine, Italy

OR8 P45 **A mass spectrometry-based multi-omics approach to explore the mechanisms of drug resistance in methicillin-resistant *Staphylococcus aureus***

Pedro C. Rosado,[1] M. Matilde Marques,[1,2] Gonçalo C. Justino [1]

[1] Centro de Química Estrutural - Institute of Molecular Sciences, Instituto Superior Técnico, Universidade de Lisboa, Lisboa, Portugal
[2] Departamento de Engenharia Química, Instituto Superior Técnico, Universidade de Lisboa, Lisboa, Portugal

---

OR9 P51 **MS fingerprinting of cyclic modified peptides and proteins with chloromethyl acryl reagents**

Maria J. S. A. Silva,[1,3] Lujuan Xu,[1,2] Pedro M. P. Gois,[3] Seah Ling Kuan,[1,2] Tanja Weil [1,2]

[1] Max-Planck Institute for Polymer Research, Mainz, Germany
[2] Institute of Inorganic Chemistry I, Ulm University, Ulm, Germany
[3] Research Institute for Medicines (iMed.ULisboa), Faculty of Pharmacy, Universidade de Lisboa, Lisbon, Portugal

---

OR10 P53 **A spatial multi-omics investigation into spinal cord remodeling in mouse mutant strains with altered myelin basic protein abundance**

Rachel Pryce,[1] Hooman Bagheri,[2] Alan C. Peterson,[2] Pierre Chaurand [1]

[1] Department of Chemistry, Université de Montréal, Montreal, Quebec, Canada
[2] Department of Neurology and Neurosurgery, McGill University, Montreal, Quebec, Canada

16:00	Workshop with Companies	
16:40	Problem solving	
17:30	*Coffee break & poster session*	
18:00	MS in lipidomics & metabolomics	P. Caboni
19:30	Awards for the best orals!	
19:40	*End of session*	
20:30	*Social dinner*	

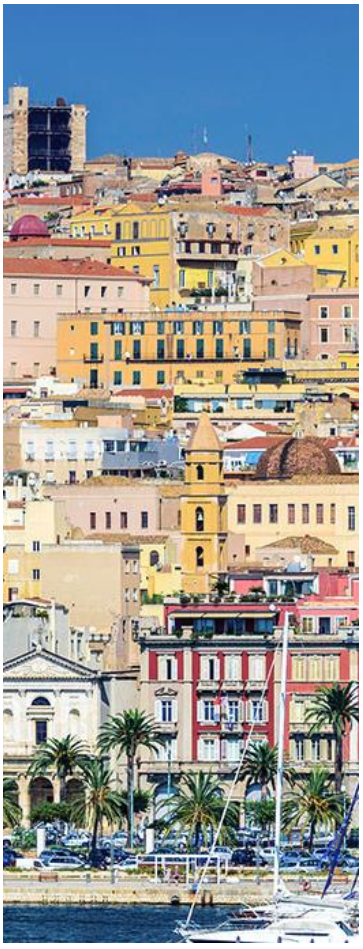

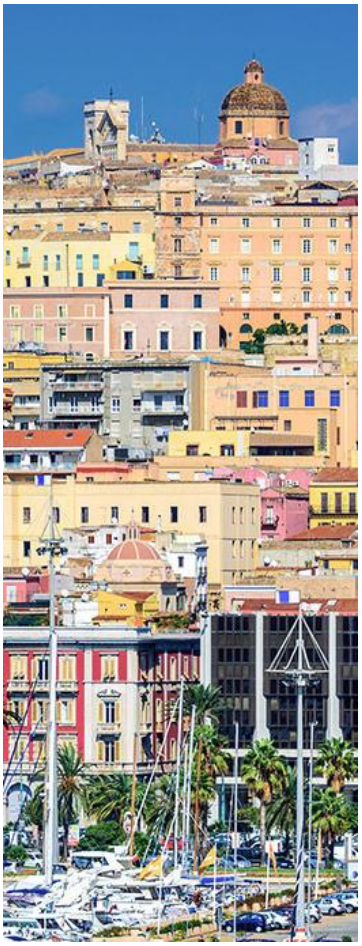

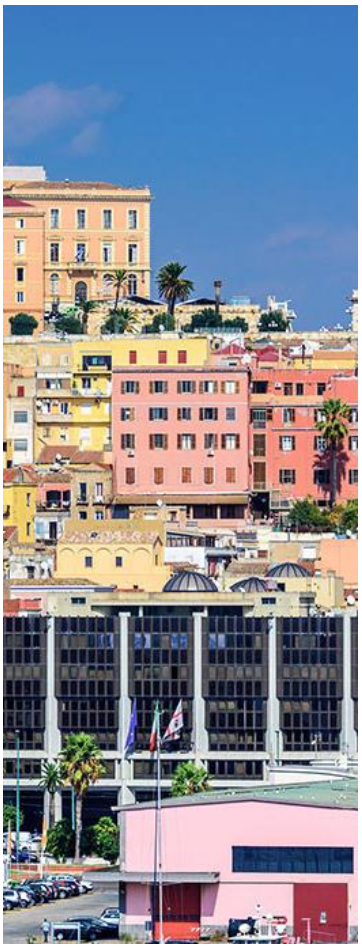

Friday, September 22

Quantitation; biomedical applications; data analysis; MS in food

8:30	Quantitation by MS and MSn	M. Marchetti-Deschmann
9:30	Biomedical applications of MS: newborn screening	G. la Marca
10:30	Data analysis	G. Paglia
11:30	*Coffee break & poster session*	
12:00	Food authentication and traceability	M. Suman
13:00	Award for the best poster!	
13:10	ECTS test	
13:30	*Arrivederci!*	

LESSONS DOWNLOAD

J. Langley

J. Langley_1	G. Giorgi	C. Cordero	C. Afonso	J. Langley_2
				

R.M.A. Heeren	M. Marchetti	C. Afonso	G. Bianco	P. Gerbaux
				

D. Cobice	C. Cordero	V. Wysocki
		

R.M.A. Heeren	V. Gabelica	Exercises	P. Caboni
			

M. Marchetti	G. La Marca	G. Paglia	M. Suman
			

POSTER SESSIONS

Poster P1-P28 **set up**: MONDAY 8:00-8:30 a.m. **Removal:** TUESDAY 6:30 p.m.

Poster P29-P55 **set up**: WEDNESDAY 8:00-8:30 a.m. **Removal**: FRIDAY 1:00 p.m.

POSTER COMMUNICATIONS

P1 **Decoding the key aroma compounds of cocoa using mass spectrometry**

Amandine André, Elodie Gillich, Lisa Ullrich, Irene Chetschik

ZHAW Zürich University of Applied Sciences, School of Life Sciences and Facility Management, ILGI Institute of Food and Beverage Innovation, Research Group Food Chemistry, 8820 Wädenswil, Switzerland

P2 **Antioxidant compounds produced by Maillard reaction between glucose and glycine: HRMS identification**

Sara Bolchini,[1] Ksenia Morozova,[1] Lucrezia Angeli,[1] Tiny van Boekel,[2] Matteo Scampicchio [1]

[1] Faculty of Agricultural, Environmental and Food Science, Free University of Bozen-Bolzano, Piazza Università 1, 39100 Bolzano, Italy
[2] Food Quality & Design, Wageningen University & Research, P.O. Box 17, 6700 AA Wageningen, The Netherlands

P3 **Method development for the determination of aflatoxin M1, aflatoxicol and sterigmatocystin in sheep, goat and buffalo cheeses in LC-MS/MS**

Stefano Sdogati,[1] Ivan Pecorelli,[1] Roberto Condoleo,[2] Guglielmo Militello,[2] Ilaria Di Marco Pisciottano,[3] Sara Lambiase,[3] Carmela Rossini,[3] Stefania Massafra,[4] Elena Torres,[4] Maurizio Cossu,[5] Giovanni Lo Cascio,[6] Antonio Macaluso,[6] Licia Pantano,[6] Bruno Neri,[2] Pasquale Gallo,[3] Marilena Gili,[4] Andrea Sanna,[5] Antonio Vella,[6] Carlo Boselli [2]

[1] Istituto Zooprofilattico Sperimentale dell'Umbria e delle Marche, Via G. Salvemini, 1 - 06126 Perugia
[2] Istituto Zooprofilattico Sperimentale del Lazio e della Toscana, Via Appia Nuova, 1411 - 00178 Roma
[3] Istituto Zooprofilattico Sperimentale del Mezzogiorno, Via Salute, 2 - 80055 Portici (Napoli)
[4] Istituto Zooprofilattico Sperimentale del Piemonte, Liguria e Valle d'Aosta, Via Bologna, 148 - 10154 Torino
[5] Istituto Zooprofilattico Sperimentale della Sardegna, Via Duca degli Abruzzi, 8 - 07100 Sassari
[6] Istituto Zooprofilattico Sperimentale della Sicilia, Via Gino Marinuzzi, 3 - 90129 Palermo

P4 **Characterization of the volatile compounds in two monovarietal wines from different worldwide origins using HS-SPME- GCxGC-ToF/MS**

Aakriti Darnal,[1,2] Simone Poggesi,[1,2] Edoardo Longo,[1,2] Emanuele Boselli [1,2]

[1] Oenolab, NOI Techpark Alto Adige/Südtirol, Via A. Volta 13B, 39100 Bolzano, Italy
[2] Free University of Bozen-Bolzano, Faculty of Agricultural, Environmental, and Food Sciences, Piazza Università 1, 39100 Bolzano, Italy

P5 **Structural elucidation of agrochemical derivatives using infrared ion spectroscopy**

T. van Wieringen,[1] M. J.A. Vink,[1] G. Berden,[1] J. Oomens,[1] S.J. Perry,[2] A. Chantzis,[2] J. Martens [1]

[1] FELIX Laboratory, Radboud Univeristy, The Netherlands
[2] Syngenta AG, Bracknell, United Kingdom

P6 **Inductively Coupled Plasma Mass Spectrometry in food analysis. Trace and toxic elements for food authentication and valorisation**

A. Mara, I. Langasco, M.I. Pilo, N. Spano, G. Sanna

Department of Chemical, Physical, Mathematical and Natural Sciences, University of Sassari, Italy

P7 **Use of mass spectrometry to characterise the unique polyphenolic profile of PIWI wines**

Gavin Duley,[1,2] Adriana Teresa Ceci,[1,2] Edoardo Longo,[1,2] Emanuele Boselli [1,2]

[1] Oenolab, NOI TechPark Alto Adige/Südtirol, Via A. Volta 13B, 39100 Bolzano, Italy
[2] Faculty of Agricultural, Environmental and Food Sciences, Free University of Bozen-Bolzano, Piazza Università 5, 39100 Bolzano, Italy

P8 **Determination of tropane alkaloids in food matrices using LC-UHPLC-MS/MS**

Larissa Caminhas, Susanne Rath

University of Campinas (UNICAMP) - Brazil

P9 **Gas chromatography-mass spectrometry method for the quantitative determination of ethylene and diethylene glycols contamination in cough syrups**

Monerah A. Altamimy, Yahya M. Alshehri, Norah Altalyan, Shaikah Alzaid

Reference Laboratory for Medicines and Cosmetics, Research and Laboratories sector
Saudi Food and Drug Authority, Riyadh, Saudi Arabia

P10 **MALDI 1 & 2 MS imaging of lipid double-bond positional isomers using off-line ozonolysis**

D. Bezdeková,[1] J. Preisler,[1] M. Hendrych,[2] K. Dreisewerd,[3] A. Bednařík [1]

[1] Chemistry Department, Faculty of Natural Sciences, Masaryk University, Czech Republic
[2] First Pathological Department, St. Anne's University Hospital Brno, Czech Republic
[3] Institute of Hygiene and Interdisciplinary Center for Clinical Research (IZKF), University of Münster, Germany

P11 **Investigating the potential of novel polymer-based MALDI matrices for the detection of compounds of low molecular weight by leveraging MALDI-HRMS analytical workflows**

E. Aleiferi,[1] M. Tsakanika,[2] D. E. Damalas,[1] A. Kritikou,[1] G. Sakellariou,[2] N. S. Thomaidis [1]

[1] Laboratory of Analytical Chemistry, Department of Chemistry, National and Kapodistrian University of Athens, Greece, Panepistimiopolis, Zografou, 15771, Athens, Greece
[2] Laboratory of Industrial Chemistry, Department of Chemistry, National and Kapodistrian University of Athens, Greece, Panepistimiopolis, Zografou, 15771, Athens, Greece

P12 **Effective temperature of porous silicon substrates in LDI-MS in function of etching parameters**

Clara Whyte Ferreira,[1,2] Bastien Cabrera-Tejera,[1] Wendy Müller,[1] Yannick Coffinier,[3] Romain Tuyaerts,[2] Gilles Scheen,[2] Gauthier Eppe,[1] Edwin De Pauw [1]

[1] Mass Spectrometry Laboratory, MolSysResearch Unit, Chemistry Department,University of Liège, Liège, Belgium
[2] Incize, Ottignies-Louvain-la-Neuve, Belgium
[3] Univ. Lille, CNRS, UMR 8520 - IEMN, Lille, France

P13 **The quest for the unambiguous identification of ß-naphthol and triarylcarbonium colorants by MeV-SIMS - Procedures for mass calibration & data evaluation**

Teodora Raicu,[1] Matea Krmpotić,[2] Zdravko Siketić,[2] Iva Bogdanović-Radović,[2] Dubravka Jembrih-Simbürger [1]

[1] Institute for Natural Sciences and Technology in the Arts (INTK), Academy of Fine Arts Vienna, Augasse 2-6, Vienna, A - 1090, Austria
[2] Ruđer Bošković Institute, Bijenička cesta 54, Zagreb, HR - 10000, Croatia

P14 Preferred protonation site of aromatic amines: elucidation via IR ion spectroscopy

Laura Finazzi,[1] *Jonathan Martens,*[1] *Giel Berden,*[1] *Jos Oomens* [1,2]

[1] FELIX laboratory, Radboud University Institute for Molecules and Materials Nijmegen, The Netherlands
[2] van 't Hoff Institute for Molecular Sciences University of Amsterdam Amsterdam, The Netherlands

P15 Structural characterization of mobility-selected ions: combining TIMS with IR ion spectroscopy on an FT-ICR MS platform

Lara van Tetering, Kas Houthuijs, Jelle Schuurman, Jonathan Martens, Giel Berden, Jos Oomens

FELIX Laboratory, Institute for Molecules and Materials, Radboud University, Nijmegen, Netherlands

P16 Mass spectrometry and photochemical study of photoisomerization and thermal back-isomerization of heteroaryl azobenzenes anchored on peptoids for the chemical storage of solar energy

Gwendal Henrard,[1,2] *Thomas Robert,*[1] *Benjamin Tassignon,*[1,2] *Julien De Winter,*[1] *Jérôme Cornil,*[2] *Pascal Gerbaux* [1]

[1] Organic Synthesis and Mass Spectrometry laboratory (S²MOs)
[2] Laboratory for Chemistry of Novel Materials (CMN), University of Mons, 23 Place du Parc, B-7000 Mons, Belgium

P17 21-T FT-ICR MS: chemical and structural characterization of complex peat- burning particulate matter

E. Schneider,[1,2] *C. P. Rüger,*[1,2] *M. L. Chacón-Patiño,*[3] *M. Somero,*[4] *M. Ruppel,*[5] *M. Ihalainen,*[4] *K. Köster,*[4] *O. Sippula,*[4] *H. Czech,*[1,6] *R. Zimmermann* [1,2,6]

[1] Department of Analytical and Technical Chemistry, University of Rostock, Rostock, Germany
[2] Department Life, Light & Matter, University of Rostock, Rostock, Germany
[3] National High Magnetic Field Laboratory, Florida State University, Tallahassee, United States
[4] Department of Environmental and Biological Sciences, University of Eastern Finland, Kuopio, Finland
[5] Atmospheric Composition Unit, Finnish Meteorological Institute, Helsinki, Finland
[6] Joint Mass Spectrometry Centre, Cooperation Group "Comprehensive Molecular Analytics" (CMA), Helmholtz Munich, 81479 Munich, Germany

P18 Contaminants of emerging concern in drinking water: integrated chemical and bioanalytical tools

M. Profita,[1] *P. Valbonesi,*[1] *I. Vasumini,*[2] *E. Fabbri* [1]

[1] Dept. of BiGeA, University of Bologna, Ravenna, Italy
[2] Romagna Acque Società delle Fonti SpA, Ravenna, Italy

P19 Detection of pesticides using Multi-Scheme Chemical Ionization (MION) Inlet and Orbitrap mass spectrometer with a filter desorbing unit

Fariba Partovi,[1,2] *Joona Mikkilä,*[1] *Jyri Mikkilä,*[1] *Tuija Jokinen,*[4] *Aleksei Shcherbinin,*[1] *Matti Rissanen* [2,3]

[1] Karsa Ltd., A. I. Virtasen aukio 1, 00560 Helsinki, Finland
[2] Aerosol Physics Laboratory, Physics Unit, Faculty of Engineering and Natural Sciences, Tampere University, 33720 Tampere, Finland
[3] Department of Chemistry, University of Helsinki, 00014 Helsinki, Finland
[4] Climate and Atmosphere Research Center (CARE-C), The Cyprus Institute, 2121 Nicosia, Cyprus

P20 Structural characterisation of glyphosate and AMPA metal complexes using ion mobility-mass spectrometry

O. Rusli, O. H. Lloyd Williams, N. J. Rijs

School of Chemistry, UNSW Sydney, Australia

P21 **Unveiling the chemical universe of PFAS in biota using a combined targeted and untargeted workflow, utilizing LC – VIP HESI(-) – tims – QToF MS**

Georgios O. Gkotsis,[1] Dimitrios E. Damalas,[1] Carsten Baessmann,[2] Bob Galvin,[2] Nikolaos S. Thomaidis [1]

[1] Nationaland Kapodistrian University of Athens, Department of Chemistry, Panepistimiopolis, 157 84 Athens, Greece
[2] Bruker Daltonik GmbH, Bremen, Fahrenheitstraße 4, 28359 Bremen, Germany

P22 **Analysis of transformation products of an emerging contaminant by HPLC-MS^n**

Federico M. Ivanic, Roberto J. Candal, Matias Butler

Instituto de Investigación e Ingeniería Ambiental (IIIA-UNSAM-CONICET), EHyS Universidad Nacional de San Martin, Buenos Aires, Argentina

P23 **The assessment of sample preparation conditions for the analysis of per and polyfluorinated alkyl substances (PFASs)**

Omotola Folorunsho

Centre for Agroecology Water and Resilience (CAWR), Coventry University Wolston Lane, Ryton on Dunsmore, CV8 3LG, UK

P24 **Evaluation for the performance of Energized Dispersive Guided Extraction system for high-throughput lipidomics studies in marine environmental matrices**

Yunhai Li,[1] Sara Finnerty,[1] Brian Kelleher,[2] Shane O'Reilly [1]

[1] Atlantic Technological University, Sligo, Ireland
[2] Dublin City University, Dublin, Ireland

P25 **Lipidomic profiling intertidal mudflat microphytobenthic biofilms**

Sara Finnerty,[1] Yunhai Li,[1] Brian Kelleher,[2] Shane O'Reilly [1]

[1] Atlantic Technological University, Sligo, Ireland
[2] Dublin City University, Dublin, Ireland

P26 **Leveraging LC-TIMS-QTOFMS for addressing analytical challenges in chemical exposome studies**

Konstantina S. Diamanti,[1] Dimitrios E. Damalas,[1] Georgios O. Gkotsis,[1] Eleni I. Panagopoulou,[1] Maria-Christina Nika,[1] Carsten Baessmann,[2] Bob Galvin,[2] Nikolaos S. Thomaidis [1]

[1] Laboratory of Analytical Chemistry, Department of Chemistry, National and Kapodistrian University of Athens, Panepistimiopolis Zografou, 15771, Athens, Greece
[2] Bruker Daltonics GmbH & Co. KG, Bremen, Germany

P27 **A bottom-up approach to characterize the proteome of natural rubbers employed in tyres production**

Ludovica Sofia Guadalupi,[1] Cosima Damiana Calvano,[1] Tommaso Cataldi,[1] Andrea Bernardi,[2] Mattia Cettolin,[2] Marco Arimondi [2]

[1] Dipartimento di Chimica, Università degli Studi di Bari Aldo Moro, 70125 Bari, Italy
[2] Chemical Laboratory - Innovations & Methods Development, Pirelli Tyre S.p.a., 20126 Milano, Italy

P28 **Saliva peptidome profiling in glioblastoma multiforme brain tumour by HPLC-MS top-down platform**

Alexandra Muntiu,[1] Diana Valeria Rossetti,[2] Federica Vincenzoni,[1,3] Irene Messana,[2] Massimo Castagnola,[4] Giuseppe La Rocca,[3,5] Alessandro Olivi,[3,5] Andrea Urbani,[1,3] Giovanni Sabatino,[3,5] Claudia Desiderio [2]

[1] Dipartimento di Scienze Biotecnologiche di Base, Cliniche Intensivologiche e Perioperatorie, Università Cattolica del Sacro Cuore, 00168 Rome, Italy
[2] Istituto di Scienze e Tecnologie Chimiche "Giulio Natta", Consiglio Nazionale delle Ricerche, Rome, Italy
[3] Fondazione Policlinico Universitario A. Gemelli IRCCS, Università Cattolica del Sacro Cuore,

Rome, Italy
4 Centro Europeo di Ricerca sul Cervello-IRCCS Fondazione Santa Lucia, Rome, Italy
5 Institute of Neurosurgery, Fondazione Policlinico Universitario A. Gemelli IRCCS, Catholic University, Rome, Italy

P29 Porphyrin derivatives as quadruplexes ligands: spectrometry and spectroscopy studies

G. Satta,[1,2] M. Carraro,[1,2] L. Pisano,[1,2] L. De Luca,[1] S. Gaspa,[1] F. Mocci,[3] C. Meloni,[3] A. Cantara,[4] J. Plavec,[5] M. Trajkovski[5]

1 Department of Chemical, Physical, Mathematical and Natural Sciences, University of Sassari, Via Vienna 2, Sassari, 07100, Italy
2 Consorzio Interuniversitario Reattività Chimica e Catalisi (CIRCC), Via Celso Ulpiani 27, Bari, 70126, Italy
3 Department of Chemistry and Geological Science, University of Cagliari, Cittadella Universitaria, I-09042 Monserrato, Italy
4 Institute of Biophysics, Czech Academy of Sciences, Královopolská 135, 612 65 Brno, Czech Republic
5 Slovenian NMR Centre, National Institute of Chemistry, Ljubljana SI-1000, Slovenia

P30 Optimization of an LC-MS/MS method for the targeted analysis of brain microdialysis samples using derivatization with dimethylaminophenacyl bromide

L. Nestor,[1] Y. Vander Heyden,[2] D. De Bundel,[1] I. Smolders,[1] A. Van Eeckhaut [1]

1 Vrije Universiteit Brussel (VUB), Research group Experimental Pharmacology (EFAR), Laarbeeklaan 103, Brussels, Belgium
2 Vrije Universiteit Brussel (VUB), Department of Analytical Chemistry, Applied Chemometrics and Molecular Modelling (FABI), Laarbeeklaan 103, Brussels, Belgium

P31 May post-translational succination be involved in cardiac arrhythmia? A joint study between (ion mobility) mass spectrometry and molecular dynamics

L. Groignet,[1,2] D. Dellemme,[2] M. Surin,[2] J.-M. Colet,[3] P. Brocorens,[2] J. De Winter [1]

1 Organic Synthesis and Mass Spectrometry Laboratory
2 Laboratory for Chemistry of Novel Materials
3 Laboratory of Human biology and Toxicology
University of Mons (UMONS), Place du Parc 23, Mons 7000, Belgium

P32 Metabolomics applied to discover prognostic markers in human heart transplantation

E.C. Montatixe Fonseca,[1] M.C. Mimmi,[3] A. Corazza,[4] M. Belliato,[2] C. Pellegrini,[1] S. Pelenghi [1]

1 Cardiac Surgery Unit 1, IRCCS San Matteo Hospital Foundation, Pavia, Italy
2 Anesthesiology and Intensive Care Unit 2, IRCCS San Matteo Hospital Foundation, Pavia, Italy
3 Department of Molecular Medicine, University of Pavia, Italy
4 Department of Medical Area, University of Udine, Italy

P33 Sterolomic profiling of human CSF and plasma to reveal altered cholesterol metabolism in Parkinson's diseases

Eylan Yutuc,[1] Manuela Pacciarini,[1] Anders Öhman,[2] Lars Forsgren,[2] Miles Trupp,[2] Yuqin Wang,[1] William J. Griffiths [1]

1 Institute of Life Science 1, Swansea University Medical School, SA2 8PP, Swansea, United Kingdom
2 Umea University, Umea, Sweden

P34 Metabolomic profiling in differential diagnosis for Parkinson's disease and atypical parkinsonisms

Erika Esposito,[1,2] Alessandro Perrone,[1,3] Chiara Cancellerini,[1] Manuela Contin,[1,4] Giovanna Calandra Buonaura,[1,4] Giovanna Lopane,[1] Jessica Fiori [1,2]

1 IRCCS Istituto delle Scienze Neurologiche di Bologna, Bologna, Italy
2 Dipartimento di Chimica "G. Ciamician", Università di Bologna, Bologna, Italy
3 Dipartimento di Scienze Mediche e Chirurgiche, Università di Bologna, Bologna, Italy
4 Dipartimento di Scienze Biomediche e Neuromotorie, Università di Bologna, Bologna, Italy

P35 **Gas chromatography-mass spectrometry reveals the metabolic signature of different phenotypes of cystic fibrosis**

Martina Spada, Cristina Piras, Vera P. Leoni, Antonio Noto, Luigi Atzori

Department of Biomedical Sciences, University of Cagliari

P36 **Novel approach to investigate highly complex pharmaceuticals utilizing ultrahigh-resolution mass spectrometry**

Ole Tiemann,[1,2] *Lukas Schwalb,*[1,3] *Christopher P. Rüger,*[1,2,4] *Martha L. Chacón-Patiño,*[4,5] *Thomas Gröger,*[3] *Ralf Zimmermann* [1,2,3]

[1] Joint Mass Spectrometry Centre (JMSC) / Chair of Analytical Chemistry, University of Rostock, 18059 Rostock, Germany
[2] Department Life, Light & Matter (LL&M), University of Rostock, 18059 Rostock, Germany
[3] JMSC / Cooperation Group "Comprehensive Molecular Analytics", Helmholtz Zentrum München, 85764 Neuherberg, Germany
[4] International Joint Laboratory - iC2MC: Complex Matrices Molecular Characterization, 76700 Harfleur, France
[5] Ion Cyclotron Resonance Program, National High Magnetic Field Laboratory, Florida State University, Tallahassee, FL 32310, USA

P37 **The role of the mass spectrometry in the discovery of new potential anticancer drugs**

Francesca Meloni,[1] *Sebastiano Masuri,*[1] *Lukáš Moráň,*[2,3] *Maria Grazia Cabiddu,*[1] *Enzo Cadoni,*[1] *Josef Havel,*[4,5] *Petr Vaňhara,*[2,4] *Tiziana Pivetta* [1]

[1] Department of Chemical and Geological Sciences, University of Cagliari, Cittadella Universitaria, 09042 Monserrato, Cagliari, Italy
[2] Department of Histology and Embryology, Faculty of Medicine, Masaryk University, 62500, Brno, Czech Republic
[3] Research Centre for Applied Molecular Oncology, Masaryk Memorial Cancer Institute, 65653 Brno, Czech Republic
[4] Department of Chemistry, Faculty of Science, Masaryk University, 62500, Brno, Czech Republic
[5] International Clinical Research Center, St. Anne's University Hospital, 65691, Brno, Czech Republic

P38 **Mass-directed preparative purification of Semaglutide batches**

Louisa O'Grady, Philip Gaffney, Paola De Luisi

Dr Reddy's Laboratories (EU) Ltd., Cambridge, UK

P39 **Investigation of the potential biotransformation of different pharmaceuticals in zebrafish embryos (*Danio rerio*), utilizing LC-QTOFMS and LC-TIMS-QTOFMS**

Eleni I. Panagopoulou, Dimitrios E. Damalas, Eleni Aleiferi, Vasiliki Tzepkinli, Nikolaos S. Thomaidis

Laboratory of Analytical Chemistry, University of Athens, Panepistimiopolis Zografou, 157 71 Athens, Greece

P40 **Antiretroviral molecules: investigating the break-down pathways**

Ambar S.A. Shaikh, Kgato P. Selwe, Ed Bergstrom, Jackie Mosely, Caroline E. H. Dessent

Department of Chemistry, University of York, Heslington, York, UK

P41 **Metabolism of nine synthetic opioid in zebrafish larvae using liquid chromatography mass spectrometry**

Sara Pesavento, Matilde Murari, Franco Tagliaro, Federica Bortolotti, Rossella Gottardo

Unit of Forensic Medicine, Department of Diagnostics and Public Health, University of Verona, Verona, Italy

P42 **Nitrating activity of the hemin-$A\beta_{16}$ complex: modifications on the peptide itself**

Silvia De Caro,[1,2] *Simone Dell'Acqua,*[1] *Enrico Monzani,*[1] *Stefania Nicolis*[1]

[1] Department of Chemistry, University of Pavia, Italy
[2] Scuola Universitaria Superiore IUSS Pavia, Italy

P43 **Chemical analysis and investigation of pharmacological activities of a birch bark extract from *Betula papyrifera***

Volodymyra Zuieva, Christina Bottaro, Rajendran Kaliaperumal, Matthias Bierenstiel

Memorial University of Newfoundland, 153 Park St, B1P 4W7, Sydney, NS, Canada

P44 **Proximity-dependent Biotin Identification (BioID): a tool for screening protein- protein interactions in living cells**

Pasquinna Sida, Mike Kinsella, David Scanlon

South East Technological University (SETU), X91 K0EK, Waterford, Ireland

P45 **A mass spectrometry-based multi-omics approach to explore the mechanisms of drug resistance in methicillin-resistant *Staphylococcus aureus***

Pedro C. Rosado,[1] M. Matilde Marques,[1,2] Gonçalo C. Justino [1]

[1] Centro de Química Estrutural - Institute of Molecular Sciences, Instituto Superior Técnico, Universidade de Lisboa, Av. Rovisco Pais, 1, 1049-001 Lisboa, Portugal
[2] Departamento de Engenharia Química, Instituto Superior Técnico, Universidade de Lisboa, Av. Rovisco Pais, 1, 1049-001 Lisboa, Portugal

P46 **Evaluation of the best HDX-MS workflow for the analysis of Meningococcal PorB in native state**

Sara Favaron,[1, 2] Veronica Nasta,[1] Elisa Fasoli,[2] Nathalie Norais,[1] Lucia Eleonora Fontana [1]

[1] GSK, Via Fiorentina 1, 53100, Siena, Italy
[2] Politecnico di Milano, Department of Chemistry, Materials and Chemical Engineering “Giulio Natta”, Piazza Leonardo da Vinci 32, 20133, Milano, Italy

P47 **Mass spectrometry’s role in the study of correlation between oxidative stress, OSAS and obesity**

Chiara Maccari,[1] Michele Miragoli,[1,2] Rosario I. Statello,[1] Agnese Martini,[3] Roberta Andreoli [1,2]

[1] Department of Medicine and Surgery, University of Parma, Parma, Italy
[2] CERT, Center of Excellence for Toxicological Research, University of Parma, Italy
[3] INAIL, the National Institute for Insurance against Accidents at Work, Department of Medicine, Epidemiology, Workplace and Environmental Hygiene, Rome, Italy

P48 **Laser settings’ optimization for single cell MALDI-TOF MS imaging of human CD19+ lymphocytes**

Ivana Marković,[1,2] Željko Debeljak,[1,2] Bojana Bošnjak,[2,3] Dario Mandić [1,2]

[1] Clinical Institute of Laboratory Diagnostics, University Hospital Centre Osijek, Osijek, Croatia
[2] Faculty of Medicine Osijek, JJ Strossmayer University of Osijek, Osijek, Croatia
[3] Clinical Institute of Transfusion Medicine, University Hospital Centre Osijek, Osijek, Croatia

P49 **BeatBox and iST for streamlined FFPE tissue processing: A xylene-free, robust, and high-throughput sample preparation for proteomic analysis**

Jasmin Johansson, Katharina Limm, Silvia Würtenberger, Marcello Stein, Nils A. Kulak, Katrin Hartinger

PreOmics GmbH, Planegg/Martinsried, Germany

P50 **Improved detection of tryptic peptides from tissue sections using Desorption electrospray ionisation mass spectrometry imaging (DESI-MSI)**

Heather Bottomley,[1] Jonathan Phillips,[1] Philippa Hart [2]

[1] University of Exeter, Stocker Road, Exeter, EX4 4PY, UK
[2] Medicines Discovery Catapult, Alderley Park, Block 35, Mereside, Macclesfield SK10 4ZF, UK

P51 **MS fingerprinting of cyclic modified peptides and proteins with chloromethyl acryl reagents**

Maria J. S. A. Silva,[1,3] Lujuan Xu,[1,2] Pedro M. P. Gois,[3] Seah Ling Kuan,[1,2] Tanja Weil [1,2]

[1] Max-Planck Institute for Polymer Research, Ackermannweg 10, 55128 Mainz, Germany

[2] Institute of Inorganic Chemistry I, Ulm University Albert-Einstein-Allee 11, 89081 Ulm, Germany
[3] Research Institute for Medicines (iMed.ULisboa), Faculty of Pharmacy, Universidade de Lisboa, 1649-003 Lisbon, Portugal

P52 Derivatization-targeted analysis of amino compounds: from neutral loss scan to dynamic multiple reaction monitoring mode

Larissa Silva Maciel,[1] *Arianna Marengo,*[2] *Michaela Hříbková,*[1,3] *Koit Herodes* [1]

[1] Institute of Chemistry, University of Tartu, Tartu, Estonia
[2] Dipartimento di Scienza e Tecnologia del Farmaco, Università di Torino, Torino, Italy
[3] Department of Pharmaceutical Chemistry and Pharmaceutical Analysis, Charles University, Hradec Králové, Czech Republic

P53 A spatial multi-omics investigation into spinal cord remodeling in mouse mutant strains with altered myelin basic protein abundance

Rachel Pryce,[1] *Hooman Bagheri,*[2] *Alan C. Peterson,*[2] *Pierre Chaurand* [1]

[1] Department of Chemistry, Université de Montréal, Montreal, Quebec, Canada
[2] Department of Neurology and Neurosurgery, McGill University, Montreal, Quebec, Canada

P54 Finding the molecules transported by SLCs: machine learning supported targeted metabolomics

Christoph Bueschl,[1] *Iciar Serrano,*[1] *Juan Sanchez,*[1] *Daniela Reil,*[1] *Kristaps Klavins,*[1] *J. Thomas Hannich,*[1] *Sabrina Lindinger,*[1] *Abigail Jarret,*[1] *Tabea Wiedmer,*[1] *Giulio Superti-Furga* [1,2]

[1] CeMM Research Center for Molecular Medicine of the Austrian Academy of Sciences, Vienna, Austria
[2] Center for Physiology and Pharmacology, Medical University of Vienna, Vienna, Austria

P55 Exploring the cellular actions of chelerythrine employing an untargeted mass spectrometry proteomics approach

Artem Petrosian, Pedro F. Pinheiro, Gonçalo C. Justino

Centro de Química Estrutural - Institute of Molecular Sciences, Instituto Superior Técnico, Universidade de Lisboa, 1049-001 Lisboa, Portugal

P56 Determination of peptide peak purity by molecular feature extraction using accurate mass LC-MS

Gregory Kelly, Peter Smith, John Malone, Philip Nicholl

Almac Group Limited, Craigavon, Ireland

POSTER ABSTRACTS

P1

Decoding the key aroma compounds of cocoa using mass spectrometry

Amandine André, Elodie Gillich, Lisa Ullrich, Irene Chetschik

ZHAW Zürich University of Applied Sciences, School of Life Sciences and Facility Management, ILGI Institute of Food and Beverage Innovation, Research Group Food Chemistry, 8820 Wädenswil, Switzerland

Summary: *The molecular basis of the so-called fine-flavour bean-to-bar chocolates is not yet fully understood. The combination of GC-O, GC-MS and HPLC-MS/MS experiments have enabled to highlight important volatile and non-volatile aroma compounds contributing to the fine-flavour property of chocolates.*

Keywords: *Cocoa, GC-O-MS, HPLC-MS/MS*

Introduction

Chocolate is a beloved product all over the world, made from the roasted beans of *Theobroma cacao*. Recent developments show a higher demand from consumers for high-quality chocolate, organic cocoa, and bean-to-bar products [1]. Bean-to-bar chocolates are made from fine or flavour cocoa of defined origin and variety. They differ in their sensory properties from the chocolates produced on a high industrial scale which are usually blending cocoa beans of bulk quality from different origins. Therefore, the diversity of chocolate flavour profiles on the market is increasing. While the sensory diversity of cocoa products, especially from defined origins and varieties, is widely described in the literature[2,3]. The molecular background of those aromas is not fully understood yet. The research group of Food Chemistry at the Zurich University of Applied Sciences (ZHAW) combines both gas and liquid chromatography techniques coupled with mass spectrometry to decipher the key cocoa aroma compounds throughout the cocoa processing chain, from beans to chocolate bars.

Experimental

In this study, bean-to-bar chocolates were investigated to understand the molecular basis of the so-called fine flavour. GC analyses coupled with olfactometry and mass spectrometry allowed to identify odor active molecules on one hand. On the other hand, the construction of a molecular network with the HPLC-MS/MS data allowed to highlight interesting differences in terms of 2,5-diketopiperazines in the different chocolates[4,5].

Results

These combined approaches have enabled to highlight important aroma characteristics of those fine-flavour chocolates at the molecular level. Using the technique of the molecular networks to visualize the chemical diversity of the dataset, 18 different diketopiperazines were identified and among them 3 were detected for the first time in chocolates. The observed clustering of the bean-to-bar chocolates according to bean variety suggests that under mild roasting conditions the bean genotype has a great influence on 2,5-diketopiperazines [5]. On the volatiles side, the fine flavour properties of chocolates such as acidic and fruity notes were associated with high dose over threshold factors (DoT factors) of acetic acid and fruity smelling esters such as ethyl 2-methylbutanaote, ethyl 3-methylbutanoate, and 3-methylbutyl acetate, respectively. Cocoa-like and roasty flavour notes were associated with high DoT factors for 2-methylbutanal, 3-methylbutanal, 4-hydroxy-2,5-dimethylfuran-3(2H)-one, and dimethyl-trisulfane. The floral and astringent flavours were linked to high DoT factors of (−)-epicatechin, procyanidin B2, procyanidin C1, and 2-phenylethan-1-ol [4].

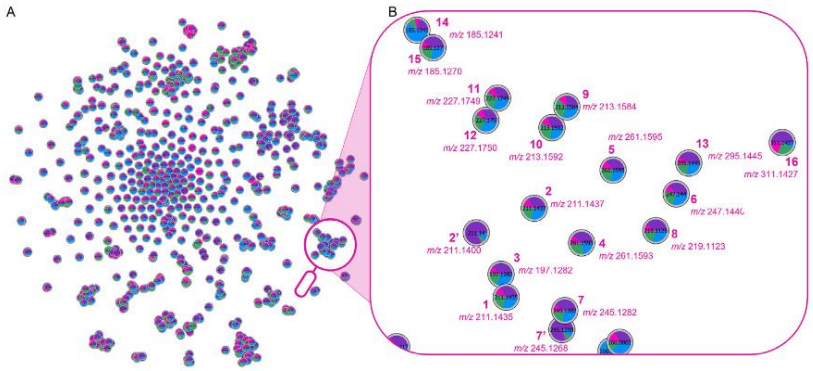

Figure 1. *Molecular Network built with the cocoa dataset (A) with a focus on the diketopiperazines cluster (B) [5].*

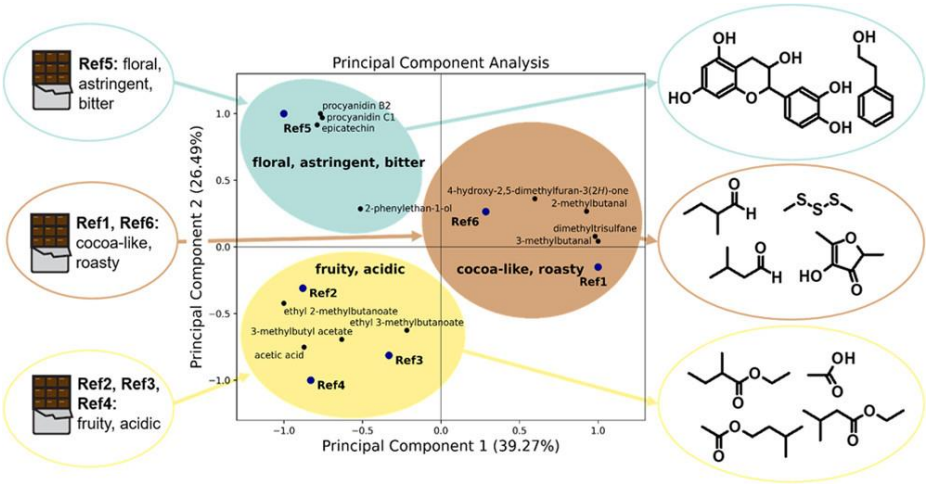

Figure 2. *Principal Component Analysis (PCA) showing the molecular composition of the different flavour-type dark chocolates [4].*

Conclusions

By combining GC and HPLC with mass spectrometry, this study showed for the first time how distinct differences in the flavour profiles of dark chocolates are reflected in molecular compositions. The results of our investigations constitute a basis for future quality assessment of cocoa and dark chocolates and the optimization of the flavour properties based on raw material selection and thoughtful processing.

References

1. Growing Cocoa. *International Cocoa Organization*. https://www.icco.org/growing-cocoa/, accessed 22.06.2023
2. Kongor, J.E.; Hinneh, M.; de Walle, D.V.; Afoakwa, E.O.; Boeckx, P.; Dewettinck, K. *Food Research International,* **2016**, *82*, pp 44–52.
3. Sukha, D.A.; Butler, D.R.; Umaharan, P.; Boult, E. *European Food Research and Technology*, **2008**, *226*, pp 405–413.
4. Ullrich, L.; Casty, B.; André, A.; Hühn, T.; Steinhaus, M.; Chetschik, I. *Journal of Agricultural and Food Chemistry.* **2022**, *70*, pp 13730–13740.
5. André, A.; Casty, B.; Ullrich, L.; Chetschik, I. *Heliyon,* **2022**, *8*.

P2

Antioxidant compounds produced by Maillard reaction between glucose and glycine: HRMS identification

Sara Bolchini,[1] Ksenia Morozova,[1] Lucrezia Angeli,[1] Tiny van Boekel,[2] Matteo Scampicchio [1]

[1] Faculty of agricultural, environmental and food science, Free University of Bozen-Bolzano, Piazza Università 1, 39100, Bolzano, Italy
[2] Food Quality & Design, Wageningen University & Research, P.O. Box 17, 6700 AA Wageningen, The Netherlands

Summary: *Maillard reaction products are reported as antioxidants by the literature, but their identification remains still unclear. Thus, this work aims to the detection (coulometric detector) and identification (HRMS) of antioxidant MRP in a glucose and glycine solution.*

Keywords: *Maillard reaction, antioxidants, High Resolution Mass Spectrometry*

Introduction

Maillard reaction is a complex series of chemical reactions that occur between reducing sugars and amino acids residues during heating of food. Maillard reaction products (MRPs) are responsible for aroma production and browning. Some of them have been reported as antioxidants, although their identification remains still unclear.
Therefore, this work aims to study the antioxidants evolved during heating a glucose-glycine model solution at 90°C and pH 6.8 starting from the kinetic model of the reaction developed in literature [1]. NMR was used to monitor the transient changes of glucose, glycine (MR reactants), acetic acid and formic acid (MR products) during time. The antioxidants produced were monitored, identified and quantified using HPLC coupled with a triple detector consisting of diode array, coulometric array and high-resolution mass spectrometer.

Materials and Methods

The study has been developed starting from the model of the reaction proposed by van Boekel [1] by monitoring the transient changes of glucose, glycine, acetic acid, formic acid and melanoidins with ^{1}H and ^{13}C NMR and spectrophotometric assays. Then, using a novel approach based on Ding et al. [2], which consisted in HPLC coupled with three different detectors, antioxidant MRPs were studied. The triple detectors consisted, respectively, of a diode array (DAD), a coulometric array (CoulArray™: CAD), and high resolution mass spectrometer (HRMS, Q Exactive Orbitrap, Thermo Scientific). DAD allowed the optimization of the separation of the analytes through the chromatographic column. CAD is a multi-channel electrochemical detector that measures the current signals generated from antioxidant analytes (redox species) eluted by the HPLC. Since the working principle of the coulometric detectors is based on the Faraday's law, it allowed the absolute quantification of the analytes. Finally, using HRMS, it was possible to identify the antioxidants previously detected and update the kinetic model of the reaction.

Results and Discussion

Kinetic model

NMR spectroscopy has been used to quantify reactants (glucose and glycine) and some products (acetic acid and formic acid) along the reaction. In Figure 1 are shown the resulting ^{1}H-NMR and ^{13}C-NMR spectra of acetic acid, formic acid, glucose and glycine.

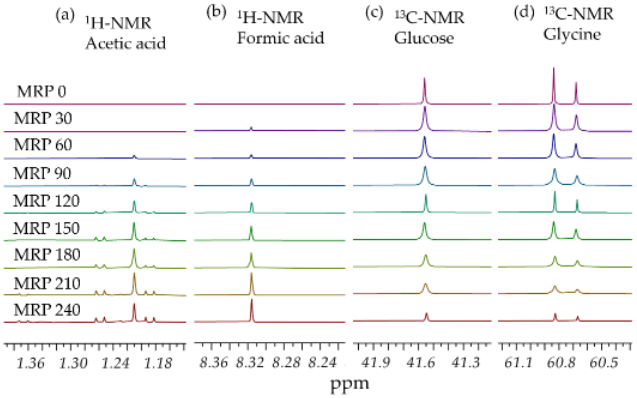

Figure 1. *(a) and (b) Stacked ^{1}H-NMR peak corresponding to acetic acid and formic acid obtained analyzing MR samples incubated for 0, 30, 60… 240 minutes at 90°C; (c) and (d) Stacked ^{13}C-NMR peak corresponding to glucose and glycine obtained analyzing MR samples incubated 0, 30, 60 … 240 minutes at 90°C.*

In details, the signals of acetic and formic acid are increasing along the MR, while glucose and glycine signals are decreasing. The transient changes of these species perfectly match the kinetic model developed in literature [1].

Antioxidant activity of MRPs and their identification

Antioxidant MRPs have been detected, identified and quantified using DAD, CAD and HRMS. In Figure 2(a) three main peaks have been detected by CAD. Also, by using HRMS, it was possible to assign those peaks to 2-acetylpyrrole and the deydrathed version of 1- and 3-deoxyglucosones (corresponding MS/MS spectra are shown in Figure 2(b)).

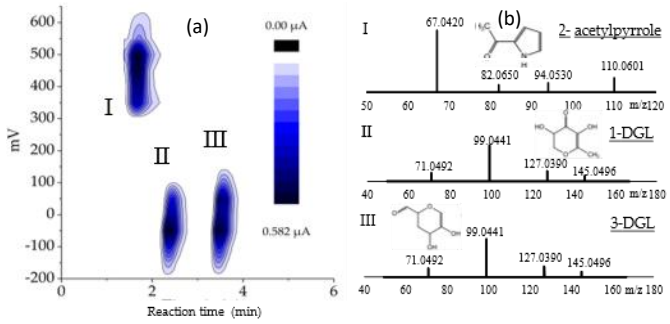

Figure 2. *(a) Contour plot of CAD signal (sum of the signals obtain from the 16 channels) of glucose-glycine MR sample after 150min at 90°C (b) MS/MS fragmentation profiles of the molecules under the three peaks and their assigned structures.*

Kinetic model update

The results achieved in this work allowed to develop a kinetic model that describe not only the evolution of MRP, confirming previous works of Van Boekel, but also the development of a new model that includes the production of antioxidant MRPs. Previous works hypothesized the formation of 2-AP [3], [4]. However, in this work, we identified the formation of 2-AP and, furthermore, we also discovered the antioxidant activity related to dehydrated version of -1 and 3-deoxyglucosones (1-DGa and 3-DGa).

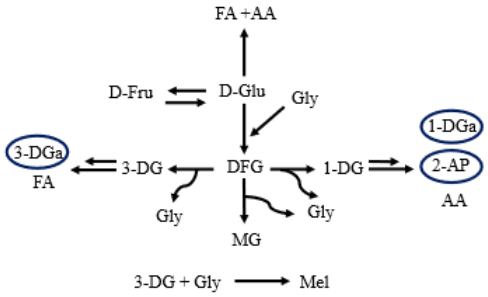

Figure 3. *Updated model of MR based on Van Boekel's one. Circled in blue, the species added: dehydrated versions of 1- and 3- deoxyglucosones (1-DGa and 3-DGa) and 2-acetylpyrrole (2-AP).*

Moreover, it was possible to follow the kinetic of production of these three species and include them in the model already developed in literature.

Conclusions

In conclusion, this study attempted to identify new species responsible for the antioxidant properties of MRP: dehydrated versions of 1- and 3- deoxyglucosones and 2-acetylpyrrole. Such findings pave the way for the synthesis of new antioxidants. Future perspectives include the production of tailored antioxidants.

References

1. Martins, Sara I.F.S., and Martinus A.J.S. Van Boekel. 2005. *Food Chemistry* 90(1–2): 257–69.
2. Ding, Yubin, et al. 2022. Lwt: 162.
3. George, R. Waller, and S. Feather Milton. 1983. Acs Symposium Series The Maillar in Foods and Nutrition.
4. Hayas, Fumitaka, Seon Bong Kim, and Hiromichi Kato. 1985. Agricultural and Biological Chemistry 49(8): 2337–41.

P3

Method development for the determination of aflatoxin M1, aflatoxicol and sterigmatocystin in sheep, goat and buffalo cheeses in LC-MS/MS

Stefano Sdogati,[1] Ivan Pecorelli,[1] Roberto Condoleo,[2] Guglielmo Militello,[2] Ilaria Di Marco Pisciottano,[3] Sara Lambiase,[3] Carmela Rossini,[3] Stefania Massafra,[4] Elena Torres,[4] Maurizio Cossu,[5] Giovanni Lo Cascio,[6] Antonio Macaluso,[6] Licia Pantano,[6] Bruno Neri,[2] Pasquale Gallo,[3] Marilena Gili,[4] Andrea Sanna,[5] Antonio Vella,[6] Carlo Boselli [2]

[1] Istituto Zooprofilattico Sperimentale dell'Umbria e delle Marche, Via G. Salvemini, 1 - 06126 Perugia
[2] Istituto Zooprofilattico Sperimentale del Lazio e della Toscana, Via Appia Nuova, 1411 - 00178 Roma
[3] Istituto Zooprofilattico Sperimentale del Mezzogiorno, Via Salute, 2 - 80055 Portici (Napoli)
[4] Istituto Zooprofilattico Sperimentale del Piemonte, Liguria e Valle d'Aosta, Via Bologna, 148 - 10154 Torino
[5] Istituto Zooprofilattico Sperimentale della Sardegna, Via Duca degli Abruzzi, 8 - 07100 Sassari
[6] Istituto Zooprofilattico Sperimentale della Sicilia, Via Gino Marinuzzi, 3 - 90129 Palermo

Summary: *Aflatoxins and related compounds are known to be extremely carcinogenic. An analytical method is being developed for the determination of aflatoxin M1, aflatoxicol and sterigmatocystin in order to evaluate occurrence in sheep, goat and buffalo cheeses and, ultimately, population exposure to the considered mycotoxins.*

Keywords: *aflatoxin M1, metabolites, cheese*

Introduction

Aflatoxins are a family of mycotoxins produced by *Aspergillus spp*. that often contaminate feed and raw materials destined to animal consumption. Among these, aflatoxin B1 (AFB1) can be transformed, after ingestion, into its metabolite aflatoxin M1 (AFM1) which is excreted through animal milk and eventually transferred to byproducts such as cheeses and serum derivates. Given the known carcinogenic properties of AFM1, EU set up maximum residue limits (MRLs) in milk (0.050 µg/kg) [1]. Together with AFM1 other relevant AFB1 metabolites / synthesis precursors may be detected in these matrices such as aflatoxicol (AFX) and sterigmatocystin (STE). Although AFX and STE showed in vitro and in vivo toxic and carcinogenic properties[2,3], no regulations were set for these chemicals in food. The aims of this project are to develop and validate an analytical method to determine AFM1, AFX and STE in sheep, goat, buffalo cheeses and serum derivates and to determine the possible concentration factor of AFM1 in these commodities. Finally, the developed method will be applied to the analysis of several cheese samples.

Experimental

Istituto Zooprofilattico Sperimentale del Lazio e della Toscana (IZSLT), as national reference center for sheep and goat milk and milk products leads this projects together with other five laboratories, belonging to the IZS italian network. A brief recap of the developed LC-MS/MS conditions by each laboratory is reported in Table 1. Method development started with the evaluation of the recovery performances obtained for two different immunoaffinity columns (IAC). Subsequently, the extraction procedure was optimized evaluating the amount of water added in the beginning of the extraction and the role of salting out as a quick and reliable purification method for fat-containing matrices such as cheeses.

Table 1. *LC-MS/MS conditions*

Lab	Instrument	Column	Mobile phase A	Mobile phase B	Polarity	Source Temp.	Ionization voltage
IZSME	QTRAP 6500+	Kinetex XB-C18 (100 × 3.0 mm; 2.6 µm)	1 mM AA in H_2O	MeOH + HCOOH 0.05%	ESI+	350 °C	4500 V
IZSPLV	TSQ Endura	Agilent Zorbax SB-Phenyl (100 × 2.1 mm; 3.5 µm)	H_2O + HCOOH 0.1%	ACN + HCOOH 0.1%	ESI+	300 °C	1500 V
IZS-Sardegna	Xevo TQ-S	Acquity UPLC BEH C18 (100 × 2.1mm; 1.7 µm)	1 mM AA in H_2O	ACN + 0.1% HCOOH	ESI+	150 °C	2000 V
IZSSI	TSQ Vantage	ZORBAX SB-C18 (50 x 2.1 mm; 1.8 µm)	1 mM AA in H_2O	ACN + 0.1% HCOOH	ESI+	300 °C	4500 V
IZSUM	QTRAP 6500+	Kinetex C18 100Å (50 x 2.1 mm; 5 µm)	1 mM AA in H_2O	ACN + 0.1% HCOOH	ESI+	350 °C	5500 V

AA: ammonium acetate

The developed method will be validated and finally applied to the analysis of 486 cheeses sampled taking into account animal origin (sheep, goat and buffalo), type (soft, semi-hard and hard) and market distribution (large distribution, discount and local dairy companies).

Results

A blank sheep cheese was spiked with 1 µg/kg of AFM1, AFX and STE, extracted with ACN:MeOH:H_2O (60:10:30, v/v/v) and 1 mL of the extract diluted with PBS. The diluted extracts were loaded in two different IACs (A and B) and the analytes eluted as suggested by each constructor. Recoveries were > 75% for AFM1 and AFX with no great differences between IACs while for STE column A (AFLATEST WBSR+) performed better than column B (Easi-Extract RP70N) in terms of recovery (75% vs 44%). Thus, further studies were carried out using AFLATEST WBSR+ as selected IACs. Cheese tends to clog when organic solvents are added therefore, for further studies, water was separately added (e.g. 5 mL ACN:MeOH 85:15 v/v + 2 mL H_2O) since it only has the role of matrix disaggregation. Moreover, a salting-out step using 1 g NaCl (180 min at -20 °C) was added to furtherly improve organic extraction of the analytes, especially the more polar one (AFM1). The updated procedure was tested with excellent recoveries and precision for AFX and STE (Table 2). AFM1 performances, in terms of recovery and precision, need to be furtherly investigated in order to assess which step of the extraction procedure is critical for its determination. Cheeses may have different degrees of humidity, depending on the type and ageing, so in order to standardize the procedure the addition of an internal labelled standard (ILS) for AFM1 may help overcome these unsatisfactory results in terms of precision and perform a more reliable quantification.

Table 2. *Preliminary recoveries for AFM1, AFX and STE in sheep cheese (n=6)*

Analyte	Rec %	RSD_{WR}	CV%
Aflatoxin M1	77	15	20
Aflatoxicol	96	10	10
Sterigmatocystin	94	7.7	8.2

Conclusions

Aflatoxins are currently regulated in many commodities although there is a lack of information on the contamination levels of many metabolites and precursors in food and animal byproducts. This methodology, once validated, could be a useful tool for filling up the knowledge gap about AFM1, AFX and STE occurrence in these particular types of cheese. On a greater perspective, the collected data will be pivotal to also determine the concentration factors for these mycotoxins in cheeses together with the population exposure to these chemicals and to draw a comprehensive risk assessment on the consumption of sheep, goat and buffalo dairy products.

Acknowledgements

This research was funded by the Ministry of Health (code: IZS LT IZS 01/21 RC “STRATEGICA”)

References

1. European Commission, Commission Regulation (EU) 2023/915 (2023), *Official Journal of the European Union,* L119, pp 105-157.
2. EFSA. EFSA CONTAM Panel (EFSA Panel on Contaminants in the Food Chain) (2013), *EFSA Journal* 2013; 11(6):3254, 81 pp.
3. Schoenhard, G. L., Hendricks, J. D., Nixon, J. E., Lee, D. J., Wales, J. H., Sinnhuber, R. O., & Pawlowski, N. E. (1981). *Cancer Research*, *41*(3), 1011–1014.

P4

Characterization of the volatile compounds in two monovarietal wines from different worldwide origins using HS-SPME- GCxGC-ToF/MS

Aakriti Darnal,[1,2] Simone Poggesi,[1,2] Edoardo Longo,[1,2] Emanuele Boselli [1,2]

[1] Oenolab, NOI Techpark Alto Adige/Südtirol, Via A. Volta 13B, 39100 Bolzano, Italy
[2] Free University of Bozen-Bolzano, Faculty of Agricultural, Environmental, and Food Sciences Piazza Università 1, 39100 Bolzano, Italy

Summary: *The aroma compounds of two bottled monovarietal wines (Pinot Gris and Pinot Noir) were investigated using bidimensional gas-chromatography coupled with time of flight mass spectrometry (HS-SPME-GCxGC-ToF/MS). Pinot Gris wines were characterized by compounds such as linalool, β-ionone, and α-terpineol while Pinot Noir by β-damascenone, trans whiskey lactone, and benzaldehyde.*

Keywords: *Pinot Gris, Pinot Noir, HS-SPME-GC x GC-TOF/MS*

Introduction

Amongst many contributing factors that have been studied for the determination of wine quality, aroma, and flavour are considered to be the most important as they also set differences between a wide number of wines and wine styles produced throughout the world[1,2]. Wine aromas are characterized by complex interactions between the vineyard soil, geographical site, and climate characteristics, grape variety, and the technical conditions of winemaking. The knowledge of aromatic compositions of wines is of great interest as it is also highly related to the flavour. In addition, the hundreds of volatile compounds that define the wine aroma also relate to the acceptance or rejection of the wines by the consumers. Comprehensive two-dimensional gas chromatography (GCxGC) has emerged as a powerful technique for identifying a substantially larger number of volatile compounds with enhanced separation efficiency compared to one-dimensional GC, reliable in both qualitative and quantitative analysis, ability to detect low concentration and thus provides a more detailed information on the wine volatile fingerprint [3]. Several studies have been carried out to associate the wine volatiles with the grape variety which is also the aim of this study.

Materials and Methods

Pinot Gris and Pinot Noir bottles from different geographical origins were kindly provided by FruitService S.r.l., a South Tyrolean trading company (Bolzano, Italy).

The volatile compounds were characterized by Head Space Solid-Phase Microextraction combined with Comprehensive Two-Dimensional GC coupled to Time-Of-Flight Mass Spectrometry (HS-SPME-GCxGC-ToF/MS) using a Flow-Modulated interface between the two capillary columns in a Pegasus® Flux BT 4D (LECO Corporation, Germany). An internal standard (2-methyl-3-pentanol) was used for checking the repeatability. The injection was carried out in a splitless mode, and the flow rate was 1 ml/min over a polar MEGA- WAX Spirit column 40m/0.18mm/0.30µm (first dimension, MEGA s.r.l) and a 1.2m/0.1mm/0.1µm MEGA 1-HT (second dimension, MEGA s.r.l). These parameters were slightly adapted methods from published reports [4]. Automatic alignment of the dataset was done using the processing software ChromaTOF® (LECO Corporation, Berlin, Germany) ver.2021. These obtained final datasets were inspected and refined prior to the statistical analysis.

Results

The GC chromatograms for both the Pinot Gris and Pinot Noir wine samples are reported in Figure 1. The volatile profiles have been analysed by Principal Component Analysis (PCA) for both varieties (Figure 2). For Pinot Gris wines, the replicate samples of each origin were well grouped. The origins were clearly separated mostly along the first principal component (Figure 2). Wines from New Zealand (Gisborne) were characterized by 2,4-di-tert-butylphenol which is a very recently identified compound in wines sealed with synthetic closures and micro agglomerated cork and were also identified in white wine samples[6,7]. The wines from Puglia-Sicilia (Southern Italy) were characterized by the volatile compounds linalool and 3-hexanol,3-ethyl while the wines from Northern Italy, Veneto-Friuli were characterized by volatile compounds ethyl phenylacetate and benzaldehyde. The wines from South Africa Western Cape (Irrigated area) were characterized by 2,3-butanediol, ethyl hexanoate, α-terpineol, ethyl octanoate while the wines from dry land were more characterized by ethyl acetate, benzenebutanal, and phenylethyl acetate The wines from New Zealand (Marlborough) were more correlated with ethyl dodecanoate, 2,3-butanediol , hexanoic acid and decanoic acid.

1) 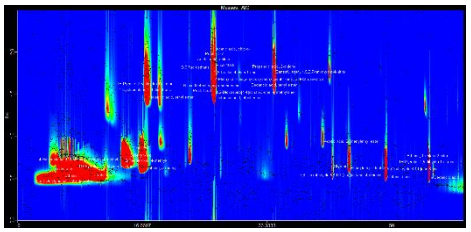 2) 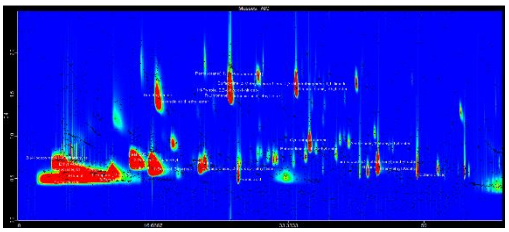

Figure 1. *GCxGC chromatogram of Pinot Gris (left) and Pinot Noir (right) sample*

For Pinot Noir wines, the replicates are grouped well in PC2 vs PC3 (Figure 4). Wines from both South Africa: Western Cape (dry land) and New Zealand showed similarity and were characterized by compounds like benzyl alcohol, trans whiskey lactone, benzaldehyde, 1-hexanol, and furfural. The Italian wines from both the Southern and Northern parts were grouped together and correlated with the compounds nerolidol, 1-butanol, 3-methyl-acetate, butyraldehyde, and phenylethyl acetate. The Chilean wines were more characterized by phenol, 4-ethyl, α-terpeniol, β-damascenone, ethyl sorbate, and butanedioic acid, diethyl ester. The wines from Argentina were more characteristic of ethyl acetate, isoamyl lactate, 2,3-butanediol, acetic acid, and β-ionone.

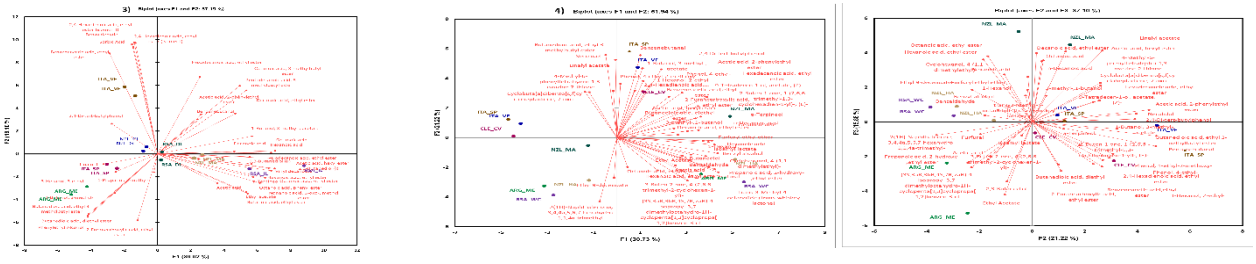

Figure 2. *PCA biplot (PC1-PC2) of Pinot Gris (left) and (PC1-PC2, PC2-PC3) of Pinot Noir wine samples (center)*
and volatile compounds (right)

Conclusion

The volatile compounds for both varieties from different origins/wineries were characterized. The volatile profiles were distinct for each variety from different countries. The wines have also been characterized for their sensory and phenolic profiles (not discussed here).

These preliminary data show that single-varietal wines of different geographic origins can differ significantly, which can lead to consumer confusion. To help producers and distributors achieve the goals of tailored commercial offerings, simplified "aroma maps" based on 2DGC chromatograms and accompanied by simple pictograms could be part of the information sheet (technical sheet) that the winery provides with the product. In this way, the information given to commercial stakeholders can be improved to meet sensory expectations related to the product offered.

References

1. E. Sánchez-Palomo, E. Gómez García-Carpintero, & G. Viñas. (2015). *South African Journal of Enology and Viticulture*, *36*(1), 117-125.
2. M.G. Álvarez, C. González-Barreiro, B. Cancho-Grande, & J. Simal-Gándara. (2011). *Food Chemistry*, *129*(3), 890-898.
3. A.L. Robinson, D.O. Adams, P.K. Boss, H. Heymann, P.S. Solomon, & R.D. Trengove. (2011). *Australian Journal of Grape and Wine Research*, *17*(3), 327-340.
4. S. Poggesi, A. Darnal, A.T. Ceci, E. Longo, L. Vanzo, T. Mimmo, & E. Boselli. (2022). 11(21), 3458.
5. M. Nishida, P. Lestringant, A. Cantu, H.J. Heymann, *Sens. Stud*. 2021, 36, e12684.
6. A.S. Oliveira, I. Furtado, M. de Lourdes Bastos, P.G. de Pinho, & J. Pinto (2020).*Food Packaging and Shelf Life*, *23*, 100465.
7. S. Han, Yang, J. Choi, K., J. Kim, K. Adhikari, & J. Lee (2022). *Foods*,*11*(4), 603.

P5

Structural elucidation of agrochemical derivatives using infrared ion spectroscopy

T. van Wieringen,[1] M. J.A. Vink,[1] G. Berden,[1] J. Oomens,[1] S.J. Perry,[2] A. Chantzis,[2] J. Martens [1]

[1] FELIX Laboratory, Radboud Univeristy, The Netherlands
[2]Syngenta AG, Bracknell, United Kingdom

Summary: *Infrared ion spectroscopy is able to determine the structure of compounds that are present in complex mixtures at very low concentration. In an automated workflow, combining liquid chromatography, mass spectrometry, infrared spectroscopy and quantum chemical calculations, derivatives related to agrochemicals are characterized.*

Keywords: *infrared ion spectroscopy, agrochemicals, toxicity*

Introduction

In plants, animals and the environment, agrochemicals undergo a variety of chemical and metabolic transformations, producing derivatives that need to be characterised to determine their toxic properties and their persistence in the environment. Using a method called infrared ion spectroscopy [1], the structure of these agrochemical derivatives can be determined. The method has the sensitivity and selectivity of mass spectrometry, while giving the structural information obtained from infrared spectroscopy.

Methods

A Bruker amaZon quadrupole ion trap was used allowing for the optical access of the FELIX IR free electron laser. The spectrum is constructed from a series of mass spectra by monitoring the fragments as the IR frequency is scanned. When the frequency of the IR laser is resonant with an absorption band of the trapped ions, photodissociation occurs, and the fragment ions are detected. The dissociation yield is calculated from the intensity of the parent ion signal (I_P) and the intensity of the fragment ion signal (I_F):

$$\text{Yield } (v) = -\ln(I_P/(I_P+\Sigma I_F)) \qquad (1)$$

The IR spectrum is computed using density functional theory (DFT). Comparing the DFT spectrum to the measured spectrum assists the structural assignment of the compound of interest.

Results

Infrared ion spectroscopy acts as a unique fingerprint, giving structural information which is able to distinguish structural isomers. Computational chemistry can predict the spectrum, based on the vibrational normal mode analysis. We show that using this technique, closely related isomeric structures can be distinguished (Figure 1).

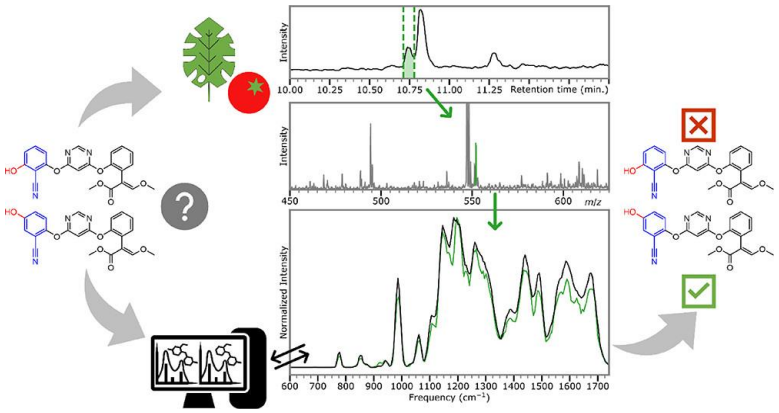

Figure 2. *Method for the analysis of plant metabolites with ion spectroscopy*

Conclusion

Agrochemical derivatives can be characterized using ion spectroscopy, with high sensitivity and little sample consumption.

References

1. M. J. A. Vink, F. A. M. G. van Geenen, G. Berden, T. J. C. O'Riordan, P. W. A. Howe, J. Oomens, S. J. Perry, J. Martens; *Environmental science and technology*, 56 (2022), pp 15563-15572.

P6

Inductively Coupled Plasma Mass Spectrometry in food analysis. Trace and toxic elements for food authentication and valorisation

A. Mara, I. Langasco, M.I. Pilo, N. Spano, G. Sanna

Department of Chemical, Physical, Mathematical and Natural Sciences, University of Sassari, Italy

Summary: *Inductively Coupled Plasma Mass Spectrometry (ICP-MS) is a powerful analytical technique for food analysis. It provides the sensitive and accurate detection of trace elements and heavy metals, thereby ensuring food safety and quality. Recent studies have highlighted the potential of these methods for food authentication.*

Keywords: *ICP-MS, Food Quality, Food Authenticity*

Introduction

Inductively Coupled Plasma Mass Spectrometry (ICP-MS) is a powerful analytical technique used in food analysis. It combines inductively coupled plasma as an ionization source with exceptional sensitivity and selectivity of mass spectrometry. ICP-MS allows for the detection and quantification of trace elements and isotopes in food samples, making it invaluable for assessing food safety, quality, and authenticity [1].

ICP-MS is considered one of the best analytical techniques because of its remarkable sensitivity and wide dynamic range, allowing both qualitative and quantitative analyses of multiple elements simultaneously. These features are crucial for studying the elemental compositions of food samples. It can determine the concentration of essential elements, such as iron, zinc, and selenium, for nutritional assessment and dietary studies. Additionally, it aids in the identification and quantification of potentially harmful elements, including lead, arsenic, cadmium, and mercury, which may be present as contaminants. This information helps regulatory bodies and food producers to ensure compliance with safety standards and implement quality control measures.

Despite these advantages, the use of ICP-MS in food analysis presents challenges. Sample preparation can be complex and time-consuming and requires careful digestion, extraction, and dilution. Interferences from matrix effects and polyatomic ions can affect the accuracy, requiring the use of different calibration strategies or instrumental parameter optimization.

This study aimed to develop and validate ICP-MS methods for food analysis to determine the elemental compositions or elemental fingerprints [2] of the most important agri-food produced in Sardinia (Italy). The foods of interest are honey [3], PDO pecorino cheese, and rice [4]. The goal was to assess the presence of contaminants, evaluate nutraceutical properties, and verify the potential use of elemental fingerprints in food authentication studies.

Experimental

The overall workflow for the development and validation of each analytical method included the use of design of experiments (DoE) for the optimization of all analytical steps to achieve the best performance in terms of detection limits, accuracy, robustness, and reduction of matrix effects and polyatomic interferences.

Elemental analyses were performed using NexION 300X ICP-MS (Perkin Elmer, Milan, Italy). Samples were prepared by microwave acid digestion using an UltraWAVE SRC (Milestone, Sorisole, Italy).

Food samples (Table 1) were collected in collaboration with the local agencies and producers.

Table 1. *Food samples and factors investigated to assess the use of elemental fingerprint for food authentication.*

Food	Factors investigated
Honey *(n=247)*	Botanic origin *(n=6)* Geographical origin *(n=2)*
Rice (*n*=234)	Genotype *(n=26)* Irrigation technique *(n=3)* Year *(n=3)*
Pecorino cheese (*n*=200)	Producing method *(n=2)* Seasonality *(n=3)* Farmer *(n=16)*

Results were elaborated using chemometric methods: principal component analysis (PCA) for data visualization, and linear discriminant analysis (LDA) for classification.

Results

Initially, analytical methods were developed, optimized, and validated step-by-step. DoE proved to be highly efficient in optimizing microwave-assisted acid digestion, maximizing the amount of digested sample, while reducing the use of oxidizing agents. Excellent yields were achieved in terms of organic matter decomposition in food samples. A library of food digestion methods was developed. Similarly, ICP-MS methods were optimized. Therefore, they were used for food analysis.

Sardinian honeys (varieties: multiflower, thistle, eucalyptus, asphodel, strawberry tree, and rosemary) are characterized by high levels of Fe and Mn, whereas heavy metals are absent and non-detectable. Trace elements allow for the discrimination of honeys based on their botanical origin. LDA demonstrated an accuracy of approximately 80%. Then, the elemental fingerprints of Sardinian honeys were compared to those of Spanish honeys (multiflower, eucalyptus, and rosemary). LDA can accurately discriminate between Sardinian and Spanish honey samples with an accuracy exceeding 90%. However, in this case, the most important markers are the major elements such as Na, K, Mg, and Ca.

ICP-MS analysis highlighted the high nutraceutical qualities of DOP pecorino cheeses. Both types of cheese, Pecorino Romano and Pecorino Sardo, have high contents of Zn (DRI = 30%, portion size 50 g) and Se (DRI = 35%, portion size 50 g). Elemental fingerprints of the products revealed that the concentrations of trace elements were influenced by the production method. The two types of cheese can be discriminated (LDA accuracy 86%) even when the same milk is used to produce them. Seasonality also affects the concentration of elements, particularly the concentrations of V and Se, which are higher in the summer products, while Zn and Cu are higher in the winter products.

Finally, for rice, the effect of intermittent irrigation methods (saturation and sprinkler) was studied in comparison to the traditional method (continuous flooding). One of the most important findings is that sprinkler irrigation can minimize the accumulation of As and Cd in rice grains, even in heavily polluted soils and water. This result is unprecedented because at the same yield, safe rice can be produced while saving water.

Conclusions

This study aimed to develop and validate new analytical methods, with particular attention to the sample preparation phase. These methods were used to study the elemental concentrations and fingerprints of Sardinian food products for valorization and food authenticity. The results highlighted the high quality in terms of nutraceutical elements and safety because of the absence of toxic elements. In addition, from the elemental fingerprints, it is possible to discriminate honeys based on their botanical and geographical origins. Moreover, pecorino cheese elements are influenced by production method and seasonality. Finally, the irrigation method is a key factor for minimizing the accumulation of toxic elements in rice.

References

1. G. Danezis et al.; *TrAC - Trends in Analytical Chemistry*, 85 (2016), pp 123-132.
2. P. Zhang and C.A. Georgiou; *Briefings in Bioinformatics,* 19 (2018), pp 524-536
3. A. Mara et al.; *Molecules*, 27 (2022), pp 2009-2025
4. A. Spanu et al.; *Science of the Total Environment,* 628 (2018), pp 1567-1581

P7

Use of mass spectrometry to characterise the unique polyphenolic profile of PIWI wines

Gavin Duley,[1,2] Adriana Teresa Ceci,[1,2] Edoardo Longo,[1,2] Emanuele Boselli [1,2]

[1] Oenolab, NOI TechPark Alto Adige/Südtirol, Via A. Volta 13B, 39100 Bolzano, Italy
[2] Faculty of Agricultural, Environmental and Food Sciences, Free University of Bozen-Bolzano Piazza Università 5, 39100 Bolzano, Italy

Summary: *LC-MS analysis of wines produced from disease resistant hybrid grape cultivars (DRHGCs) and from* Vitis vinifera *shows that the DRHGC wines (PIWI wines) are distinctive, and are defined not only by compounds such as diglucoside anthocyanins but also by triglucoside anthocyanins.*

Keywords: disease resistant grape cultivars, anthocyanins, polyphenols, wine

Introduction

Disease resistant hybrid grape cultivars (DRHGCs) are increasingly topical, particularly since EU legislation changed to allow their use in DOC wines [1]. DRHGCs allow for the production of healthy, high quality grapes with minimal pesticide usage, and thus effecting positive social and environmental transitions [2]. However, the chemistry of DRHGCs is unique, and this can create challenges for the production of high quality wines (PIWI wines)[1,3].

Methods

Wines produced from both DRHGCs and conventional *Vitis vinifera* cultivars were compared using LC-MS, colorimetry (CIELab color space), oenological multiparametric analysis and sensory characterization. The preliminary results presented here are from wines used for a 'round table' sensory session (used to generate sensory attributes for training and wine description).

Preliminary results

As expected, the anthocyanin content of the red wines were particularly distinctive [4]. DRHGC wines (PIWI wines) contained diglucoside and triglucoside anthocyanins, which were not present in *Vitis vinifera* wines. In addition, anthocyanin rhamnoside derivatives were present. Work on quantification has yet to be undertaken, but the patterns of anthocyanins differs between DRHGCs and *V. vinifera* (Figure 2). Structures of the anthocyanins and fragmentation patterns were hypothesised based on a comparison of retention times and MS/MS with red cabbage extract [5] (Figure 1); other LC-MS peaks that presented the same mass/charge ratio but much higher RT have been observed, and their identification is in progress. These differences were also reflected in the wine colour, with the DRHGCs being darker, more yellow, and more magenta than the *V. vinifera* wines.

Differences in the polyphenol of red wines were also noted, with a PCA providing good separation between DRHGC and *V. vinifera* wines. The separation was not as obvious for white wines. In contrast, preliminary results suggest that the peculiar proanthocyanidin (PAC) patterns observed may be more valuable for white wines than for red wines.

Preliminary sensory analysis of white wines has begun, and reinforces the distinctiveness of DRHGCs shown by LC-MS analysis. Interestingly, sensory analysis has so far shown no preference towards *V. vinifera* wines, in contrast to other studies[6,7].

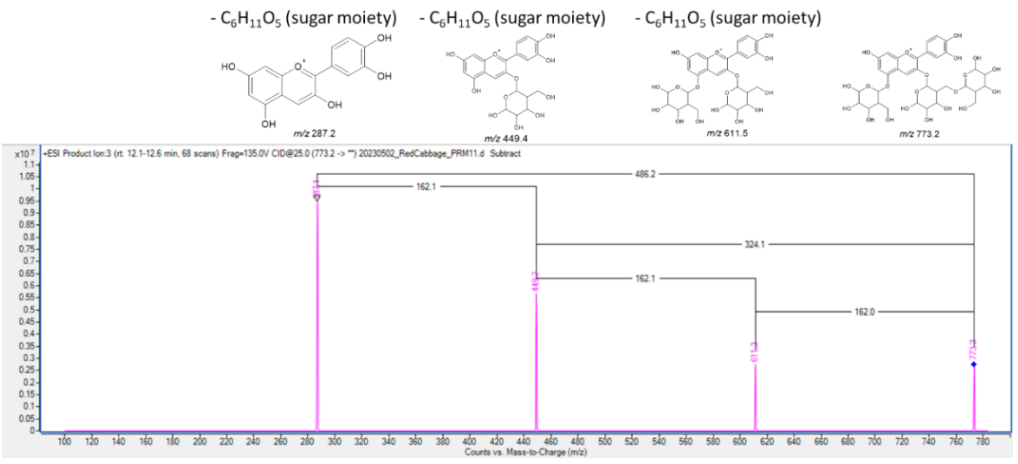

Figure 1. *MS/MS fragmentation of red cabbage cyanidin triglucoside*

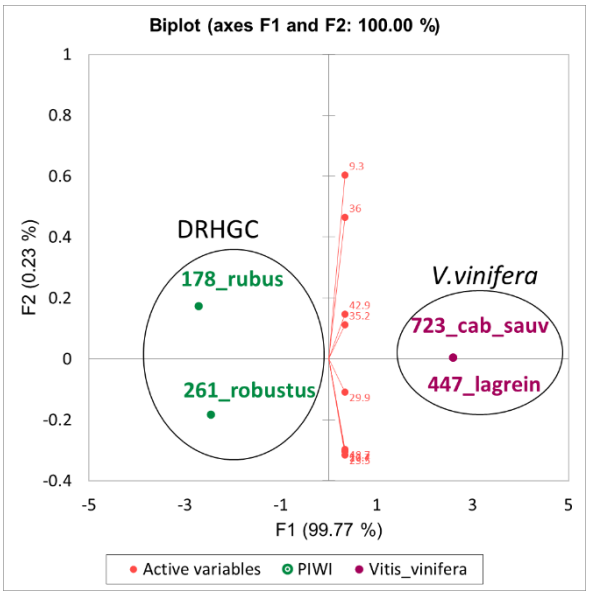

Figure 2. *PCA of round table red wines anthocyanins, showing clear separation between DRHGC wine (Rubus and Robustus, both blends of 'Monarch' and 'Cabernet Cortis') and Vitis vinifera blends ('Lagrein' and 'Cabernet Sauvignon') on PC1.*

Preliminary conclusions and future work

From the preliminary analysis already conducted, it can be seen that PIWI wines are distinctive in terms of their chemical profiles. While our results are still preliminary, they show the distinctive character of PIWI wines from South Tyrol. These results were also reflected by the sensory analysis. Interestingly, no differences in consumer preference between DRHGC and *V. vinifera* wines were noted.

Wineries may efficiently adapt the winemaking practices required for processing PIWI grapes. In addition, educated consumers may be well receptive to the flavours and aromas of PIWI wines, thus supporting the efforts of the EU policy towards the ecological transition.

References

1. G. Duley, A.T. Ceci, E. Longo, E. Boselli; Comprehensive Reviews in Food Science and Food Safety (2023).
2. K. Pedneault, C. Provost; Scientia Horticulturae 208 (2016) pp. 57–77.
3. P-L Teissedre; OENO One 52 (2018) pp. 211–217.
4. M. De Rosso, L. Tonidandel, R. Larcher, et al.; Analytica Chimica Acta 732, 120–129 (2012).
5. Wiczkowski, W, Szawara-Nowak, D & Topolska, J. Red cabbage anthocyanins: Profile, isolation, identification, and antioxidant activity. Food Research International 51, 303–309 (2013).
6. A. Fuentes Espinoza, A. Hubert, Y. Raineau, C. Franc & É. Giraud-Héraud; OENO One 52 (2018).
7. L. Nesselhauf, R. Fleuchaus, L. Theuvsen; International Journal of Wine Business Research 32 (2019) pp. 96–121

P8

Determination of tropane alkaloids in food matrices using LC-UHPLC-MS/MS

Larissa Caminhas, Susanne Rath

University of Campinas (UNICAMP) - Brazil

Summary: *The monitoring of tropane alkaloids cereal-based food has emerged as a significant concern. A novel method for the determination of scopolamine and hyoscyamine in corn and buckwheat samples, using solid-liquid extraction at low temperature and quantification by bidimensional chromatography coupled to tandem mass spectrometry is presented.*

Keywords: *LC-UHPLC-MS/MS; tropane alkaloids; food analysis*

Introduction

In recent years, the monitoring of tropane alkaloids, particularly hyoscyamine and scopolamine, in food has emerged as a significant concern. The rising number of reports regarding food contamination with these compounds globally has heightened awareness of the potential risks associated with their consumption[1,2]. Two main matrices prone to contamination are corn and buckwheat. Both crops are favourable to the growth of tropane alkaloids-rich weeds, such as *Datura Stramonium* and have been reported to contain significant levels of hyoscyamine and scopolamine[3]. The EFSA have created efforts to regulate and monitor tropane alkaloids in food matrices[4]. For unprocessed buckwheat, the maximum acceptable level is 10 µg kg^{-1}.

The present work introduces a novel method for the determination of scopolamine and the sum of (+)-hyoscyamine and (–)-hyoscyamine in buckwheat-based matrices, using solid-liquid extraction at low temperature (SLE-LTP) and quantification by bidimensional chromatography coupled to tandem mass spectrometry (LC- UHPLC-MS/MS).

Experimental

Sample and materials

All grains and coarse flours were milled adding dry ice with a blade grinder (Hamilton Beach). Different corn and buckwheat products (64 samples) were purchased from local stores in Campinas, SP, Brazil, between 2022 and 2023. Standard solutions were prepared using a mix of atropine ((±)hyoscyamine) and scopolamine. Atropine-d_3 and scopolamine-d_3 were used as internal standards.

Sample preparation

The QuEChERS approach and solid-liquid extraction with low temperature partitioning (SLE-LTP) were assessed for the extraction of TAs and clean-up of the sample matrix. Although the results were similar, the latter exhibited a lower matrix effect. The sample preparation procedure involved weighing 1.00 g of the sample and adding 200 µL of a 50 ng mL^{-1} internal standard solution. After the solvent evaporated, 5 mL of water, 15 mL of acetonitrile, and 1 g of $MgSO_4$ were added. The mixture was agitated in a chamber for 30 minutes at 25 °C, allowed to equilibrate for 1 h, and then frozen at -22°C. After a minimum of 6 hours, the liquid fraction was collected, dried, and resuspended in 500 µL of methanol and 4.50 mL of water. The solution was then filtered (0.22 µm) and analyzed.

Instrument setup

The analyses were carried out using an LC- UHPLC-MS/MS system (Waters, USA), which was equipped with an autosampler having a single injection capacity of 250 µL, binary (BSM) and quaternary (QSM) solvent pumps, a column manager, and a triple quadrupole mass detector (Xevo TQD Zspray, Waters). The electrospray ionization source (ESI) was operated in the ion positive mode.

Chromatographic conditions were optimized using an OASIS HLB in the first dimension (^{1}D) and an Acquity BEH C18 in the second one (^{2}D). This arrangement allows to select the fraction of TAs in the 2D column and transfer this fraction to the D column, which provides an additional clean-up of the sample matrix. Different additives in the mobile phase were tested to improve peak symmetry and ionization. Sample injection volume was set to 100 µL. Quantitation transitions (m/z) were: 304 → 156 and 290 → 124 for scopolamine and (±)hyoscyamine, respectively.

The method was fully validated for linear range, linearity, precision, accuracy, matrix effect, LOD and LOQ.

Results

Sample preparation

Different sample preparation procedures were tested and the selected one was SLE-LTP due to its better matrix cleanup.

Analytical Method

The strategy of using two-dimensional chromatography enables selection of the fraction containing the

analytes (TAs) in the ^{1}D column and the transfer of this fraction to the ^{2}D column, where the separation of the analytes occurs. Optima conditions comprised: sample injection volume (100 µL), loading volume (2 mL), loading solvent (water), additives (ammonium carbonate) for both loading and elution steps, stationary phases for both columns.
The optimized method was validated in buckwheat matrix and extrapolated for other flours by evaluating accuracy through recovery test. The results showed that the method is comprehensive and applicable to corn products.

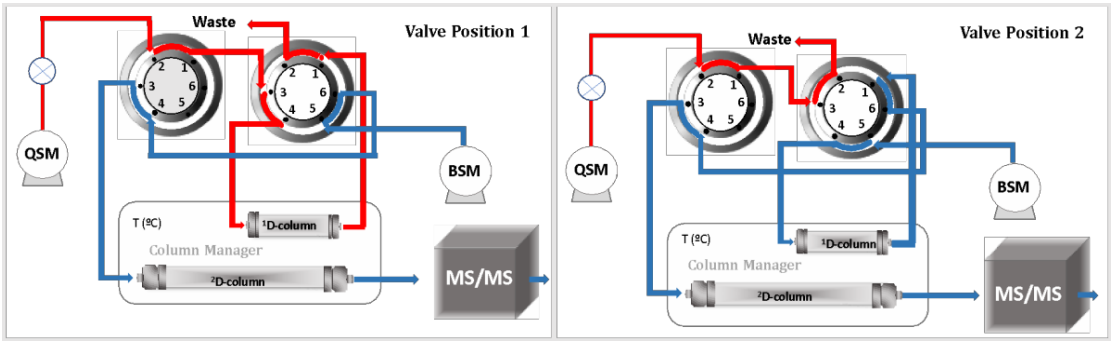

Figure 1. *Diagram of the LC-UPLC-MS/MS system*

Table 1. *Validation parameters of the method using LC-UHPLC-MS/MS for the determination of hyoscyamine and scopolamine in food matrices*

Parameter	Atropine		Scopolamine	
Linear range (matrix-matched calibration curve)	2.5 – 15 µg kg^{-1}		2.5| - 15 µg kg^{-1}	
Linearity (r)	0.9978		0.9974	
Precision, intra-day (RSD), n=5 (%)	2.5 10 15	8.5 2.8 0.8	2.5 10 15	7.4 3.1 1.1
Precision, inter-day (RSD), n=11 (%)	2.5 10 15	5.9 3.8 11.0	2.5 10 15	10.0 4.3 4.9
Accuracy, mean (s), n=5 (%)	97 (7.4) 96 (2.3) 100 (3.3)		103 (7.5) 99 (3.8) 102 (1.6)	
Matrix effect	+27		+11	
LOQ	2.5 µg kg^{-1}		2.5 µg kg^{-1}	
Extraction efficiency (recovery)	90-123 %		80-125%	
Selectivity	No interference observed in blank samples		No interference observed in blank samples	

Sample analysis
Analysis of 64 commercial samples indicated no contamination above legislation limits of 10 µg kg1.

Conclusions
Bidimensional chromatography coupled to tandem mass spectrometry (LC-UHPLC-MS/MS) is a novel method for the determination of TAs, with the advantage of online sample clean-up. Solid-liquid extraction at low temperature (SLE- LTP) is suitable for the efficient extraction of hyoscyamine and scopolamine from cereal-based food. The method was validated and provided LOQ values of 2.5 µg kg^{-1} for atropine and hyoscyamine. Analyses were made of 64 locally purchased samples of buckwheat grain and flour, cornmeal, popcorn, corn flour, and it was observed that all the samples had contamination levels below the established guidelines.
These data provide insights into the likelihood of Tas contamination in food in Brazil and demonstrate the effectiveness of the method developed in this study.

References

1. L. Perharič, K. A. Juvan, and L. Stanovnik, *J. Appl. Toxicol.*, vol. 33, no. 9, pp. 980–990,
2. P. P. J. Mulder *et al.*, “Occurrence of tropane alkaloids in food,” *EFSA Support. Publ.*, vol. 13, no. 12, 2016.
3. F. S. Series, *Joint FAO/WHO Expert Meeting on Tropane Alkaloids*, no. April. FAO, 2020.
4. European Commission (EU), “COMMISSION REGULATION (EU) 2016/239 of 19 February 2016,” *Off. J. Eur. Union*, pp. 19–21, 2016.

P9

Gas chromatography-mass spectrometry method for the quantitative determination of ethylene and diethylene glycols contamination in cough syrups

Monerah A. Altamimy, Yahya M. Alshehri, Norah Altalyan, Shaikah Alzaid

Reference Laboratory for Medicines and Cosmetics, Research and Laboratories sector
Saudi Food and Drug Authority, Riyadh, Saudi Arabia

Summary: *Ethylene glycol (EG) and diethylene glycol (DEG) are contaminants known to cause a variety of health problems to humans. These contaminants can be present in glycerol based drug syrups. We report a gas chromatography-mass spectrometry (GC-MS) Method for the identification and quantification of EG and DEG in cough syrups.*

Keywords: *Glycols, cough syrups, Mass Spectroscopy*

Background

Ethylene glycol (EG) and diethylene glycol (DEG) are contaminants known to cause various human health problems. These contaminants can be found in glycerol or polyethylene glycol (PEG) based drug syrups. Throughout history, there have been mass poisonings due to the consumption of EG and DEG-contaminated pharmaceuticals. The most recent incident occurred by the end of 2022, in which several batches of cough and antihistaminic syrups were reported to have an unacceptable level of EG or DEG in several countries, which resulted in serious injuries and deaths.[1] Several analytical methods were reported for determining EG and DEG in pharmaceutical products. These include high-performance liquid chromatography-tandem mass spectrometry (HPLC-MS/MS), fourier transform infrared (FT-IR) and near-infrared (NIR) spectroscopy for the determination of DEG, thin layer chromatography (TLC), and capillary gas chromatographic method with flame ionization (GC/FID) for the determination of both EG and DEG.[2,3] We propose a selective GC-MS method for quantitatively determining EG and DEG in cough syrups in a single run.

Methods

EG and DEG were analyzed by Shimadzu GC–MS/MS model TQ8050 (Kyoto, Japan), equipped with a PAL AOC 6000 Autosampler operating in electron impact (EI) ionization (70eV). The column was Stabilwax-MS, length: 30 m, thickness: 0.25 µm, and a diameter of 0.25 mm. We used a column oven temperature of 80◦C, injection temperature of 250◦C, injection volume of 1.0 µl, splitless injection mode, and pressurized flow control mode. The pressure was set at 65.2 kpa, the total flow was 4.0mL/min, and the column flow was 1.0 mL/min, and we used a linear velocity of 36.8 cm/s, purge flow of 3.0 mL/min. The oven was programmed to 80◦C for 1 min, then 10◦C/min up to 245◦C, and then held for 3.5 min. The detection mode was single ion monitoring (SIM), and the ions were selected as 31.00, 33.00, and 43.00 for EG, 45.00, 75.00, and 43.00 for DEG, and 31.00, 49.00, and 77.00 for the internal standard (2,2,2-trichloroethanol). Methanol was used as a diluent for standards and samples preparation.

Results

The developed method met the current ICH method validation guidelines. The method's selectivity was proven by the absence of interferences with other peaks in the reference standard solutions and native cough syrup (unspiked). Linearity was examined by assaying EG and DEG standard solutions over the concentration range of 1 – 10 µg/mL. The calibration curves were obtained by plotting the peak response ratio of each standard solution relative to the internal standard (ISTD). The correlation coefficients for the calibration curves were $>$ 0.98 for both EG and DEG. The residuals for the calibration curves were distributed randomly across the calibration range, confirming the absence of bias and the linearity of the results. The limit of detection (LOQ) for both EG and DEG was 400 ng/mL, and the limit of quantitation (LOQ) was 1 µg/mL. The method's accuracy was tested by preparing triplicate samples of cough syrup spiked with three different concentrations of EG and DEG. The average recoveries for each level and the mean calculated from three levels of EG and DEG in each run met the accuracy acceptance criterion (80-120% recovery).

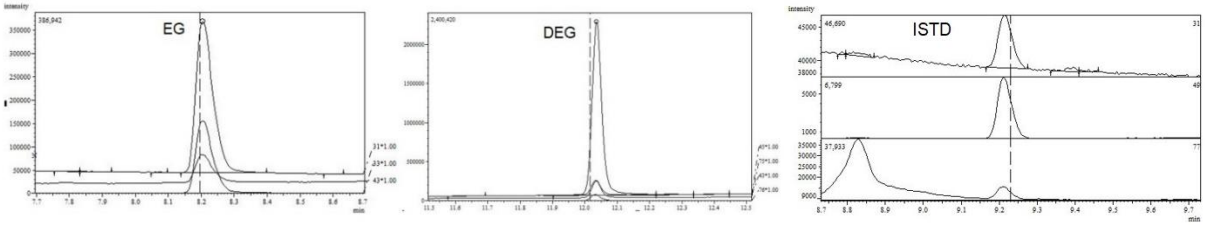

Figure 3. *Glycols standard chromatogram*

Conclusion

A new GC-MS method was developed to determine and quantify EG and DEG in cough syrups. This method is quick, simple, highly selective, provides good separation between EG and DEG, and does not require glycol derivatization or sample cleanup. The method can be applied in analyzing EG and DEG in glycerin as raw material and glycerin-containing cough syrups. Furthermore, the procedure was successfully used to analyze cough syrups collected from the local market.

References

1. Sharma DC. *The Lancet*. 2022;400:1395.
2. Barr DB, Barr JR, Weerasekera G, Wamsley J, Kalb SR, Sjödin A, et al. *Journal of Analytical Toxicology*. 2007;31:295–303.
3. Ahmed MK, McLeod MP, Nézivar J, Giuliani AW. *Journal of Spectroscopy*. 2010;24 : 601–608

P10

MALDI 1 & 2 MS imaging of lipid double-bond positional isomers using off-line ozonolysis

D. Bezdeková,[1] J. Preisler,[1] M. Hendrych,[2] K. Dreisewerd,[3] A. Bednařík [1]

[1] Chemistry Department, Faculty of Natural Sciences, Masaryk University, Czech Republic
[2] First Pathological Department, St. Anne's University Hospital Brno, Czech Republic
[3] Institute of Hygiene and Interdisciplinary Center for Clinical Research (IZKF), University of Münster, Germany

Summary: *This research focuses on the application of off-line ozonolysis in MALDI 1 & 2 imaging of lipid, mainly phosphatidylcholines and phosphoethanolamines', positional double-bond isomers in mouse embryonal and clinical tissue samples.*

Keywords: *lipid double-bond positional isomers, ozonolysis, MALDI 1 & 2 MS imaging*

Introduction

Mass spectrometry mapping of the distribution of glycerophospholipid isoforms, in which the carbon-carbon double bond (db) position resides, is enjoying increasing success. However, classical imaging mass spectrometry with laser desorption and matrix-assisted ionization (MALDI MSI) itself is rather insufficient to reveal the individual differential distribution of isomers in tissues. Therefore, over time, several (not only) derivatization strategies have been developed that allow the position of the C=C double bond to be determined and subsequently contribute to the spatial visualization of particular db isoforms. An important derivatization technique includes an off-line reaction with ozone, which in the past was used to visualize the distribution of phosphatidylcholine (PC) isomers in sections of the mouse brain and human colon tissues.[1] Although the cells are compositionally a mixture of different lipid classes, due to the strong PC ion signal in the MALDI positive mode, classes such as phosphatidylethanolamines (PE) or diacylglycerols (DAG) are significantly suppressed by their presence. As one solution, the combination of MALDI with laser post ionization, referred to as the MALDI 2 technique, was recently introduced, in which a second MALDI- like process appears after the initial ionization step, significantly amplifying the signals of glyco- and phospho-lipids.[2,3]
This work is focused on the application of off-line reaction with ozone, as a technique for lipid db isomers' differentiation, in combination with MALDI 1 & 2 MS imaging. The spatial arrangement of positional isoforms of phosphatidylcholines (PC), phosphoethanolamines (PE), and diacylglycerols (DAG) was visualized in mouse pre- and post- natal tissues and in clinical samples (healthy and cancer human colon tissues).

Experimental

Firstly, 10 µm sections of mouse embryonal and human colon tissues embedded on microscopic slides were desalted three times by repeated 5-s immersion in a cold 50 mM ammonium acetate solution. After careful drying with nitrogen, tissue sections were ozonized during an optimized reaction time of 3 min. Ozone was produced by an off-line O_3 generator, fed with technical oxygen (99.5%), in the amount of approximately 7g/hour, and blown into the reaction vessel, on the bottom of which a glass with a sample was placed. Finally, sections were covered with MALDI matrix 2,5-dihydroxybenzoic acid (0.033 mg/cm^2) by sublimation method (heating temperature 130 °C, time ~15 min) and analyzed by MALDI 1 & 2 MS and MS/MS imaging techniques. All the data were acquired using a modified timsTOF fleX (Bruker)[4] mass spectrometer with a MALDI ion source and two lasers: a primary laser - 355 nm Bruker SmartBeam 3D Laser with the pulse frequency of 1 000 Hz and a post ionization laser – 266 nm NL 204-1k-FH, EKS-PLA Nd:YAG laser, pulse time 7 ns, pulse frequency 1 000 Hz, max. pulse energy ~500 µJ, central distance of the beam from the sample surface ~500 µm, time between pulses of the two lasers 10 µs, beam width ~85 µm. The mass resolution was 40,000 (lipid m/z area) and the deviation from the theoretical mass was ≤2 ppm. In MS/MS experiments, the collision energy was most of the time set to 30, and the width of the selection window was 1 Da. In addition, a constant data collection speed was 33 pixels/s, and the size of a pixel was 50 or 70 µm. MS and MS/MS images were generated using SCiLS Lab software.

Results

First, the potential of the off-line ozonolysis in combination with MALDI 2 MS and MS/MS was tested, using PC, PE standards, and mouse brain homogenates. After the instrument parameter optimization, it was found that comparatively fragile ozonides of PEs and DAGs can survive laser post-ionization and MS/MS fragmentation reveals observable diagnostic ions revealing corresponding lipid double-bond isomers. An example of such an MS/MS spectrum is provided in Figure 1A, where the ozonide of PE 34:1 (m/z 766.53) is fragmented, showing two diagnostic ion pairs (aldehyde and carboxylic acid ion) with the mass difference of

one oxygen (m/z 15.99), corresponding to two isomers – PE 34:1 (Δ9) (m/z 467.37 & 483.37) and PE 34:1 (Δ11) (m/z 495.41 & 511.40). In the second part, the mouse embryonal and clinical tissue sections exposed to ozone were visualized in MALDI 2 MS/MS imaging mode. As an example, the distribution of PE 36:1 isomers in human colon cancer (low-grade adenocarcinoma) tissue is provided in Figure 1B. The green color represents the spatial arrangement of the isomer PE 36:1 (Δ7) and the pink color belongs to the isomer PE 36:1 (Δ9). In comparison with the histological analysis (Figure 1C), the light green area represents the tumor, which corresponds to the areas with increased content of the PE 36:1 (Δ7) isomer (the green part in Figure 1B). The purple region on the left side of Figure 1C was identified as mucosa, the red part as submucosa, the dark blue color represents stroma, light blue color muscle, and the yellow color was identified as immune cells.

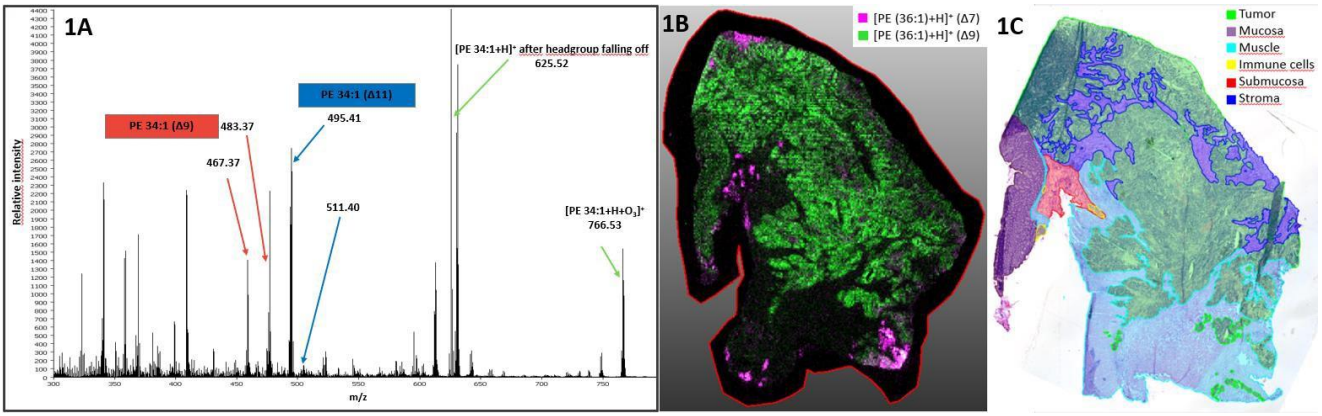

Figure 1. *(1A) The MALDI 2 MS/MS spectrum of the PE 36:1 ozonide (m/z 766.53), showing two diagnostic ion pairs corresponding to two isomers* ***–*** *PE 34:1 (Δ9) and PE 34:1 (Δ11); (1B) The MALDI 2 MS/MS image of the distribution of PE 36:1 (Δ7) (the green color) & PE 36:1 (Δ9) (the pink color) isomers in human colon cancer tissue, (1C) The histological analysis of the human colon cancer tissue*

Conclusions

Analyses showed that the ozonides of PEs and DAGs can survive the MALDI laser post- ionization and subsequently can be fragmented in MS/MS, revealing diagnostic ion pairs specific for positional double-bond isomers of the given lipid. Based on the acquired knowledge and data, the potential of the ozone reaction was proved to be applicable in MALDI 2 MS and MS/MS imaging of the distribution of lipids and their isoforms in tissues. The increased content of certain PC & PE db isomers in certain regions of clinical samples revealed the possible recognition between cancerous and healthy tissue, pointing towards the promising tool for a better understanding of specific functions of lipids in lipid metabolism and the diagnosis of certain diseases.

References

1. *Bednařík, A.* et al.; *Analytical Chemistry* 2020, 92, 9, 6245-6250.
2. *Boskamp, M.* et al.; *Analytical Chemistry .* 2020, 92, 7, 5222-5230.
3. *Soltwisch, J.* et al.; *Science* 2015, 348, 6231, 211-215.
4. *Soltwisch, J.* et al.; *Analytical Chemistry* 2020; 92, 13, 8697-8703.

We gratefully acknowledge the Czech Science Foundation (19-20927Y) and the Project of Specific Research at Masaryk University (MUNI/A/1192/2020 MŠMT) for the financial support.

P11

Investigating the potential of novel polymer-based MALDI matrices for the detection of compounds of low molecular weight by leveraging MALDI-HRMS analytical workflows

E. Aleiferi,[1] M. Tsakanika,[2] D. Damalas,[1] A. Kritikou,[1] G. Sakellariou,[2] N. S. Thomaidis [1]

[1] Laboratory of Analytical Chemistry, Department of Chemistry, National and Kapodistrian University of Athens, Greece, Panepistimiopolis, Zografou, 15771, Athens, Greece
[2] Laboratory of Industrial Chemistry, Department of Chemistry, National and Kapodistrian University of Athens, Greece, Panepistimiopolis, Zografou, 15771, Athens, Greece

Summary: *Small molecule analysis with Matrix Assisted Laser Desorption Ionization Mass Spectrometric (MALDI-MS) techniques is gaining relevance in various fields of research. In this study, the potential of new polymer-based MALDI matrices was investigated for the efficient ionization and detection of small molecules, utilizing high resolution mass spectrometry (MALDI-HRMS) workflows.*

Keywords: *MALDI-HRMS, polymer-based matrices, small molecule analysis*

Introduction

Nowadays omics research (e.g., metabolomics, lipidomics) in the environmental and medical field has skyrocketed. Allowing the direct detection of biomolecules of interest such as metabolites, or/and lipids, the determination of their abundance as well as the elucidation of their localization in tissue samples, imaging can provide with insightful information regarding disease pathways (e.g., carcinogenesis) and lead to new biomarkers of disease discovery. Due to the above-mentioned advantages, imaging techniques, such as Matrix Assisted Laser Desorption Ionization Mass Spectrometry Imaging (MALDI-IMS), have been gaining momentum in clinical and biomedical research[1-5]. Hence, the importance of applying MALDI analysis of small molecules is gaining more and more attention as well by the scientific community.

Nevertheless, analysis of low molecular weight compounds (LMWCs) via MALDI-MS techniques has not been hitherto as extensively exploited as with larger biomolecules or has even been considered for a long time non-feasible [5]. This is mostly due to the fact that the common matrices used in MALDI techniques are typically small organic molecules (SOMs), such as α-Cyano-4-hydroxycinnamic acid (α-CHCA), 2,5-Dihydroxy-benzoic acid (2,5 – DHB), 9-Aminoacridine (9AA), etc, which during the desorption and ionisation processes can produce large background interfering peaks related to the matrix itself (e.g. adduct clusters or fragmentation) at the lower m/z range of small molecule analysis. Their presence can therefore interfere with and hindrance the detection of LMWCs [6-8].

For this reason, various strategies have been developed to overcome the aforementioned problem. Employing polymer matrices which are of higher molecular weight than that of the analytes of interest is such an approach [9]. Even though applications of this strategy are limited, the results of the available studies thus far seem to be promising regarding the applicability of polymers such as poly(3-dodecylthiophene-2,5-diyl) (P3DDT) etc, as matrices for the ionization of small molecules in MALDI-MS and MALDI-IMS applications[7,10].

Experimental

The focal scope of this study was: i) the exploration of the potential of the newly synthesized polymers for efficient ionization and detection of small molecules (e.g., pharmaceuticals, pesticides etc.), and ii) the development and optimization of High-Resolution Mass Spectrometric methods (MALDI-HRMS) and analytical workflows for low molecular weight compounds (LMWCs) with commercially available polymer matrices (e.g., P3DDT).

For this purpose, newly synthesized and characterized polymer-based MALDI matrices were first developed to investigate their potential for efficient ionization of small molecules. The synthesis design of these matrices was performed to demonstrate desired physicochemical properties as MALDI matrices, as well as to ensure effective laser absorption at the wavelength of the MALDI laser.

Secondarily, analytes of low molecular weight (e.g., pharmaceuticals) were spotted with the synthesized matrices on a ground steel MTP 384 plate (Bruker, Germany) and analysed on a timstof flex (Bruker, Germany) instrument in positive or/and negative ionization mode. Different parameters such as sample preparation protocols (e.g., spotting method) and instrumental parameters (e.g., %laser power) were tested aiming at discovering the conditions for which optimal results could be obtained.

Results

From the experiments that were conducted with the commercially available polymers as MALDI matrices, various factors such as sample preparation (e.g., spotting, matrix concentration) and instrumental parameters, were found to significantly affect the obtained results. The conditions for which optimum results

could be obtained were therefore selected, and the newly synthesized polymers were tested as MALDI matrices with these abovementioned optimal parameters. The results on the small molecules' ionization showcase the potential of the polymer-based MALDI matrices application in future LMWC analysis with MALDI-HRMS workflows.

References

1. P. M. Vaysse, R. M. Heeren, T. Porta, B. Balluff; Analyst, 142 (15), (2017), pp. 2690-2712.
2. K. Chughtai, R. M. Heeren; Chemical reviews, 110, (5), (2010), pp. 3237-3277.
3. M. Giampà, M. B. Lissel, T. Patschkowski, J. Fuchser, V. H. Hans, O. Gembruch, H. Bednarza, K. Niehaus; Chemical Communications, 52, (2016), pp. 9801-9804.
4. J. J. van Kampen, P. C. Burgers, R. de Groot, R. A. Gruters, T. M. Luider; Mass spectrometry reviews, 30 (1), (2011), pp. 101-120.
5. C. D. Calvano, A. Monopoli, T. R. Cataldi, F. Palmisano; Analytical and bioanalytical chemistry, 410, (2018), pp. 4015-4038.
6. K. Horatz, M. Giampà, Z. Qiao, S. A. Moestue, F. Lissel;,ACS Applied Polymer Materials, 3 (8), (2021), pp. 4234-4244.
7. K. Horatz, M. Giambà, Y. Karpov, K. Sahre, H. Bednarz, A. Kiriy, B. Voit, K. Niehaus, N. Hadjichristidis, L. D. Michels, F. Lissel; American Chemical Society, 140 (36), (2018), pp. 11416–11423.
8. I. P. Smirnov, X. Zhu, T. Taylor, Y. Huang, P. Ross, I. A. Papayanopoulos, S.A. Martin, D. J. Pappin; Analytical chemistry, 76 (10), (2004), pp. 2958-2965.
9. Z. Qiao, F. Lissel; Chemistry–An Asian Journal, 16 (8), (2021), pp. 868-878.
10. K. Horatz, K. Ditte, T. Prenveille, K. N. Zhang, D. Jehnichen, A. Kiriy, A. Kiriy, B. Voit, F. Lissel; ChemPlusChem, 84 (9), (2019), pp. 1338-1345.

P12

Effective temperature of porous silicon substrates in LDI-MS in function of etching parameters

Clara Whyte Ferreira,[1,2] Bastien Cabrera-Tejera,[1] Wendy Müller,[1] Yannick Coffinier,[3] Romain Tuyaerts,[2] Gilles Scheen,[2] Gauthier Eppe,[1] Edwin De Pauw [1]

[1] Mass Spectrometry Laboratory, MolSysResearch Unit, Chemistry Department,University of Liège, Liège, Belgium
[2] Incize, Ottignies-Louvain-la-Neuve, Belgium
[3] Univ. Lille, CNRS, UMR 8520 - IEMN, Lille, France

Summary: *Substituted benzylpyridinium (BP) compounds are used as thermometer ions to characterize porous silicon (PSi) substrates in terms of their effective temperature in LDI-MS. The PSi substrates are produced by electrochemical etching of boron-doped silicon wafers/or surfaces. Porosification parameters are tuned to obtain different morphological features (i.e. porosity, pore size, porous layer thickness).*

Keywords: *Porous silicon, LDI-MS, thermometer ions*

Introduction

Surface-Assisted Laser Desorption Ionization Mass Spectrometry (SALDI-MS) is an analytical technique that uses inorganic substrates as assisting materials to improve the desorption/ionisation process.
To be efficient assisting material candidates, these inorganic substrates need strong absorption in the laser's wavelength, to allow its efficient absorption of the laser energy; low heat capacity and large surface area per volume unit, both ensuring rapid heating, highly localized, and uniform energy distribution. Several substrates have been proposed for SALDI based on semiconductors, carbon, metals, and composite materials[1]. Among many examples, desorption/ionization on porous silicon (DIOS) is one of the most prominent substrates for SALDI-MS[2].
The exact mechanism behind the desorption/ionization process in these inorganic substrates is not fully understood. However, it is clear that the surface chemical properties and surface morphology are key parameters. In this work, porous silicon (PSi) bearing different morphological features is investigated as an inorganic substrate in LDI-MS.
These substrates can be fabricated by electrochemical etching of silicon substrates in electrolytes containing hydrofluoric acid (HF). The morphology of PSi substrates can be characterized by three parameters: porosity, pore size and layer thickness. Different parameters play a role in pore formation: current density (mA/cm^2), electrolyte composition, etching time, substrate doping.
Generally, mesoporous PSi ($2\ nm < d < 50\ nm$) is obtained from highly doped p-type wafers, where an increasing current density yields higher porosity and pore size (until electropolishing regime is reached when the pore walls become too thin and the pores merge), and thickness increases with etching time[3].
In order to compare the impact of these different morphologies in SALDI-MS, substituted benzylpyridinium (R-BnPy+) ions are used as model analytes [4]. Experimental conditions are fixed and the internal energies are calculated (E_0). The fraction of surviving precursor ions can be obtained from the survival yield (SY)

$$SY = \frac{I_P}{I_P + I_F}$$

where I_P and I_F are the intensities of intact precursor and fragment ions, respectively. Finally, the SY values are plotted as a function of the dissociation energy barrier for each thermometer ions. An internal energy distribution can be obtained from the derivative of the sigmoidal curve. By applying a Maxwell-Boltzmann distribution fit (assuming that the fragmentation proceeds statistically and that the collisions in the source lead to a Maxwell- Boltzmann-like distribution of the internal energy) one can extract the thermodynamic temperature (i.e. effective temperature) for the different PSi morphologies.
Through this data analysis procedure, it is possible to compare the different surfaces in terms of the harshness of the desorption/ionization process.

Experimental

Materials

Boron-doped silicon wafers (<100> crystalline orientation, 10-20 mOhm.cm) were acquired from SIEGERT WAFER GmbH (Aachen, Germany). Octadecyl trimethoxysilane (OTS) was purchased from ABCR (Germany). Aqueous hydrofluoric acid (HF, 49%) was purchased from Chem-Lab, NV (Zeldegem, Belgium), and isopropanol was purchased from VWR Chemicals (Leuven, Belgium).

Porous silicon fabrication

The silicon wafers were first oxidized in a tubular furnace at 1000 °C, under 1.5 L/min O_2, for 3 h to obtain

100 nm thick SiO_2. This oxide was etched in buffered HF solution (7:1 volume ratio of 40% NH_4F in water to 49% HF in water) to eliminate the influence of the sacrificial layer. Porosifications were conducted using a 3:3:4 HF(49%):IPA:H_2O electrolyte. The porosification parameters were tuned to yield porosities around 50% and 80%; and thicknesses of 200 nm and 1 µm. The surfaces were then oxidized at 350 °C for 1h under oxygen.

Porous silicon characterization

The thickness and the porosity of the PSi was characterized through spectroscopic liquid infiltration method (SLIM), using a fibre-coupled Ocean Optics JAZ spectrometer and a 10-mW halogen light source. These parameters were also evaluated using an ellipsometry model (Sentech SE850). Thickness values were confirmed by scanning-electron microscopy (SEM) using a Zeiss Auriga FIB-SEM.

Silanization of surfaces using octadecyltrimethoxysilane (OTS)

To allow thermometer ions deposition on localized spots, the porous silicon surface needs to be surrounded by a hydrophobic area. The surfaces were plunged in 10^{-3} M solution of OTS in a 7:3 hexane: CH_2Cl_2 during 6h at room temperature in sealed glass jars. The surfaces were then rinsed with CH_2Cl_2, isopropyl alcohol and dried by a stream of nitrogen. The application spots were obtained by local degradation of the grafted monolayer with the aid of a patterned quartz mask under UV-ozone.

Benzylpyridinium ions synthesis

The synthesis protocol of the benzylpyridinium ions was performed as described by E De Pauw et al. [5].

LDI-MS analysis

For LDI-MS analysis, a ToF instrument (rapifleX, Bruker Daltonics, Bremen, Germany) was used. Different laser parameters (laser power, shots number, and repetition rate) were tested to find an optimal value to be used for all analyses and thus allowing relative comparison. The instrument was calibrated using red phosphorous freshly suspended in acetone.

Results

Porous silicon characterization yielded 52-56% porosity for the 20 mA/cm^2 samples and 80-89% porosity for the 100 mA/cm^2 samples. Furthermore, the etching rates in terms of layer thickness are 14 nm/s at 20 mA/cm^2 and 55 nm/s at 100 mA/cm^2 in average. Top and cross view SEM images are shown in Figure 1.

The LDI-MS experiments and subsequent data analysis to extract the surface effective temperatures through the thermometer ions SY is currently on going, a schematic representation of this analysis is shown if Figure 2.

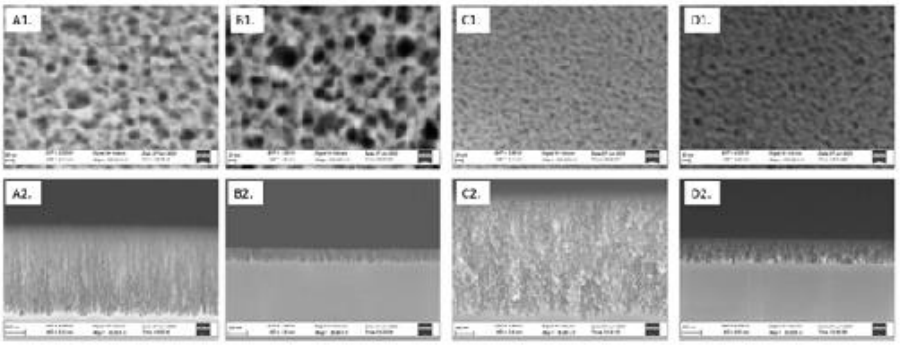

Figure 1 *- SEM images of PSi samples, numbers 1 and 2 correspond to top and cross view respectively. The etching conditions are: A) 100mA/cm^2, 17s; B) 100mA/cm^2, 3s; C) 20mA/cm^2, 85s; D) 20mA/cm^2, 18s*

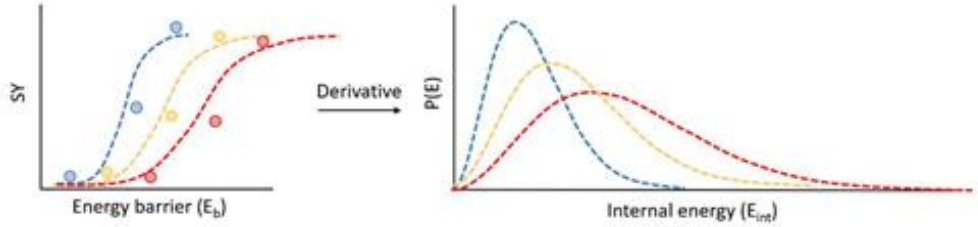

Figure 2. *Schematic representation of the sigmoid fit of SY values as a function of the dissociation energy barrier of the thermometer ions, and the subsequent derivation to obtain Maxwell-Boltzmann-like distributions – ion population P(E) as a function of the internal energy. Each color represents a different porous silicon morphology.*

References

1. W. H. Müller, A. Verdin, C. Malherbe, G. Eppe and E. De Pauw, Mass Spec Rev, 41:373–42 (2022)
2. Q. Zhu, Z. Wang, Y. Wang, F. Teng, J. Du, S. Dou, and N. Lu, J.Phys. Chem. C, 124, 4, 2450–2457 (2020)
3. M. J. Sailor, Porous Silicon in Practice: Preparation, Characterization and Applications, Wiley (2011)
4. C. Collette and E. De Pauw, Rapid Communications In Mass Spectrometry, 12, 165–170 (1998)
5. E. De Pauw, G. Pelzer and P. Natalis, Springer Ser. Phys. 9, 103 (1986)

P13

The quest for the unambiguous identification of ß-naphthol and triarylcarbonium colorants by MeV-SIMS - Procedures for mass calibration & data evaluation

Teodora Raicu,[1] Matea Krmpotić,[2] Zdravko Siketić,[2] Iva Bogdanović-Radović,[2] Dubravka Jembrih-Simbürger [1]

[1] Institute for Natural Sciences and Technology in the Arts (INTK), Academy of Fine Arts Vienna Augasse 2-6, Vienna, A-1090, Austria
[2] Ruđer Bošković Institute, Bijenička cesta 54, Zagreb, HR-10000, Croatia

Summary: *The MeV-SIMS spectra mass calibration and evaluation procedures that were employed in the first attempt to the identification of β-naphthol and triarylcarbonium pigments used in artworks are shown and discussed.*

Keywords: *MeV-SIMS, mass calibration, synthetic organic colorants*

Introduction

This research presents the mass calibration and evaluation procedures of the MeV-SIMS spectra employed in the first attempt to the unambiguous identification of β-naphthol and triarylcarbonium pigments used for artistic purposes. 31 colorants have been examined, which belong to the materials collection of 19th and 20th century of the Institute for Natural Sciences and Technology in the Arts (INTK) at the Academy of Fine Arts Vienna. As these materials serve as references for materials to be identified in modern and contemporary artworks (such as prints, drawings, paints, etc.) exact identification of these synthetic organic colorants is necessary. MeV-SIMS is a soft-ionization accelerator-based mass spectrometry technique that is of particular interest to Cultural Heritage as it requires just a microscopic sample that can be analysed without any chemical preparation or treatment prior to the measurements. Additionally, the sample is still available after the analysis. Moreover, the efficiency of this technique has already been proven in the identification of (protonated) molecular ions and fragment ions of various other synthetic organic pigments even if they were not pure and had been mixed with other colorants and binders in paints [1–3] due to its low-degree of fragmentation. However, since no reference MeV-SIMS spectra were available for β-naphthol and triarylcarbonium pigment classes the mass calibration and evaluation of the data involved a thorough study of the literature on other mass spectrometry techniques that had been applied in the analysis of β-naphthol and triarylcarbonium pigments and on their corresponding dyes/lakes.

Materials and Methods

The measurements were carried out using the MeV-SIMS setup with a linear TOF spectrometer attached to the heavy-ion microbeam beamline at the Ruđer Bosković Institute, which follows the setup used in previous authors' works for SOPs identification [1–3] and presented by Tadić *et.al.* [4]. A pulsed 5 MeV Si^{4+} primary ion beam focused to 10 x 10 μm^2 with currents in the fA range was used for the analysis. The beam was scanned across a 1000 x 1000 μm^2 sample area. Samples were kept at a potential of +5 kV (positive-ion mode) and -4 kV (negative-ion mode). Mass calibration was performed for each spectrum separately using the SPECTOR software[4] since it is known that there are differences in the sample geometry (e.g. uneven surface), which generate variations in the arrival time of the secondary ions[5]. Initially, for the calibration low-mass ions were selected such as H^+, H_2^+, and $C_xH_y^+$ fragments (generally up to an *m/z* value of 220) and finally, higher-mass ions, mostly molecular ions corresponding to the analyzed pigments (in the *m/z* range of 290-480) that could be extracted from the data published on other mass spectrometry techniques such as DTMS [6], MALDI-TOF-MS or MALDI-MS[7,8], LDI-MS or LDI-TOF-MS[9,10], TOF-MS [11], and from the keV-SIMS database "The Static SIMS Library" (version 4) from SurfaceSpectra[12]. However, the ions selected for performing the mass calibration varied for the positive and negative-ion modes, respectively. For the positive-ion mode the molecular ions and sometimes one of the most important fragment ions were selected, which were, thus, organic species. Contrarily, for the negative-ion mode anions characteristic of precipitating agents such as phosphotungstic molybdic acid – PO_3^- (*m/z* 78.9585), MoO_3^- (*m/z* 145.8902), WO_3^- (*m/z* 231.9357) – (in the case of triarylcarbonium pigments) or constituent radicals – $NO_2^{\bullet-}$ (*m/z* 45.9935), $SO_3^{\bullet-}$ (*m/z* 79.9574) – (in the case of β-naphthol pigments) were selected, which were inorganic species. The sole exception was encountered in the case of the β-naphthol pigment lakes (Pigment Red 49 (C.I. 15630) – a sodium salt - and Pigment Red 53:1 (C.I. 15585:1) – a barium salt) that were mostly characterized by inorganic species in the positive-ion mode and, thus, the following ions were employed in the calibration: Na^+ (*m/z* 22.9898), Na_2OH^+ (*m/z* 62.9817), $Na_2SO_3^+$ (*m/z* 125.9364) (for Pigment Red

49), and Ba^+ (*m/z* 137.9052), $BaOH^+$ (*m/z* 154.9080), and $BaCl^+$ (*m/z* 172.8741) (for Pigment Red 53:1). Moreover, in the negative-ion mode of Pigment Red 53:1 the calibration was based on the molecular ion peak that was observed. ChemDraw (version 16.0.1.4) was used to obtain the exact masses of the species. The spectra analysis was performed using mMass - Open Source Mass Spectrometry Tool (version 5.5.0)[13], which allowed a straightforward comparison of the spectra using base peak normalization. The *m/z* values acquired from the other mass spectrometry techniques mentioned before were used for the assignment of the peaks. When no information was found on a particular pigment a potential fragmentation pattern and peak assignment were proposed such as in the case of Pigment Blue 3 (C.I. 42140:1).

Results

The positive-ion mode generally provided the (protonated) molecular ions together with the main fragment ions. In the case of the triarylcarbonium pigments, fragmentation seems to have been principally generated via demethylation and/or deethylation (thus a methyl or an ethyl group was lost and then replaced by a hydrogen atom), which corresponds to the findings in the literature[11]. The ß-naphthol pigment lakes were the sole exceptions in the positive-ion mode as the spectra could only show the adduct ions and the positive secondary ions of their constituent metallic salts. However, in the case of Pigment Red 53:1 the negative-ion mode provided the molecular ion along with the fragment ions. Overall, the negative-ion mode spectra of the other pigments gave additional information on the molecular structure such as constituent radicals in the case of ß-naphthols such as $NO_2^{\bullet-}$ (*m/z* 45.9935) and $SO_3^{\bullet-}$ (*m/z* 79.9574), and components of heteropolyacids in the case of triarylcarbonium pigment lakes such as $W_2O_6^-$ (*m/z* 463.8719), and $Mo_2O_6^-$ (*m/z* 291.7809).

Conclusions

The employed mass calibration and evaluation procedures for the MeV-SIMS spectra both in positive and negative-ion modes led to the exact identification of β-naphthol and triarylcarbonium pigments and lakes in the pigment samples (mixtures). The outcome of these measurements will have a high impact on Heritage Science since many artworks, *e.g.* prints, paints, etc. have been rendered through the use of pigments/lakes from the ß-naphthol and triarylcarbonium classes.

Acknowledgement

The authors gratefully acknowledge the European project “RADIATE” (within Horizon 2020) for funding the MeV-SIMS measurements (proposal no. 22003068-ST-1.1-RADIATE).

References

1. I. Bogdanović Radović, Z. Siketić, Z, D. Jembrih-Simbürger, N. Marković, M. Anghelone, V. Stoytschew, M. Jakšić; *Nucl. Instrum. Methods Phys. Res. Sect. B Beam Interact. Mater. At.,* 406 (2017), pp. 296–301.
2. M. Krmpotić, D. Jembrih-Simbürger, Z. Siketić, N. Marković, M. Anghelone, M., T. Tadić, D. Plavčić, M. Malloy, I.B. Radović; *Anal. Chem.,* 92 (2020), pp. 9287–9294.
3. M. Krmpotić, D. Jembrih-Simbürger, Z. Siketić, M. Anghelone, I. Radovic; *Polym. Degrad. Stab.*, 195 (2021), pp. 109769.
4. T. Tadić, I. Bogdanović Radović, Z. Siketić, D.D. Cosic, N. Skukan, M. Jakšić, J. Matsuo; *Nucl. Instrum. Methods Phys. Res. Sect. B Beam Interact. Mater. At.*, 332 (2014), pp. 234–237.
5. F.M. Green, I.S. Gilmore, M.P. Seah; *J. Am. Soc. Mass Spectrom,* 17 (2006), pp 514–523.
6. T. Learner editor, *Modern Paints Uncovered: Proceedings from the Modern Paints Uncovered Symposium*, Los Angeles (2007).
7. C. Weyermann, D. Kirsch, C. Costa Vera, B. Spengler; *J. Am. Soc. Mass Spectrom.,* 17 (2006), pp. 297–306.
8. Soltzberg, L.J.; Hagar, A.; Kridaratikorn, S.; Mattson, A.; Newman, R. *J. Am. Soc. Mass Spectrom.,* 18 (2007), pp. 2001–2006.
9. Siegel, J.; Allison, J.; Mohr, D.; Dunn, J. *Talanta,* 67 (2005), pp. 425–429.
10. Papson, K.; Stachura, S.; Boralsky, L.; Allison, J. *J. Forensic Sci.,* 53 (2008), pp. 100–106.
11. Costa, K.F.F.; Brand, G.D.; Grobério, T.S.; Braga, J.W.B.; Zacca, J.J. *Microchem. J.,* 147 (2019), pp. 1123–1132.
12. A. Henderson, D. Briggs, J.C. Vickerman; The SurfaceSpectra Static SIMS Library: Version 4, 2006.
13. MMass - Open Source Mass Spectrometry Tool Available online: http://www.mmass.org/ (accessed on 1 August 2023).

P14

Preferred protonation site of aromatic amines: elucidation via IR ion spectroscopy

Laura Finazzi,[1] *Jonathan Martens,*[1] *Giel Berden,*[1] *Jos Oomens* [1,2]

[1] FELIX laboratory, Radboud University Institute for Molecules and Materials Nijmegen, The Netherlands
[2] van 't Hoff Institute for Molecular Sciences University of Amsterdam Amsterdam, The Netherlands

Summary: *Aromatic amines can protonate either on the amino nitrogen or on a carbon atom of the aromatic ring(s). The preferred protonation site may vary and is dependent on different environmental conditions. In this work, we aim to elucidate the preferred protonation sites in aromatic amines, specifically for aminonaphthalene and aminoanthracene.*

Keywords: *IRMPD spectroscopy, DFT calculations, aromatic amines*

Introduction

Aniline and its polycyclic derivatives are a class of compounds that possess basic character resulting from the presence of the lone pair of electrons on the nitrogen atom. Aromatic amines present two kinds of possible protonation sites: the lone pair of the nitrogen atom of the amino group or one of the carbon atoms of the aromatic ring(s). However, the preferred protonation sites in the gas phase may differ from the ones in solution as the solvation energy is typically much larger for the charge-localized amine-protonated tautomer as compared with charge-delocalized ring protonated tautomers. For this reason, the structural elucidation of protonated aniline and substituted anilines has been a topic of extensive theoretical [1] and experimental work[2,3], which led to the conclusion that proton affinities are highly dependent on experimental conditions and level of theory employed. Spectroscopic studies of aromatic amines in the gas phase allows to assign the protonation site of the system, while helping to discern electronic effects from solvation effects.
In our previous experiments, we addressed the protonation site in radical cationic aniline and the final results have been published [4]. The following research question we want to tackle is how the presence of additional aromatic rings influences the favoured protonation site in aromatic amines. The candidates that we propose to study for this project are two possible constitutional isomers of aminonaphthalene and aminoanthracene.

Experimental

In this work, we employ a combination of infrared multiple photon dissociation (IRMPD) spectroscopy and density functional theory (DFT) calculations. IRMPD experiments coupled with quantum chemical calculations allow us to precisely assign the structure of the ion of interest and assess the effect of additional aromatic rings on the protonation site. Furthermore, varying experimental conditions, such as employing different ionization sources (e.g. electrospray ionization and atmospheric pressure chemical ionization), helps to elucidate their influence on the protonation site of these systems.

Results and Future Outlook

Preliminary experiments on 1-aminonaphthalene, 2-aminonaphthalene and 2-aminoanthracene have already been started and the recorded IRMPD spectra at the modified 3D ion trap mass spectrometer (Bruker AmaZon Speed ETD) revealed the presence of multiple isobaric species contributing to the observed bands. Determining which tautomer gives rise to the observed features will be carried out on a Bruker-FTICR mass spectrometer which is equipped with a trapped-ion mobility spectrometry (TIMS) unit, which not only can measure mobilities and collisional cross-sections but also might be used as a filter to record IRMPD spectra of mobility-selected ions. Preliminary TIMS studies revealed the presence of three distinct mobility peaks for all the considered molecules (Figure 1). We aim to repeat these measurement, including 1-aminoanthracene in the experiments, and record mobility selected IRMPD spectra of all the isobaric species.

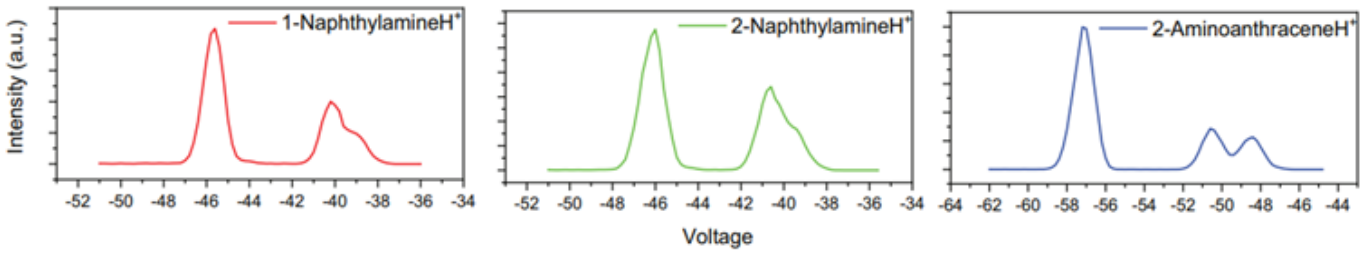

Figure 1. *Ion mobilogram measured for the protonated species.*

References

1. N. Russo, M. Toscano, A. Grand, and T. Mineva, *The Journal of Physical Chemistry A*, vol. 104, no. 17, pp. 4017– 4021, 2000.
2. Z. Karpas, Z. Berant, and R. M. Stimac, *Structural Chemistry*, vol. 1, no. 2-3, pp. 201–204, 1990.
3. R. Flammang, N. Dechamps, L. Pascal, Y. V. Haverbeke, P. Gerbaux, P.-C. Nam, and M. T. Nguyen, *Letters in Organic Chemistry*, vol. 1, no. 1, pp. 23–30, 2004.
4. L. Finazzi, J. Martens, G. Berden, and J. Oomens, *Molecular Physics*, p. e2192307, 2023.

P15

Structural characterization of mobility-selected ions: combining TIMS with IR ion spectroscopy on an FT-ICR MS platform

Lara van Tetering, Kas Houthuijs, Jelle Schuurman, Jonathan Martens, Giel Berden, Jos Oomens

FELIX Laboratory, Institute for Molecules and Materials, Radboud University, Nijmegen, Netherlands

Summary: *The combination of mass spectrometry with trapped ion mobility spectrometry and infrared ion spectroscopy was realized on a new FT-ICR MS platform, enabling the characterization of various saccharide isomers. Mobility separation revealed distinct peaks for isomeric species, and infrared ion spectroscopy combined with calculations aided in assigning their structures.*

Keywords: *trapped ion mobility spectrometry, infrared ion spectroscopy*

Introduction

Mass spectrometry (MS) often faces challenges when it comes to assigning the complete molecular structure of detected compounds. To overcome this bottleneck, MS is frequently combined with techniques like infrared ion spectroscopy (IRIS) to characterize the structure of gas-phase ions. However, IRIS alone cannot provide isomer-selective infrared spectra from a mixture. With trapped ion mobility spectrometry (TIMS) such isomers can be separated based on their mobility, thereby extending the selectivity of MS and IRIS. This combination was realized on a new instrument that includes ion mobility, ultra-high mass resolution and IRIS: a prototype TIMS-enabled FT-ICR MS connected to the beamline of the free-electron laser FELIX.

Methods

A Bruker solariX XR 7T FT-ICR instrument is coupled to the FELIX beamline, where optical laser access is provided to ions within the ICR cell through an IR window located at the instrument's rear. The instrument features an ESI/MALDI dual source, allowing to analyse complex mixtures as well as to perform MALDI imaging. Moreover, the instrument is equipped with a prototype version of trapped ion mobility spectrometry (TIMS) by changing the ion funnel in the source vacuum housing with a modified tunnel. By utilizing this modified funnel as a filter, IR spectra of ions selected based on their mobility can be recorded using both ESI and MALDI techniques.

Results

First results obtained from this set-up include the analysis of several mono-, di- and trisaccharide isomers. The preliminary mobility data of sodiated monosaccharides (see Figure 1) are fascinating, as galactose and glucose exhibit more than one mobility peak. Furthermore, glucose elutes at a different voltage (i.e., mobility) as its isomers. Therefore, to distinguish isomeric species within the same sample, we intend to use the far-IR range (300-1000 cm^{-1}) of FELIX to utilize the mobility filter to separate these isomers within the same sample, as it has been shown that this wavelength range provides well-resolved and diagnostic features for oligosaccharides [1]. In addition, by utilizing the mobility set-up, it is possible to investigate the origin of the three mobility peaks observed for the Na^+ adduct of galactose in greater detail. An aggregate IR spectrum of all conformations can be decomposed into its different contributions using TIMS separation, so that individual conformational structures can be established using infrared ion spectroscopy and DFT calculations. Additionally, it was observed that the trisaccharide maltotriose exhibits two mobility peaks for the Cs^+-adduct (see Figure 2), suggesting the presence of two reducing-end anomers for this ion. By employing TIMS, the combined IR spectrum of the two conformations can be deconvoluted, and their structures can be assigned using quantum-chemical calculations.

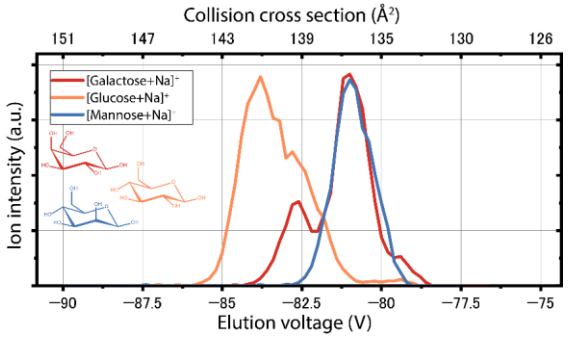

Figure 1. *Mobilogram recorded for sodiated galactose, glucose, and mannose. As glucose elutes before galactose and mannose, this ion can be separated from its isomers in a mixture to record a mobility-selected infrared spectrum.*

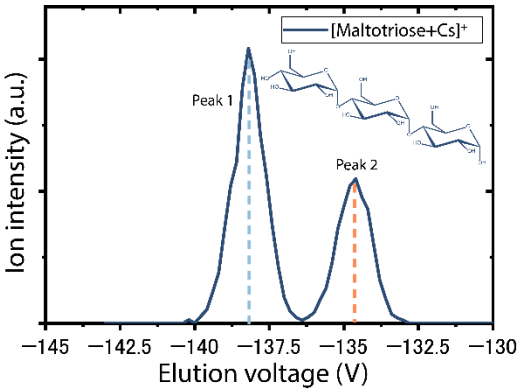

Figure 2. *Mobilogram measured of the trisaccharide maltotriose showing two mobility peaks.*

References

1. R.E. van Outersterp, P.C. Kooijman, J. Merx, et al.; Distinguishing Oligosaccharide Isomers Using Far-Infrared Ion Spectroscopy: Identification of Biomarkers for Inborn Errors of Metabolism, *Analytical Chemistry* (2023)

P16

Mass spectrometry and photochemical study of photoisomerization and thermal back-isomerization of heteroaryl azobenzenes anchored on peptoids for the chemical storage of solar energy

Gwendal Henrard,[1,2] *Thomas Robert,*[1] *Benjamin Tassignon,*[1,2] *Julien De Winter,*[1] *Jérôme Cornil,*[2] *Pascal Gerbaux* [1]

[1] Organic Synthesis and Mass Spectrometry laboratory (S²MOs)
[2] Laboratory for Chemistry of Novel Materials (CMN)
University of Mons, 23 Place du Parc, B-7000 Mons, Belgium

Summary: *Storing renewable energies represents a major challenge in modern science. The most abundant energy source is undoubtedly the Sun. Several storage concepts have already been studied and among them, chemical storage with MOlecular Solar Thermal systems (MOST) appears promising though challenging.*

Keywords: *Solar Energy, Storage, Mass Spectrometry*

Introduction

Molecules that undergo light-induced isomerization to a metastable isomer can be used to store solar energy. Such systems are known as MOlecular Solar Thermal systems. Exposing compound to sunlight generates a high energy photoisomer whose lifetime is considered as a key criterion for storage purpose. When energy is needed, the photoisomer is converted back to the stable compound, releasing the excess energy in the form of heat. Azobenzenes (ABs) with their E → Z photoisomerization are among the most widely studied molecular photo-switches. Properties such as storage enthalpy and half-life time need to be improved. To do so, grafting azobenzenes at selected positions all along a polymer backbone appears to be an elegant strategy to enhance these properties thanks to cooperative effects between the chromophores [1].

Experiment

At UMONS, two strategies to enhance the solar energy absorption, the storage enthalpy and the metastable isomer half-life time of MOST azobenzene-like candidates are considered; (i) the replacement of one phenyl group by a thiazolyl moiety is envisaged to red shift the absorption of the chromophores in the visible region [2], and (ii) the grafting of several azobenzene residues at selected positions all along the polymer backbone. Anchoring AB photoswitches on a peptoid chain is performed using an on-resin step-by-step synthetic procedure allowing to incorporate different side chains at selected positions. Three different residues are incorporated in our photoactive peptoids; i.e. methylamine (*me*), (S)- phenylethylamine (*spe*) and (E)-4-(thiazol-2- yldiazenyl) aniline (*azo*).

Results

Two peptoids have been successfully synthesized, namely N*spe*N*azo*N*spe* and N*me*N*azo*N*me*, and their sequences are confirmed based on MSMS analysis. Both peptoids are subjected to photoillumination experiments. LC-MS experiments are carried out before and after irradiation to separate/identify/quantify the stereoisomers. Before irradiation, only the stable E-isomers are detected for both structures provided the peptoid solutions are protected against ambient light. After UV-vis irradiation, only the Z-isomers of the Nspe containing peptoid are detected, pointing to a fast retro isomerization of the Z-isomers of the methyl-containing peptoid.

Conclusions

With this work combining synthesis and photochemical characterization, we demonstrated that peptoids can be a good template to improve MOST properties of azobenzene. The spe side chains position greatly influence the half life time as opposed to methyl side chain. The stabilizing effect of the phenyl ring of the N*spe* residue within the Z-isomers is currently tested by preparing defined sequence peptoids incorporating the N*azo*, the N*spe* and the N*me* residues at key positions.

References

1. L. Dong, Y. Feng, L. Wang, W. Feng, *Chem. Soc. Rev*. 47 (2018), pp 7339–7368.
2. H. Abdallah Abomelha, *Text. Res. J.* 90 (2020), pp 1396-1403.

P17

21-T FT-ICR MS: chemical and structural characterization of complex peat- burning particulate matter

E. Schneider,[1,2] *C. P. Rüger,*[1,2] *M. L. Chacón-Patiño,*[3] *M. Somero,*[4] *M. Ruppel,*[5] *M. Ihalainen,*[4] *K. Köster,*[4] *O. Sippula,*[4] *H. Czech,*[1,6] *R. Zimmermann* [1,2,6]

[1] Department of Analytical and Technical Chemistry, University of Rostock, Rostock, Germany
[2] Department Life, Light & Matter, University of Rostock, Rostock, Germany
[3] National High Magnetic Field Laboratory, Florida State University, Tallahassee, United States
[4] Department of Environmental and Biological Sciences, University of Eastern Finland, Kuopio, Finland
[5] Atmospheric Composition Unit, Finnish Meteorological Institute, Helsinki, Finland
[6] Joint Mass Spectrometry Centre, Cooperation Group "Comprehensive Molecular Analytics" (CMA) Helmholtz Munich, 81479 Munich, Germany

Summary: *The combination of electrospray ionisation (ESI) and atmospheric pressure photoionisation (APPI) direct-infusion 21 T Fourier Transform Ion Cyclotron Resonance Mass Spectrometry (FT-ICR MS) supported by infrared multiple photon dissociation (IRMPD) fragmentation, enables unprecedented insights into the chemical properties of climate and health relevant peat-burning aerosol.*

Keywords: *FT-ICR MS, biomass burning, aerosol*

Introduction

Biomass burning (BB) emissions are a major contributor to the global budget of particulate matter (PM), affecting air quality, scattering and absorption of radiation as well as cloud formation. Climate change increases the frequency of wildfire events in regions like Europe where, in addition to industrial air pollution, implications of wildfire PM emissions are an important field of research in environmental science. Furthermore, several adverse health effects of BB emissions are known, including induction of diseases via inflammatory and gene-toxic pathways.

Large-scale peat fires can release large amounts of CO_2 as well as organic carbon (OC), especially Brown Carbon (BrC), due to the predominant smouldering conditions in peat fires (low temperature, low oxygen). [1] The higher frequency of extreme drought events resulting from climate change, as well as thawing of permafrost grounds in the Arctic, also increases the frequency and scale of peat fires in the northern hemisphere, where by far the most peat deposits are located. [2]

The application of the highest magnetic field FT- ICR MS system in the world (21 T), and the resulting improvement of resolving power (R > 1,200,000 @ *m/z* 600), mass accuracy and dynamic range for the assignment of elemental compositions based on the exact mass (Smith et al, 2018), revealed an extremely complex mixture of organic compounds. Additional structural information was obtained by infrared multiple photon dissociation (IRMPD) fragmentation.

Experimental

To characterize the OC emitted from peat burning, four peat samples and one Finnish boreal forest duff sample were dried and burned in lab experiments simulating wildfire emissions. Two peat samples originate from peatlands in Finland (Lakkasuo, Siikaneva), only few kilometres apart, while the others originate from the Arctic in northwest Russia (Rogovaya) and Norway (Alkehornet, Spitsbergen). Peat burning emissions of PM were collected on quartz fibre filters and extracted by Methanol/Dichloromethane for consequent characterization of OC by electrospray ionisation (ESI) in positive and negative mode, as well as atmospheric pressure photoionisation (APPI) 21 T FT-ICR MS.

Results

The chemical characterization of peat burning PM revealed an average assigned compound number larger than 30,000, in the range of 180–1400 Da, containing the heteroelements oxygen, nitrogen, sulphur. A high abundance of heavily oxygenated and nitrogen- containing compounds with up to six nitrogen atoms was detected, as well as typical BB markers like levoglucosan (decomposition of cellulose) and a broad range of additional high molecular weight BB markers including e.g., terpenoids from resins (Figure 1).

The smouldering combustion of biomass also leads to the emission of partially oxidized, aromatic and condensed-aromatic structures. These compounds are of reasonable concern regarding human health due to their increase ability to form reactive oxygen species (ROS). [3]

The comparison of peat burning aerosol from several locations revealed distinct differences in the chemical composition, resulting from regional influences of vegetation. Also, more than 10,000 common compounds were identified in all peat samples, which could be described as a base set of peat burning OC, containing mostly CHO and CHNO compounds. Particularly, PM emitted from the combustion of peat from Arctic

locations revealed a set of unique compounds, with increased nitrogen content. Compounds containing e.g., nitro or nitrate functional group as well as aromatic structures may impact the optical properties of the PM due to their increased light-absorption properties. [4]

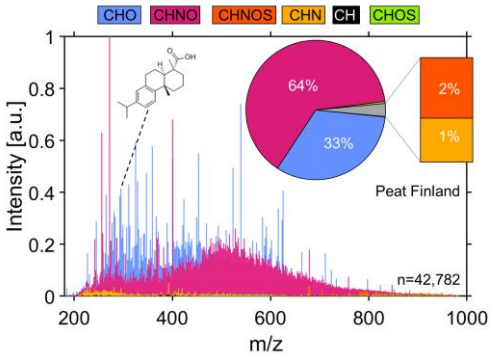

Figure 1. *Mass spectrum (ESI+) of assigned elemental compositions in peat burning aerosol from Finland (Siikaneva) with compound classes indicated by colour and pie chart showing relative number distribution.*

In-cell fragmentation by IRMPD of two quadrupole-isolated mass ranges (2 Da window) at m/z 448 and m/z 560 revealed distinct structural differences of the peat burning organic compounds. While e.g., one Finnish peat sample displayed mainly fragmentation into partially aromatic hydrocarbon ring structures (Figure 2) with only minor abundance of heteroelements, the boreal forest surface samples showed an abundant de-alkylation pattern of CHN and CH compounds, in addition to a similar hydrocarbon ring structure pattern.

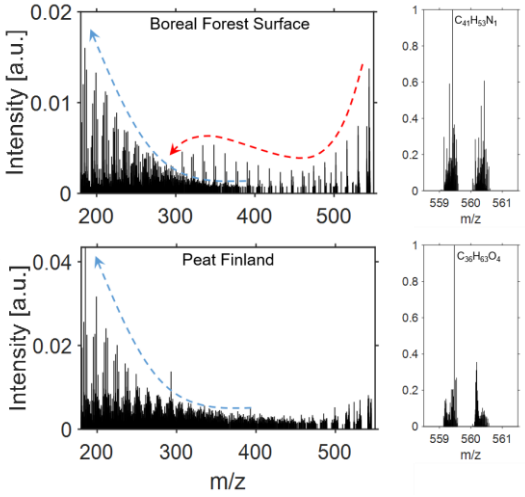

Figure 2. *Mass spectra (APPI+) of assigned fragment and precursor compounds in peat and boreal forest surface burning aerosol from Finland from IRMPD fragmentation of the isolated m/z 560 (2 Da window).*

Conclusion

The application of 21 T FT-ICR MS improves our understanding of the composition of organic aerosol from peat burning. It revealed a highly complex mixture with abundant oxygen, nitrogen and sulphur-containing compounds, highlighting the benefits of the applied instrument and its unique capabilities. Knowledge of molecular properties based on the elemental composition as well as structural information from IRMPD fragmentation is necessary to evaluate the impact peat fires may have on the atmosphere.
The presented results are a starting point for further studies, aiming to understand the effect of regional peat composition on the emission profile, as well as the impact of atmospheric aging during transport of biomass burning plumes.

Acknowledgment

A portion of this work was performed at the National High Magnetic Field Laboratory, which is supported by National Science Foundation Division of Materials Research and Division of Chemistry through DMR-2128556 and the State of Florida.

References

1. Chakrabarty, R. K. et al. (2016) *Atmos. Chem. Phys*. 16 (5), 3033–3040.
2. Langmann, B. et al. (2009) *Atmos. Env*. 43 (1), 107–116.
3. Clergé, A., Le Goff, J., Brotin, E. et al. (2023) *Environ. Mol. Mutagen*. 64 (3), 179-186.
4. Laskin A., Laskin J., Nizkorodov S. A. (2015) *Chem. Rev*. 115 (10), 4335-4382

P18

Contaminants of emerging concern in drinking water: integrated chemical and bioanalytical tools

M. Profita,[1] *P. Valbonesi*,[1] *I. Vasumini*,[2] *E. Fabbri* [1]

[1] Dept. of BiGeA, University of Bologna, Ravenna, Italy
[2] Romagna Acque Società delle Fonti SpA, Ravenna, Italy

Summary: *The work investigated emerging contaminants, focusing on endocrine-disrupting chemicals (EDCs), in drinking water. It assessed EDC occurrence in drinking water from three drinking water treatment plants serving the Romagna area (Italy), evaluated treatment effectiveness, and examined potential health impacts. Integrated chemical analysis and bioassays highlighted water quality and treatment efficiency.*

Keywords: *Endocrine-disrupting chemicals (EDCs), drinking water, chemical and bioanalytical tools*

Introduction

In the last few decades, the water cycle has become afflicted with contaminants of emerging concern, posing a significant threat to the quality of both environmental and drinking waters. Among these contaminants, endocrine-disrupting chemicals (EDCs) have gained growing attention due to their potential to cause severe adverse health effects, even at low concentrations[1]. Recognizing this risk, the recent revision of the EU Drinking Water Directive has, for the first time, included EDCs in drinking water legislation[2]. However, drinking water treatment plants (DWTPs) does not effectively remove most emerging contaminants, making the detection and removal of EDCs in DWTPs a crucial challenge.

The aim of this project was to assess the presence of suspected EDCs (hormones and phenolic compounds), in drinking waters across the Romagna area (Italy) (Figure 1). The main objectives were:

(i) Assessing the occurrence of EDCs in source water and drinking water from three DWTPs,
(ii) Characterizing the effectiveness of various water treatment processes in removing them, and
(iii) Evaluating their potential biological impact.

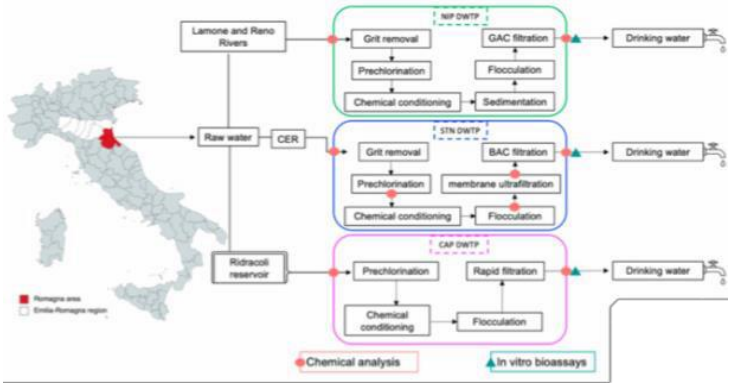

Figure 1. *Schematic representation of treatment processes at the three studied DWTPs (NIP; Standiana, STN; Capaccio, CAP).*

Methods

A complementary approach employing both target chemical analysis and effect-based methods[3] was adopted (Figure 2).

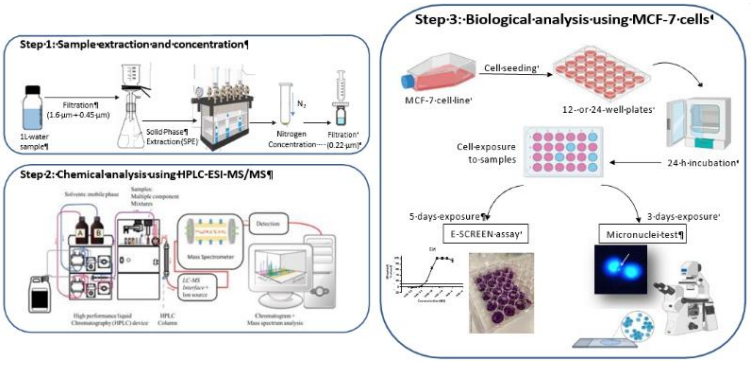

Figure 2. *Analytical approaches used in this work.*

Results

Chemical analysis conducted using HPLC- MS/MS revealed that Nonylphenol (NP) prevailed in all the raw water samples, followed by Bisphenol A (BPA) (Table 1). Although the measured concentrations of EDCs in drinking water did not surpass the threshold guideline values.

Table 1. *Levels of suspected EDCs (ng/L) measured in water samples from three DWTPs.*

BPA (ng/L)	July 2020	Sept. 2020	July 2021	Sept. 2021	July 2022	Sept. 2022
NIP IN	13.36	7.37	3.80	3.55	2.96	13.87
NIP OUT	5.63	6.29	**5.22**	<0.99	<0.99	<0.99
CAP IN	3.35	3.52	<0.99	<0.99	1.67	<0.99
CAP OUT	1.91	3.37	<0.99	<0.99	<0.99	<0.99
STN IN	3.04	4.15	3.71	3.81	1.64	<0.99
STN OUT	**3.48**	2.02	<0.99	<0.99	<0.99	<0.99

NP (ng/L)	July 2020	Sept. 2020	July 2021	Sept. 2021	July 2022	Se
NIP IN	9.01	7.50	8.21	99.93	6.28	5.97
NIP OUT	**11.97**	2.43	**36.73**	4.58	**22.91**	**14.82**
CAP IN	22.27	9.05	12.76	6.13	12.00	42.65
CAP OUT	3.19	2.19	3.31	3.42	**22.75**	11.77
STN IN	18.26	12.72	4.58	83.43	8.73	30.53
STN OUT	8.67	6.83	**12.76**	10.13	4.95	6.04

Notably, an increase in BPA and NP levels was observed during the pre-chlorination, flocculation, and ultrafiltration steps (Table 2).

Table 2. *Levels of suspected EDCs (ng/L) measured in water samples during treatment processes performed by Standiana DWTP.*

Sampling	Standiana	BPA (ng/L)	NP (ng/L)
July 2020	IN	3.04	18.26
	PRECL	1.55	**27.51**
	FLOCC	**3.62**	16.51
	ULTR	**5.35**	14.95
	OUT	3.48	8.67
September 2020	IN	4.15	12.72
	PRECL	2.03	**16,73**
	FLOCC	**4.39**	**22.88**
	ULTR	**5.37**	1.50
	OUT	2.02	**6.83**
July 2021	IN	3.71	4.58
	PRECL	< LOQ	2.60
	FLOCC	< LOQ	**5.68**
	ULTR	**2.48**	**132.61**
	OUT	< LOQ	12.76
September 2021	IN	3.81	83.43
	PRECL	< LOQ	14.13
	FLOCC	< LOQ	7.74
	ULTR	**1.50**	5.31
	OUT	< LOQ	**10.13**
July 2022	IN	1.64	8.73
	PRECL	**1.99**	**53.43**
	FLOCC	**2.05**	14.36
	ULTR	**3.40**	**14.83**
	OUT	< LOQ	4.95
September 2022	IN	< LOQ	30.53
	PRECL	**1.42**	**143.30**
	FLOCC	**1.88**	14.95
	ULTR	< LOQ	12.15
	OUT	< LOQ	6.04

Regarding the biological assessments conducted on finished water, no notable bioactivity was observed,

except for a few treated water samples that exhibited estrogenic responses (Figure 3). However, these effects were well below the available effect-based trigger values and in line with the existing scientific consensus on endocrine effects in drinking water.

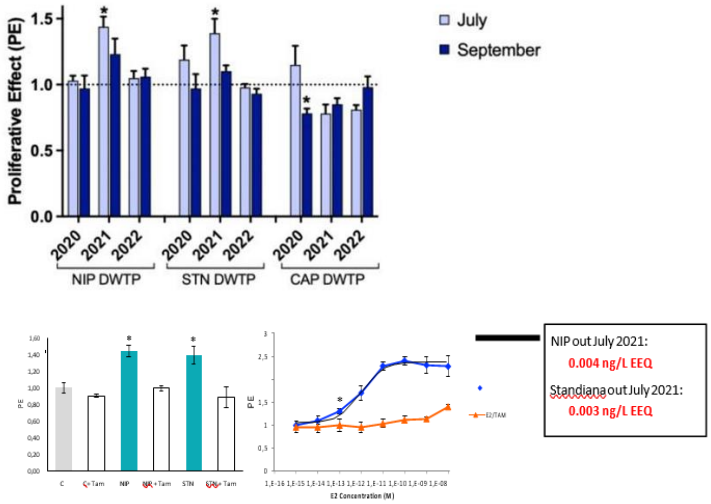

Figure 3. *Estrogenic activity observed after exposure of MCF-7 cells to drinking water samples from three DWTPs.*

Conclusion

Our research has revealed valuable insights into the occurrence, treatment efficiency, and potential health impacts of suspected EDCs in drinking water. By implementing comprehensive monitoring strategies4 and employing advanced treatment technologies, we can enhance the efficiency of DWTPs and safeguard the quality of our drinking water. Overall, our data emphasize the high quality of the produced drinking water and highlight the value of integrating chemical analysis and in vitro bioassays for robust water quality assessment.

References

1. Profita M., Fabbri E., Spisni E., Valbonesi P. Biology of Reproduction, 2021, 105, 1355–136.
2. Directive 2020/2184/EU on the quality of water intended for human consumption.
3. Valbonesi P., Profita M., Vasumini I., Fabbri E. Science of Total Environment, 2021, 758, 143624.
4. Escher B., Neale P., Leusch F. IWA Publishing, 2021.

P19

Detection of pesticides using Multi-Scheme Chemical Ionization (MION) Inlet and Orbitrap mass spectrometer with a filter desorbing unit

Fariba Partovi,[1,2] Joona Mikkilä,[1] Jyri Mikkilä,[1] Tuija Jokinen,[4] Aleksei Shcherbinin,[1] Matti Rissanen [2,3]

[1] Karsa Ltd., A. I. Virtasen aukio 1, 00560 Helsinki, Finland
[2] Aerosol Physics Laboratory, Physics Unit, Faculty of Engineering and Natural Sciences, Tampere University, 33720 Tampere, Finland
[3] Department of Chemistry, University of Helsinki, 00014 Helsinki, Finland
[4] Climate and Atmosphere Research Center (CARE-C), The Cyprus Institute, 2121 Nicosia, Cyprus

Summary: *In this study, the effectiveness of the MION-Orbitrap setup in rapidly identifying diverse pesticides with distinct functional groups in air samples was demonstrated. Assessment using standard mixtures successfully detected over 500 pesticides. This technique exhibits potential as a valuable tool for pre-screening of pesticides in real extract and fruit samples.*

Keywords: *MION-Orbitrap, Pesticides, Air samples, Rapid identification, Pre-screening*

Introduction

In this study, we focused on analyzing air samples to detect various pesticides with different functional groups. Our method uses a Multi-Scheme Chemical Ionization (MION) (Rissanen *et al.*, 2019)inlet with a filter desorbing unit (Karsa Ltd.) connected to a high-resolution orbitrap mass spectrometer.

Materials and method

The MION-Orbitrap setup enables rapid and specific detection of pesticides by altering between reagent ions of different polarities. Air samples were obtained by drawing in 60 liters per minute of air through a filter situated in a filter holder that was connected to a pump. The filters containing the air samples were then placed in the filter desorption unit and subjected to a temperature ramping process ranging from 30°C to 250°C. The total measurement time for each filter was 3 minutes.
To validate our method, we tested standard mixtures purchased from LGC standards and extract juice mixtures from Finnish customs, comparing the results to samples collected directly on the filter. Each measurement took about 5 minutes, and we were able to inject the next sample quickly, facilitating high throughput.

Results

By using different reagents in different modes, we detected more than 500 pesticides, including some of the most widely used ones. Additionally, we investigated the matrix effect by mixing two different pesticide standard solutions and found that the presence of other targets did not affect the chemical ionization of individual pesticides at this concentration level. We also tested actual extract and fruit samples and detected the presence of pesticides, demonstrating the potential of our method as a fast-pre-screening technique.

Conclusion

In conclusion, our study shows that the MION-Orbitrap setup is a fast and specific method for detecting various pesticides with different functional groups in air samples. The method was validated using standard mixtures and extract juice mixtures, and more than 500 pesticides were detected. The technique also showed promise as a fast-pre-screening tool for detecting pesticides in actual extract and fruit samples.

References

Rissanen, M.P. *et al.* (2019) 'Multi-scheme chemical ionization inlet (MION) for fast switching of reagent ion chemistry in atmospheric pressure chemical ionization mass spectrometry (CIMS) applications', *Atmospheric Measurement Techniques*, 12(12), pp. 6635–6646. Available at: https://doi.org/10.5194/amt-12-6635-2019.

P20

Structural characterisation of glyphosate and AMPA metal complexes using ion mobility-mass spectrometry

O. Rusli, O. H. Lloyd Williams, N. J. Rijs

School of Chemistry, UNSW Sydney, Australia

Summary: *Glyphosate is a herbicide heavily used globally. AMPA is Glyphosate's main metabolite. Both Glyphosate and AMPA are very good chelating agents and could form various metal complexes, but the structures are not well understood. This project aims to use to IM-MS to characterise the metal complexes of Glyphosate and AMPA.*

Keywords: *Herbicide, Roundup, IMS-MS*

Introduction

N-(phosphonomethyl)glycine or Glyphosate is the most used herbicide globally. First developed in the 1970s, it quickly gained popularity due to its extreme efficacy and its non-selective trait in exterminating weeds. Recent studies have also linked Glyphosate and its primary metabolite, aminomethylphosphonic acid (AMPA), to multiple adverse health effects from metalloenzyme inhibiting activities to non-Hodgkin's lymphoma.[1,2] Both Glyphosate and AMPA are zwitterionic and have multiple reactive functional; groups that can readily participate in coordination bonding, and polymerisation, allowing them to easily form various complexes with divalent metal cations, including multiply charged species.[3,4] The metal complexes formed possess extraordinarily rich structural variability. Structural characterisation of these complexes is highly desirable as that would provide better mechanistic understanding of their behaviour, characteristics, interactions, and biological and environmental fate. Ion mobility is an analytical technique where ions are separated based on their interaction with an inert drift gas under the influence of an electric field. In addition to the separation, ion mobility also allows users to access an additional analytical dimension which is ions' collisional cross sections. In tandem with mass spectrometry, the technique is fit for this purpose as it can separate isomers that are cannot be resolved over mass spectrometry alone, making it the perfect technique for structural characteristion.

Experimental

The sample solutions were made by mixing Glyphosate or AMPA crystals with metal salts dissolved in 1:1 H_2O/MeOH. Here, target $[Glyphosate+M-H]^+$ and $[AMPA+M-H]^+$ complexes where M = Mg^{2+}, Ca^{2+}, Sr^{2+}, Ba^{2+}, Mn^{2+}, Co^{2+}, Cu^{2+}, and Zn^{2+} were structurally characterised using .multiple IMS-MS techniques including drift tube (DTIMS), trapped (TIMS) and travelling wave (TWIMS) to robustly characterise the Glyphosate and AMPA metal complexes under different instrumental conditions. Density functional theory (DFT) structures were generated to computationally predict potential collisional cross sections. These theoretical values were compared to the experimentally obtained values to gain further structural insight.

Conclusions

Experimental results have confirmed that both Glyphosate and AMPA form various metal complexes with divalent metal ions. Some of the structures of these metal complexes have been successfully characterised by using IMS-MS, however there are still many structures that haven't been characterised. More research would need to be conducted to fully understand the characteristics of Glyphosate and AMPA metal complexes.

References

1. Chang, V. C. et al. *JNCI: Journal of the National Cancer Institute* **2023**, djac242. https://doi.org/10.1093/jnci/djac242.
2. Giannousis, P. P.; Bartlett, P. A. *J. Med. Chem.* **1987**, *30* (9), 1603–1609. https://doi.org/10.1021/jm00392a014.
3. Gimsing, A. L.; dos Santos, A. M. *Biogeochemistry of Chelating Agents*; ACS Symposium Series; American Chemical Society, 2005; Vol. 910, pp 263–277. https://doi.org/10.1021/bk-2005-0910.ch016.
4. Freuze, I.; Jadas-Hecart, A.; Royer, A.; Communal, P.-Y. *Journal of Chromatography A* **2007**, *1175* (2), 197–206. https://doi.org/10.1016/j.chroma.2007.10.092.

P21

Unveiling the chemical universe of PFAS in biota using a combined targeted and untargeted workflow, utilizing LC – VIP HESI(-) – tims – QToF MS

Georgios Gkotsis,[1] Dimitrios E. Damalas,[1] Carsten Baessmann,[2] Bob Galvin,[2] Nikolaos S. Thomaidis [1]

[1]Nationaland Kapodistrian University of Athens, Department of Chemistry, Panepistimiopolis, 157 84 Athens, Greece
[2] Bruker Daltonik GmbH, Bremen, Fahrenheitstraße 4, 28359 Bremen, Germany

Summary: *The aim of the present study was the establishment of an efficient workflow for the comprehensive monitoring of PFAS in complex environmental matrices, such as biota. More broadly, the present study aimed to demonstrate the overall analytical performance of RPLC-VIP HESI(-)-TIMS-QTOF MS in environmental applications.*

Keywords: *per- and polyfluoroalkyl substances (PFAS), ion mobility spectrometry (IMS), high resolution mass spectrometry (HRMS)*

Introduction

Per- and Polyfluoroalkyl Substances (PFAS), also known as “forever chemicals”, due to their persistent, bioaccumulative and toxic (PBT) properties, and their ubiquitous presence in the environment and organisms, are in the spotlight of environmental studies. Currently, around 5,000 PFAS are marketed worldwide, making the systematic monitoring of PFAS in the environment a challenging task. The integration of trapped ion mobility spectrometry (TIMS) to LC-HRMS workflows, allows a more comprehensive monitoring of organic micropollutants (PFAS, pharmaceuticals, pesticides, etc.) in complex environmental matrices, such as biota, through targeted and untargeted workflows. Here we present an LC-TIMS-HRMS based workflow, combining CCS-aware target analysis with wide-scope suspect and non- target screening, as a complete solution for PFAS characterization in environmental samples.

Experimental

Extracted suitable for untargeted screening were generated through a generic sample preparation protocol developed for the simultaneous extraction of 56 PFAS from different sub-groups. The analysis was conducted using RPLC-VIP HESI(-)-TIMS- QTOF MS. Data independent (bbCID) acquisition and PASEF, an efficient data- dependent mode, were used for targeted and untargeted workflow, respectively. The 4D target analysis was performed using a target list of 56 PFAS. In the untargeted data processing workflow, after the transformation of the raw data into a comprehensive feature table, the detected features were prioritized using Kendrick mass analysis and further annotated using a PFAS suspect list with approximately 5,000 compounds. In-silico prediction of MS/MS spectra and CCS values for the suspected compounds was performed to facilitate their identification.

Results

Due to PFAS structure, there is a high probability of generating PFAS isomers, making their separation and structure elucidation even more demanding. Therefore, through target analysis, TIMS capabilities to separate coeluting isobaric and isomeric analytes were evaluated. The results indicate higher sensitivity and, thus, lower detection limits of the targeted PFAS and full-scan MS and bbCID MS/MS spectra of significantly higher quality, due to mobility filtrating. Finally, the use of collisional cross sections (CCS), as additional identification criterion, enhanced the identification confidence.

A feature table containing thousands of features was created by the untargeted workflow. Kendrick mass defect filtered out of the matrix several features as potential PFAS, based on the high fluorine content (repeating CF2 unit) of PFAS. Wide-scope suspect screening (5,000 suspect PFAS) using in-silico MS/MS and CCS value prediction was evaluated as a comprehensive approach for a fast and efficient identification of PFAS.

Examples highlighting the prioritization and annotation of suspected features as PFAS- related compounds were revealed. The combination of advanced tools and manual spectral interpretation to assist structure elucidation was demonstrated through the identification of completely unknown features as potential PFAS. The extensive MS2 coverage provided by PASEF facilitated the identification process.

Conclusions

The proposed workflow provides a comprehensive solution for PFAS characterization, combining LC-TIMS-HRMS with target, suspect and non-target screening. Therefore, it will assist understanding the chemical universe of PFAS in the environment and protecting environment, wildlife, and human health in a One Health approach.

P22

Analysis of transformation products of an emerging contaminant by HPLC-MS^n

Federico M. Ivanic, Roberto J. Candal, Matias Butler

Instituto de Investigación e Ingeniería Ambiental (IIIA-UNSAM-CONICET), EHyS
Universidad Nacional de San Martin, Buenos Aires, Argentina

Summary: *Transformation products of the emerging contaminant oxytetracycline were detected and their structures elucidated using tandem mass spectrometry, from the simulated environmental degradation in water and sediment under aerobic and anaerobic conditions.*

Keywords: *Tandem Mass Spectrometry, Degradation Products, Emerging Pollutant*

Introduction

Oxytetracycline (OTC) is a broad-spectrum antibiotic that, due to its intensive use in livestock, is regarded as emerging contaminant (EC). As other ECs, OTC may degrade in the environment, generating transformation products (TPs), which could potentially be more harmful and/or persistent than their parent compound. The degradation trend of OTC was studied by coupling laboratory experiments simulating aerobic and anaerobic environmental conditions with HPLC-MS. Particularly, the chemical structure of multiple TPs of low abundance were elucidated through tandem mass spectrometry (MS^n).

Experimental

Aerobic and anaerobic OTC degradation experiments (AX and ANX, respectively) were carried out in water/sediment reactors, based on existing guidelines[1,2], at pH 5.5, under biotic and abiotic conditions, during 45 days. High OTC concentrations were employed to facilitate TPs characterization. Aqueous and sediment samples were taken periodically and, after conditioning and applying a desorption method [3], were analysed using HPLC-MS^n (Figure 1).

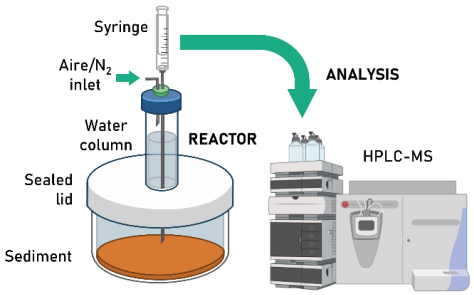

Figure 4. *Workflow showing coupling of degradation experiments in reactors with HPLC-MS.*

Multiple tandem mass spectra were acquired using a linear ion trap mass spectrometer (Thermo LTQ XL) equipped with an electrospray source in positive-ion mode. Search of transformation products was accomplished by an untargeted screening approach, using MatLab software to filter potential candidates. Fragmentation patterns were analysed to propose chemical structures for the more abundant or environmentally relevant TPs.

Results

Biotic degradation of OTC in solution proved to be faster in both AX and ANX than under abiotic conditions, rendering also a higher number and diversity of TPs, specially at short times (Figure 2).

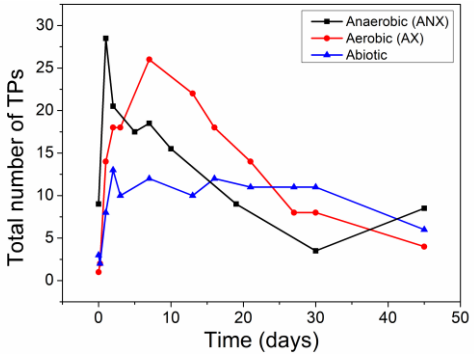

Figure 2. *Evolution in time of number of TPs in water for the three studied conditions.*

No significant differences in OTC degradation kinetics were observed between AX and AXN in water, both achieving non detectable concentrations by the end of the experiment. Nonetheless, OTC was observed to be more persistent in sediment, being able to detect a remanent percentage of 3.5%, 2.9% and 8.8% for aerobic, anaerobic and abiotic experiments, respectively. Likewise, most detected TPs showed a higher persistence in sediment than in water.
Untargeted screening revealed a higher number of detected TPs for ANX than AX, 56 and 44 respectively. A total of 20 TPs were structurally characterized after analysis of multiple fragmentation experiments. Focus was brought into TPs showing environmental relevance, that is, being persistent after long periods of time, when OTC was no longer detected. Proposed structures for some of the detected TPs are shown in Figure 3. No correlation between structural changes and persistence was found but, interestingly, OTC may go through different types of reactions when degraded, such as alcohol oxidation, demethylation, hydrolysis, etc.

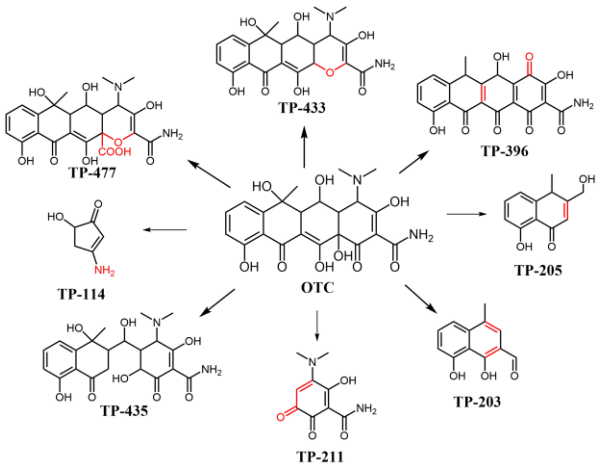

Figure 3. *Chemical structure of OTC and some of the detected TPs in both AX and ANX.*

Although most of the TPs were detected in both ANX and AX, time evolution in water and sediment mostly differs between conditions, affecting their final persistence. Some differences between conditions can be noted, e.g. ANX showing a higher percentage of smaller m/z ions and AX presenting predominantly TPs coming from oxidation processes. These results show that OTC degradation and its fate in the environment depend on the studied conditions.

Conclusions

Batch simulated degradation experiments have proven to be a powerful tool when combined with HPLC-MS^n to examine the fate of emerging contaminants such as OTC in water/sediment systems under different conditions. Employing this methodology, 20 TPs were characterized and their persistence was studied. Although OTC is fully degraded in water, TPs can still be found in both water and sediment, which must be taking into consideration when developing monitoring and remediation strategies.

References

1. Baginska E., Kümmerer K., *Biodegradation screening of chemicals in an artificial matrix simulating the water-sediment interface*. Chemosphere, 119, 1240-1246 (2015).2
2. Organization for Economic Co-operation and Development (OECD), *Aerobic and Anaerobic Transformation in Aquatic Sediment Systems*. OECD guidelines for Testing of Chemicals 308 (2002).
3. Cheng D., Hao Ngo H., Guo W., Chang S.W., Nguyen D. D., Liu Y., Wei Q., Wei D., *Simultaneous Determination of 32 Antibiotics and 12 Pesticides in Sediment Using Ultrasonic-assisted Extraction and High Performance Liquid Chromatography-tandem Mass Spectrometry*. Journal of Hazardous Materials 387, 121682 (2015).

P23

The assessment of sample preparation conditions for the analysis of per and polyfluorinated alkyl substances (PFASs)

Omotola Folorunsho

Centre for Agroecology Water and Resilience (CAWR), Coventry University
Wolston Lane, Ryton on Dunsmore, CV8 3LG, UK

Per and poly-fluoroalkyl substances (PFASs) are compounds whose persistent nature in the environment and potential toxicity have led to their recognition as new and emerging pollutants(NEPs) and persistent organic pollutants (POPs). The detection and quantitation of these compounds remain an analytical challenge due to their diverse properties and occurrence at low concentrations in the environment which also calls for necessary preparatory steps before analysis. These steps, such as sample collection, storage and preparation, usually involve the use of labware materials, e.g. glass and plastic, whose interaction with PFASs can potentially lead to their losses and ultimately cause errors when reporting results. For this reason, guidelines such as the United States Environmental Protection Agency (EPA) 533 suggest the use of labware materials made of polypropylene during measurement. However, recent studies on the show the adsorption of PFASs in polypropylene. In this study, we evaluated the losses of a suite of 18 PFASs, consisting of short, and long-chain PFASs to different materials, including polypropylene (PP), polystyrene (PS), polypropylene co-polymer (PP-CO), polyethene terephthalate (PET), polytetrafluoroethylene (PTFE) and glass (GL). We also examined the influence of storage and preparation conditions, including storage time, solvent composition and temperature, on PFASs adsorption. Our results which will be presented in the poster highlights the importance of choosing suitable laboratory materials and conditions for the assessments of PFASs at trace levels.

P24

Evaluation for the performance of Energized Dispersive Guided Extraction system for high-throughput lipidomics studies in marine environmental matrices

Yunhai Li,[1] *Sara Finnerty,*[1] *Brian Kelleher,*[2] *Shane O'Reilly* [1]

[1] Atlantic Technological University, Sligo, Ireland
[2] Dublin City University, Dublin, Ireland

Summary: *Our research interest is the bioprospecting of novel marine terpenoids across selected underexplored organisms and niches in Irish waters. There is a large number of samples that need to be extracted preliminarily which leads to the significance of a high-throughput method. Here, we will establish a method by an automated extraction system compared to traditional approaches.*

Keywords: *Lipidomics, Marine, Biofilm, High-throughput extraction*

Introduction: The discovery of drugs and other products from natural compounds requires extraction of often large masses of material. The lack of robust, high-throughput extraction technologies hinders natural product discovery as part of the ProspecTER projects, bio-guided fractionation workflows are being designed for discovery of high-potential terpenoids and related lipid compounds. Here, we tested the performance of an Energized Dispersive Guided Extraction system (EDGE, CEM Corp.) for the recovery of crude lipid yields and specific lipid classes from marine environmental matrices. The EDGE system was compared to established extraction methodologies, namely the modified Bligh & Dyer method and ultrasonication-assisted extraction.

Methods: To facilitate comparison of different methods, 10.00 g freeze dried microphytobenthic biofilm, sampled from Ballysadare Bay, Sligo Ireland were weighed and spiked with known quantities of the following internal standards: nonadecanoic acid and cholestane. For the EDGE method we tested 2:1 (v:v) methanol: dichloromethane, and the following parameters: 20 mL top volume, 10 mL bottom volume, 35 °C, a 2-min hold time, and three wash cycles. For Modified Bligh & Dyer and ultrasonication, we refer to the literature that reported[1,2]. In brief, we weighed 10.00 g of the same sample and added 2:1:0.8 (v:v:v) of methanol: dichloromethane: phosphate buffer and sonicated for 10 min at 37°C. After adjusting to a final ratio of 1:1:0.9 (v:v:v), we collected the lower organic phase. The crude lipid yield was determined gravimetrically. The recovery of internal standards and the distributions of analytes from several lipid classes (e.g., sterols, fatty acids, triterpenoids, alkanes) were determined following identification and quantification by gas chromatography mass spectrometry. The relative abundance of intact complex lipids was also determined using thin layer chromatography.

Preliminary data and findings: The EDGE protocol tested significantly reduces time per extraction compared to other methods. Additionally, it is estimated that significant cost savings would be realized in the long term through reduced solvent consumption and solvent waste per sample. Initial findings, together with a review of the literature, indicate that the EDGE system also produces comparable results in terms of crude lipid yield and a representative distribution of key lipid classes. The robustness and reproducibility of a broad range of lipids for untargetted and targetted lipidomic profiling needed in modern natural products chemistry will be evaluation and discussed in detail.

References

1. Balser T.C. Phospholipid Fatty-acid Analysis (PLFA). [cited 2023 May 18]
2. Silvia R. S and Walter V., *Phytochemical Analysis*, 11 (2000), pp 69-73.

P25

Lipidomic profiling intertidal mudflat microphytobenthic biofilms

Sara Finnerty,[1] Yunhai Li,[1] Brian Kelleher,[2] Shane O'Reilly [1]

[1] Atlantic Technological University, Sligo, Ireland
[2] Dublin City University, Dublin, Ireland

Summary: *The marine world offers a diverse range of resources, potentially valuable for human health. Marine natural product discovery holds great potential, but faces many challenges. The ProspecTER project will explore marine organisms for novel bioactive terpenoids. In this preliminary research, biofilms from Irish coastal intertidal mudflats are sampled and characterised.*

Keywords: *marine, terpenoid, biofilm*

Introduction

The marine environment holds great potential for natural product discovery. Several marine natural products, such as Adcetris® (brentuximab vedotin) and Yondelis® (trabecetidin), have successfully reached the drug market and are positively impacting society. Despite these success stories, marine environments and organisms are relatively unexplored in comparison to terrestrial environments [1]. Microphytobenthic biofilms are found in intertidal regions and contain a diverse range of prokaryotic and eukaryotic organisms, which live in a complex competitive community within a matrix of extracellular polymeric substances [2]. This biological and chemical diversity, coupled with accessibility, renders them suitable targets for marine natural product research. Terpenoids are isoprene-based lipids that have garnered interest due to their biological activity and potential therapeutic value. The ProspecTER project aims to use a bio-guided fractionation workflow that mass spectrometry-based metabolite and lipid profiling and structure elucidation with genomics approachesto find novel terpenoids with bioactivity. Here we present preliminary results in experiments to extract and analyse the lipid profile of microphytobenthic biofilms.

Methods

Microphytobenthic biofilms were sampled from intertidal mudflats and sandflats in Ballysadare Bay, Sligo, on the northwest coast of Ireland. A biofilm sample was taken using a $1m^2$ quadrat under low-tide conditions. Water conductivity, pH and dissolved oxygen readings were taken at both water's edge and the sampling location. The sample was stored frozen. In this preliminary work, lipid extraction was performed using a modified Bligh and Dyer extraction protocol [3]. Extraction of the freeze-dried sample was performed using methanol, dichloromethane and phosphate buffer, to separate into two phases: one aqueous and one organic. The identity and relative abundances of key complex neutral and polar lipids were determined using thin layer chromatography. Detailed analysis of sterol, triterpenoid, fatty acid, fatty alcohol and other core lipids was performed by analysis of an aliquot of the extract by gas chromatography-mass spectrometry (GC-MS) after derivatization by acid methanolysis and silylation.

Preliminary data and findings

A microphytobenthic biofilm was sampled from Ireland's coastline. A lipid fraction was successfully extracted using a modified conventional lipid extraction method and chemical profiles obtained.

References

1. Sigwart JD, Blasiak R, Jaspars M, Jouffray JB, Tasdemir D. *Natural Product Reports.* 2021;38(7):1235–42.
2. Hubas C, Passarelli C, Paterson DM. *Mudflat Ecology.* 2018. p. 63–90.
3. Balser TC. Phospholipid Fatty-acid Analysis (PLFA); Available from: https://nature.berkeley.edu/soilmicro/methods/BalserPLFA.pdf

P26

Leveraging LC-TIMS-QTOFMS for addressing analytical challenges in chemical exposome studies

Konstantina S. Diamanti,[1] *Dimitrios E. Damalas,*[1] *Georgios O. Gkotsis,*[1] *Eleni I. Panagopoulou,*[1] *Maria-Christina Nika,*[1] *Carsten Baessmann,*[2] *Bob Galvin,*[2] *Nikolaos S. Thomaidis* [1]

[1] Laboratory of Analytical Chemistry, Department of Chemistry, National and Kapodistrian University of Athens, Panepistimiopolis Zografou, 15771, Athens, Greece
[2] Bruker Daltonics GmbH & Co. KG, Bremen, Germany

Summary: *The exposome characterization is a complicated task. Through human biomonitoring, exposure to xenobiotics is evaluated by analyzing human biospecimens. Mass spectrometry coupled to chromatography is the preferred technique, but an additional dimension is often demanded to address several analytical challenges. Thus, the benefits of TIMS dimension into LC-HRMS are investigated.*

Keywords: *trapped ion mobility spectrometry, human biomonitoring, exposomics*

Introduction

Thousands of chemicals are produced and used daily, several of which are estimated to be dispersed in the environment via anthropogenic activities. Thus, human exposure to chemicals is an inevitable part of life and occurs via multiple routes, such as inhalation, ingestion and dermal contact. The term 'exposome' refers to the environmental agents to which human is exposed and the body's biological response to these exposures from prenatal period and throughout lifetime [1]. Through human biomonitoring, the chemical fingerprint of the xenobiotics exposure is revealed by directly analyzing human biological samples.

The comprehensive chemical characterization of the exposome is challenging. Today, various chemical classes can be simultaneously and reliably identified and quantified by target screening using high-resolution mass spectrometry. However, the sample complexity (endogenous metabolome) often results in high matrix effects and thus hampers the detection of compounds with low concentration. Reliable detections are also prevented by the complexity of MS/MS data produced by data-independent acquisition (DIA) modes. Therefore, apart from the established target screening protocols using retention time, MS and MS/MS information, an additional dimension and an extended workflow are required to identify xenobiotics with high confidence.

This study investigates the incorporation of trapped ion mobility spectrometry (TIMS) into LC-HRMS wide-scope target screening of biological samples for detection of xenobiotics. A workflow for establishing a database with ion mobility-derived collision cross section (CCS) values and a 4D target screening methodology for data treatment, as well as a quality assurance protocol for acquiring high quality LC-TIMS-HRMS data, are presented. Moreover, the benefits of leveraging LC-TIMS-QTOFMS for addressing analytical challenges in chemical exposome characterization are explored.

Experimental

Reference standard solution mixes of xenobiotics from different classes, such as pharmaceuticals, personal care products, drugs of abuse, plant protection products, plasticizers, flame retardants, preservatives, etc., were prepared for developing a CCS-aware database. Human urine samples were selected for exploring the added value of LC- TIMS-HRMS target screening, which were spiked with xenobiotics at a wide concentration range. For extracting semi-polar to polar xenobiotics from urine samples, the 'dilute-and-shoot' method was implemented. Standard solutions were analyzed in triplicate using LC-TIMS-QTOFMS with optimized broad mass and mobility bbCID and PASEF modes (data independent and data dependent modes, respectively). Samples were analyzed in bbCID mode, both by switching TIMS OFF and ON. Quality control standard solution mixes were also prepared and analyzed during the analytical run, which included compounds with reference values for evaluation of LC-TIMS-QTOFMS performance. The software used for data treatment was Bruker's DataAnalysis 5.3 and TASQ 2023.

Results

As a first step of the workflow, the high quality of the CCS measurements was assured by comparing the experimental CCS values with reference single-field CCS values from the Unified CCS Compendium in order to have accurate and reproducible results [2]. The extensive dataset that was developed for hundreds of xenobiotics included for each analyte the precursor ion formula, retention time (RT), full-scan MS and bbCID MS/MS qualifier ions, and the additional information of ion mobility-derived CCS values. Thorough evaluation for CCS values extraction was performed regarding adduct ions, isomers, protomers, etc. Then, the criterion of an allowed CCS window (ΔCCS ±1%) was added to the established parameters of mass accuracy (Δm/z ±2 mDa), RT shift (ΔRT ± 0.20 min), isotopic pattern fitting, and presence of qualifier ions, so that 4D wide-

scope target screening could be performed in real samples.
Finally, target screening was applied in both timsOFF and timsON data of spiked urine samples. With the addition of TIMS dimension, the signal-to-noise ratios were improved. By processing the data with an optimal ion mobility filtering (that was proved to be $1/K_0 = \pm 0.02$ V·s/cm^2 for the majority of the analytes), full-scan MS and bbCID MS/MS spectra and chromatograms of higher quality were obtained because of the deconvolution of the background signal caused by the presence of co-eluting isobaric analytes and matrix components. Thus, additional compounds out of the total number of spiked compounds were detected in ion mobility- filtered timsON data compared to timsOFF data. Overall, the improved MS signals and the detection of qualifier ions due to mobility filtering in many cases, as well as the additional orthogonal identification parameter of CCS, resulted in enhanced identification confidence by reducing false positive and false negative results.

Conclusions
This study proved that the incorporation of TIMS into LC-QTOFMS addresses several analytical challenges and offers great advantages with 4D wide-scope target screening of biosamples to detect xenobiotics, assisting in studies for the chemical characterization of the exposome.

References
1. C.P. Wild; *Cancer Epidemiology, Biomarkers and Prevention*, 14 (8) (2005), pp 1847-50.
2. J.A. Picache; *Chemical Science*, 10 (2019), pp 983-993.

P27

A bottom-up approach to characterize the proteome of natural rubbers employed in tyres production

Ludovica Sofia Guadalupi,[1] Cosima Damiana Calvano,[1] Tommaso Cataldi,[1] Andrea Bernardi,[2] Mattia Cettolin,[2] Marco Arimondi [2]

[1] Dipartimento di Chimica, Università degli Studi di Bari Aldo Moro, 70125 Bari, Italy
[2] Chemical Laboratory - Innovations & Methods Development, Pirelli Tyre S.p.a., 20126 Milano, Italy

Summary: *The protein content plays a crucial role in determining the quality of natural rubber and tyres as end products. This research project aims to characterize the proteome and establish its correlation with the performance of natural rubber. A bottom-up approach was adopted, involving trypsin digestion followed by LC-ESI-MS/MS analysis.*

Keywords: *natural rubber, proteomics, LC-ESI-ddMS²*

Introduction

Liquid chromatography coupled with tandem mass spectrometry (MS) is considered the method of choice for the identification and quantification of proteins [1]. The most widely used strategy is the data-dependent acquisition (DDA) mode, where fragment ion spectra (MS^2) from the most intense precursor ions are generated. Then, the collected MS^2 spectra are assigned to their corresponding peptide sequences by database searching [2]. This method can be applied to different fields such as food, cultural heritage, pharmaceutical or, in this specific case, to characterize the proteome of natural rubber (NR). The information on protein nature and content could help in modulating the mechanical and technological properties of finished tyres, resulting in high-performing products [3]. NR, mainly produced from *Hevea brasiliensis*, has a distinctive internal network structure that creates properties such as low thermogenesis and excellent durability during exhaustion cycling. In detail, proteins and lipids relate to the linear polyisoprene chains, generating a complex network structure with branching termed a " *naturally occurring network*" [4]. The great challenge in protein analysis is signified by their low content (about 1.5-4% w/w) and by their complex network interactions, which result in a very challenging extraction process from NR.

Experimental

Due to the tricky matrix, several extraction protocols were investigated. Starting from pulverized NR obtained by cryogenic milling, the most performing "one pot" protocol includes the use of a mix of reducing agent tris(2-carboxyethyl) phosphine, alkylating agent 2-chloroacetaide, ionic detergent sodium deoxycholate and ammonium bicarbonate alongside an ultrasonic homogenizer. The isolated proteins were digested by trypsin and subjected to LC-ESI-$ddMS^2$ analysis; the tandem mass spectra generated were interpreted through dedicated software/databases and manually validated.

Results

As reported in the literature [5], the proteome of NR revealed the occurrence of two major proteins: rubber elongation factor (REF) and small rubber particle protein (SRPP), which are water-insoluble acidic proteins of 14.7 and 22.3 kDa, respectively [5]. Both proteins were mapped with coverage of 52.2% and 36.3%. To allow the selection of precursor ions with lower signal intensity in DDA mode, an *ad hoc* exclusion list of REF and SRPP peptides in the tandem MS/MS spectra collection was generated. This strategy aims at characterizing minor proteins of NR. Currently, several enzymes and minor proteins have been identified, but further research is needed to confirm their presence and increase their coverage.

Conclusions

A "one-pot" protein extraction protocol to recover the NR proteins is proposed. The identification of NR proteins was based on LC-ESI-MS/MS analyses. Although the most predominant proteins, REF and SRPP, were identified with satisfying coverage, further work is required for a detailed description of minor ones.

References

1. Y. Zhang, B. R. Fonslow, B. Shan, M. Baek, and J. R. Yates, *Chemical reviews*, 113 (2013), pp 2343–2394.
2. B. Domon, and R. Aebersold, *Science*, 312 (2006), pp 212-217.
3. Y. Zhan, Y. Wei, J. Tian, Y. Gao, M. Luo, and S. Liao, *Scientific Reports* (2020), 10:16417.
4. K. Kosugi, and S. Kawahara, *Colloid and Polymer Science*, 293 (2015), pp 135-141.
5. K. Berthelot, S. Lecomte, Y. Estevez, and F. Peruch, *Biochimie*, 106 (2014), pp 1-9.

Acknowledgements
Project funded under the National Recovery and Resilience Plan (PNRR), Mission 4, Component 2 “Dalla Ricerca all'Impresa” - Investment 3.3 “Introduzione di dottorati innovativi che rispondono ai fabbisogni di innovazione delle imprese e promuovono l’assunzione dei ricercatori dalle imprese” - Call for tender No. 352 of 09 April 2022 of Italian Ministry of University and Research MUR under the DM 352/22 co-funded by Pirelli Tyre SPA; grant code 38-033-02-DOT1302393-3131; CUP H91I22000460007; Project title “Caratterizzazione di gomme naturali impiegate per la produzione di pneumatici mediante spettrometria di massa ad alta risoluzione”.

P28

Saliva peptidome profiling in glioblastoma multiforme brain tumour by HPLC-MS top-down platform

Alexandra Muntiu,[1] Diana Valeria Rossetti,[2] Federica Vincenzoni,[1,3] Irene Messana,[2] Massimo Castagnola,[4] Giuseppe La Rocca,[3,5] Alessandro Olivi,[3,5] Andrea Urbani,[1,3] Giovanni Sabatino,[3,5] Claudia Desiderio [2]

[1] Dipartimento di Scienze Biotecnologiche di Base, Cliniche Intensivologiche e Perioperatorie, Università Cattolica del Sacro Cuore, 00168 Rome, Italy
[2] Istituto di Scienze e Tecnologie Chimiche "Giulio Natta", Consiglio Nazionale delle Ricerche, Rome, Italy
[3] Fondazione Policlinico Universitario A. Gemelli IRCCS, Università Cattolica del Sacro Cuore, Rome, Italy
[4] Centro Europeo di Ricerca sul Cervello-IRCCS Fondazione Santa Lucia, Rome, Italy
[5] Institute of Neurosurgery, Fondazione Policlinico Universitario A. Gemelli IRCCS, Catholic University, Rome, Italy

Summary: *Peptidome investigation of the acid soluble fraction of glioblastoma multiforme saliva samples collected at different times, before and after surgery, revealed distinct molecular profiles using a top-down proteomic strategy by nano-LC-ESI-Orbitrap MS.*

Keywords: *Top-down; Saliva; Glioblastoma.*

Introduction

Glioblastoma multiforme (GBM) is an aggressive and high recurrence rate brain tumour, still demanding elucidation of the molecular mechanisms of onset and progression and the identification of diagnostic biomarkers. To date, surgery is the unique treatment for this tumour followed by a co-adjuvant chemo-radiotherapy combined treatment[1]. The present study provides the first attempt to investigate the peptidome of saliva pools collected from newly diagnosed GBM patients before surgery (T0) and one (T1) and three (T3) months after the surgery (before and after radiotherapy/ chemotherapy combined treatment, respectively), using a top-down strategy by nano-LC-ESI-Orbitrap MS platform. Top-down proteomics is the strategy of choice for characterizing small proteins and peptides in their intact form, suitable for studying proteoforms, identifying and localize post-translational modifications (PTM), investigating the naturally occurring protein fragmentome, including cryptides with proper biological activity[2].

Experimental

Saliva samples were treated with formic acid solution and the acid soluble fraction analysed by reverse phase LC in coupling with high resolution ESI-Orbitrap tandem mass spectrometry in gradient elution after filtering on FASP device equipped with 10kDa membrane filter. Proteomic data filtered for high confidence have been processed by bioinformatics tools to perform gene ontology and functional interaction analysis, pathway categories and over-representation, considering both shared and exclusive peptide elements identified at the different time of collection and condition, and their relative Uniprot accession[3].

Results

The peptides identified were related to 37 proteins that commonly characterized all saliva samples analysed, and to 6, 13 and 12 proteins instead exclusive of T0, T1 and T3 saliva, respectively. Noteworthy correlations have been found between the present results and previous data obtained from GBM CUSA aspirate fluid proteomic analysis[4]. The peptides exclusive of T0 saliva included, in addition to peptides relative to Histone H1.2, Homeodomain-only protein, Cytidine deaminase, DAZ-associated protein 1 and Neuroblast differentiation-associated protein AHNAK, the N-terminal peptide 2-12 of Fatty acid-binding protein 5, a Cancer Related protein, that was previously characterrized interestingly in newly diagnosed and recurrent GBM Cavitating Ultrasonic Aspirator (CUSA) fluid aspirate[5]. LC-MS data were also analysed to study the dark proteome of GBM saliva allowing the identification of proteins belonging to the uPE1, PE2 and PE3 classes, with uncharacterized function or missing mass spectrometry identification yet.

Conclusions

This pilot investigation revealed alterations of salivary proteome at the different time of collection and demonstrated the potential of saliva biofluid to discover GBM disease biomarkers for future perspectives of early diagnostic application and of the patient follow-up.

References

1. Bikfalvi, C. A. da Costa, T. Avril, J. V. Barnier, L. Bauchet, L. Brisson, T. Virolle; *Trends in Cancer*, 2022.
2. F. Iavarone, C. Desiderio, A. Vitali, I. Messana, C. Martelli, M. Castagnola, T. Cabras; *Biochem Mol Biol*. 2018; 53(3):246-263.
3. The UniProt Consortium, UniProt: the Universal Protein Knowledgebase in 2023, *Nucleic Acids Research*, Volume 51, Issue D1, 6 January 2023, Pages D523–D531, https://doi.org/10.1093/nar/gkac1052
4. G. La Rocca, G. A. Simboli, F. Vincenzoni, D. V. Rossetti, A. Urbani, T. Ius, G.M. Della Pepa, A. Olivi, C. Desiderio; *Cancers,* 2020. 13(1), 30.

P29

Porphyrin derivatives as quadruplexes ligands: spectrometry and spectroscopy studies

G. Satta,[1,2] M. Carraro,[1,2] L. Pisano,[1,2] L. De Luca,[1] S. Gaspa,[1] F. Mocci,[3] C. Meloni,[3] A. Cantara,[4] J. Plavec,[5] M. Trajkovski[5]

[1]*Department of Chemical, Physical, Mathematical and Natural Sciences, University of Sassari, Via Vienna 2, Sassari, 07100, Italy*
[2] *Consorzio Interuniversitario Reattività Chimica e Catalisi (CIRCC), Via Celso Ulpiani 27, Bari, 70126, Italy*
[3] *Department of Chemistry and Geological Science, University of Cagliari, Cittadella Universitaria, I-09042 Monserrato, Italy*
[4] *Institute of Biophysics, Czech Academy of Sciences, Královopolská 135, 612 65 Brno, Czech Republic*
[5] *Slovenian NMR Centre, National Institute of Chemistry, Ljubljana SI-1000, Slovenia*
g.satta@studenti.uniss.it

Summary: *Inhibition of telomerase activity is a promising cancer therapy strategy. G-quadruplex structures formed in telomeres can block telomerase, and new derivatives of tetra pyridyl porphyrin were synthesized and evaluated for their ability to stabilize them. NMR Spectroscopy and Mass Spectrometry were used to study complex structure and stability.*

Keywords: *Cancer, G-Quadruplex, Porphyrins,*

Introduction

A recent strategy pursued for cancer therapy is the inhibition of telomerase activity. Telomerase is an enzyme that counteracts the shortening of telomeres and therefore programmed cell death by senescence. In cancer cells, telomerase activity is often elevated and makes them able to evade the normal replication limit. As a result, tumour growth and survival are promoted[1]. Since human telomeres are rich in guanine, in the presence of monovalent metal cations as sodium or potassium, they can form non-canonical quaternary structures called G-quadruplexes (GQs), that consist of two or three stacked G-tetrads, with each G-tetrad comprising four guanines arranged in a square planar structure stabilized by Hoogsteen hydrogen bonds. The presence of these structures can inhibit telomerase activity[2]. Different molecules have been studied as ligands for GQs with the scope to stabilize them, one of the most known is tetra-(*N*-methyl-4-pyridyl) porphine (TMPyP4)[3]. Our research group synthetized some new derivatives of tetra pyridyl porphyrin to study their ability in the G4s coordination.

Experimental

Tetra pyridyl porphyrin derivative bearing amide substituent on the pyridinium nitrogen has been synthetized starting from a condensation reaction between pyrrole and 4-pyridinecarboxaldehyde to obtain 5,10,15,20-tetra(4-pyridyl) porphyrin (TPyP). The amide substituents were added by reacting TPyP with an alpha-brominated amide; the reaction follows an S_N2 mechanism, giving the tetra cationic porphyrin salt in almost quantitative yield. An initial analysis of interaction of porphyrins with 1XAV[4] (c-Myc) and 1KF1[5] (hTel) sequences by molecular dynamics and molecular modelling has been performed, followed by in vitro tests, UV-visible melting curves and displacement assays. To confirm complex formation, NMR spectroscopy has been used performing NOESY and COSY experiments. The mass spectrometry experiments[6] were performed using a Thermo Finnigan Q-Exactive high-resolution mass spectrometer with API-HESI source and Fourier Transform orbital trap (Orbitrap). Putative quadruplex sequence derived from c-Myc called CMT (with parallel topology) were folded in 100mM tetramethylammonium acetate (TMAA) buffer and 1mM KCl at pH=7[7]. TMPyP4 (used as reference ligand) and our derivative P11b were alternatively added on fractions of the same DNA sample, in a 1.75:1 ligand: DNA ratio. After identification by full MS scan analysis (Figure 1), the complex's peak was isolated by MS/MS experiment and subjected to fragmentation by increasing the collision energy in the Orbitrap analyser. The relative intensity (1) was calculated as follows: and correlated with the logarithm of the collision energy.

$$Relative\ Intensity = \frac{I_{Complex}}{I_{Complex} + I_{Dissociation\ \ Products}} \qquad (1)$$

Results

The intrinsic stability of free Quadruplex was evaluated by submitting it to MS/MS experiments as reported in the experimental section. The analyses were conducted in the presence of two different ligands TMPyP4 and P11b. From the curves reported in Figure 2 it is possible to see that both ligands show stabilising activity towards the free sequence. This can be confirmed by a significant increase of the $E_{COM}^{50\%}$ value (Table 1).

Compared to TMPyP4, P11b shows a further increase of $E_{COM}^{50\%}$ value of 4 eV.

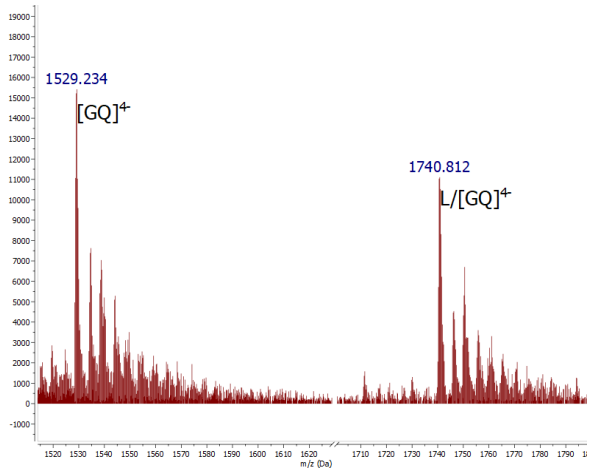

Figure 5. *L = P11b. Full MS scan analysis of complex solution whit GQ:L ratio 1:1,75*

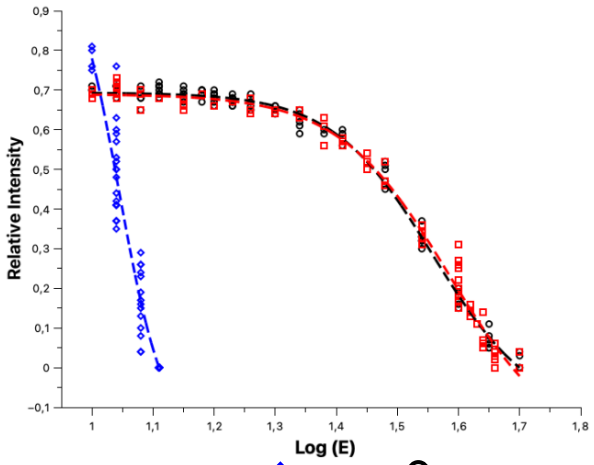

Figure 6. *Complex collision induced dissociation study. ◇free CMT, ○CMT/TMPyP4 complex, □CMT/P11b complex*

Table 2. *$E_{COM}^{50\%}$ quadruplex and complexes*

Sample	$E_{COM}^{50\%}$ Quadruplex	
	Log (E)	E (eV)
CMT	1.04	11,12
CMT vs P0	1.56	35,48
CMT vs P11b	1.58	39,81

Conclusions

The derivative synthesized by our group have demonstrated the ability to bind and stabilize putative G-quadruplex sequences. When compared to a porphyrin derivative already reported in the literature, they show similar or even superior activity. The obtained results have provided interesting insights for further evaluation, e.g. test on different DNA sequences are undergoing.

References

1. J. Shay and B. SA, *European journal of cancer (Oxford, England : 1990)* 33 (1997), pp. 787–91.
2. N. Kosiol, S. Juranek, P. Brossart, A. Heine and K. Paeschke, *Molecular Cancer* 20 (2021), pp. 40.
3. H. Arthanari, S. Basu, T.L. Kawano and P.H. Bolton, *Nucleic Acids Research* 26 (1998), pp. 3724–3728.
4. *RCSB PDB - 1XAV* Available at https://www.rcsb.org/structure/1xav.
5. *RCSB PDB - 1KF1* Available at https://www.rcsb.org/structure/1kf1.
6. F. Rosu, E. De Pauw and V. Gabelica, *Biochimie* 90 (2008), pp. 1074–1087.
7. A. Marchand and V. Gabelica, *J. Am. Soc. Mass Spectrom.* 25 (2014), pp. 1146–1154.

P30

Optimization of an LC-MS/MS method for the targeted analysis of brain microdialysis samples using derivatization with dimethylaminophenacyl bromide

L. Nestor,[1] Y. Vander Heyden,[2] D. De Bundel,[1] I. Smolders,[1] A. Van Eeckhaut [1]

[1] Vrije Universiteit Brussel (VUB), Research group Experimental Pharmacology (EFAR), Laarbeeklaan 103, Brussels, Belgium
[2] Vrije Universiteit Brussel (VUB), Department of Analytical Chemistry, Applied Chemometrics and Molecular Modelling (FABI), Laarbeeklaan 103, Brussels, Belgium

Summary: *The analysis of a broad range of neurochemicals in volume-limited samples, such as brain microdialysate, poses several challenges. In this project, a targeted LC-MS/MS method is currently being developed for the sensitive quantification of more than 100 neurochemicals using sample derivatization with dimethylaminophenacyl bromide.*

Keywords: *targeted metabolomics, brain extracellular fluid, derivatization*

Introduction

Microdialysis is the gateway for researchers to gain insights into the neuronal and glial release of neuroactive substances. Indeed, gaining insights into the healthy and diseased brain for biomarker discovery and unravelling new therapeutical targets remains important as current therapies for some neurodegenerative diseases are still insufficient. Microdialysis sampling does not only result in low sample volumes, but the analytes are also present in low concentrations[1]. Moreover, neurochemicals possess a wide range of physicochemical properties, making their simultaneous analysis challenging in volume-limited samples [2]. The overall aim of this project is to develop a sensitive liquid chromatography (LC) tandem mass spectrometry (MS) method that allows the simultaneous quantification of a broad range of low-concentrated neurochemicals - including carboxylic acids, amines, thiols - in volume-limited brain samples. To enhance separation in reversed-phase LC, to increase sensitivity and stability, and to allow ionization of all metabolites in electrospray positive mode, sample derivatization is performed using dimethylaminophenacyl bromide (DmPABr). This derivatization reagent allows a broad metabolome coverage as it reacts with amines, thiols and carboxylic acids [3]. In this study, 8 neurochemicals with different properties were selected to optimize the method. These compounds are glutamate, gamma-aminobutyric acid (GABA), cysteine, ornithine, butyrate, lactate, spermidine and kynurenic acid. First, the MS parameters of these compounds were determined. Second, the LC parameters, mobile phase gradient steepness (%B/min) and column temperature, were optimized using an experimental design approach. Thirdly, also optimization of the derivatization reaction was started.

Experimental

Sample derivatization was performed using 750 mM DmPABr in acetonitrile, at 65°C in the presence of triethanolamine (TEOA) as alkaline compound. After 1 hour derivatization, the reaction was quenched with formic acid [3]. Sample analysis was performed on a Waters Acquity UPLC system equipped with a Waters Acquity BEH C18 column (2.1 x 100 mm, 1.7 µm) using gradient elution. Mobile phases A and B consist of 0.1% formic acid in water and in acetonitrile, respectively. Mass spectrometry was performed on a Waters TQ-MS triple quadrupole system, equipped with an electrospray ionization source, which was operated in electrospray positive mode.

Results and discussion

Optimization of the method was performed on 8 neurochemicals, selected based on their functional groups, physicochemical properties, and biological relevance. First, the selected reaction monitoring (SRM) parameters (precursor and product ion, cone voltage and collision energy) were optimized. For this purpose, automatic tuning via IntelliStart® was performed, followed by manual tuning for verification purposes. For each neurochemical, a quantifier and qualifier transition were selected. The quantifier product ion always had a mass to charge ratio of 134.1, while a unique qualifier product ion was selected for every compound, except for butyrate and lactate. Secondly, a capillary voltage of 1.5 kV was selected based on signal intensity and signal-to-noise ratio of the different compounds. Thirdly, to minimize matrix effects and ion suppression, the column temperature and gradient slope were optimized using a three-level two-factor full factorial design. Considering minimal peak resolution and optimal peak shape as responses, a column temperature of 60°C and a linear gradient slope of 7%B/min over 10 minutes with a starting condition of 10%B were selected. The MS parameters and retention time for the 8 compounds, after optimization, are presented in Table 1.
For the derivatization reaction, different dilution solvents for TEOA were compared (water, dimethylsulfoxide/

dimethylformamide and acetonitrile). With the exception of glutamate, water had a negative influence on the derivatization reaction. This is in line with the literature, where water content is described to be of influence on the reaction efficiency [3]. Acetonitrile was chosen as optimal solvent for TEOA.

***Table 1**: Optimized MS parameters and retention times for the 8 selected compounds.*

Compound	**Retention time *(min)***	**Cone voltage *(V)***	**Quantitative parameters**		**Qualitative parameters**	
			SRM transition	**Collision energy *(eV)***	**SRM transition**	**Collision energy *(eV)***
Butyrate	6.1	30	250.2 > 134.1	25	250.2 > 165.0	20
Cysteine	8.8	45	766.4 > 134.1	55	766.4 > 426.6	25
GABA	5.9	45	587.3 > 134.1	30	587.3 > 438.2	20
Glutamate	8.4	46	792.4 > 134.1	42	792.4 > 585.3	24
Kynurenic acid	7.5	40	512.3 > 134.1	30	512.3 > 305.3	30
Lactate	3.7	25	252.1 > 134.1	25	252.1 > 165.0	25
Ornithine	7.7	50	938.5 > 134.1	60	938.5 > 599.3	30
Spermidine	5.5	50	951.8 > 134.1	75	951.8 > 394.2	35

Future perspectives

Further optimization of the derivatization reaction will be performed to allow sensitive analysis of the different compounds in the aqueous microdialysis samples. Moreover, a stable isotope labeled form of the derivatization reagent will be used to perform isotope-coded derivatization. In this way, an isotopically labeled internal standard for all analytes of interest is formed, enabling to correct for matrix effects for every metabolite. To maximize sensitivity, the method will be transferred to a UPLC-ionKey system coupled to a Xevo TQ-XS triple quadrupole MS (Waters). Before validating the method for microdialysis sample analysis, the list of compounds will be further expanded to more than 100 relevant neurochemicals.

References

1. M-L Custers, et al. *Pharmaceutics,* 14 (2022), 1051.
2. K Segers, et al. *Bioanalysis,* 11 (2019), 2297-2318
3. CCW Willacey, et al. *Journal of Chromatography A*, 1608 (2019), 460413.

P31

May post-translational succination be involved in cardiac arrhythmia? A joint study between (ion mobility) mass spectrometry and molecular dynamics

L. Groignet,[1,2] D. Dellemme,[2] M. Surin,[2] J.-M. Colet,[3] P. Brocorens,[2] J. De Winter [1]

[1] Organic Synthesis and Mass Spectrometry Laboratory
[2] Laboratory for Chemistry of Novel Materials
[3] Laboratory of Human biology and Toxicology
University of Mons (UMONS), Place du Parc 23, Mons 7000, Belgium

Summary: *This study focuses on 3D structures of proteins before and after a spontaneous post-translational modification called "succination", which involves a Michael addition of fumarate to a free thiol carried by a cysteine. To study the 3D structure, 2 main approaches are considered: ion mobility mass spectrometry and theoretical chemistry.*

Keywords: *Proteomics, Ion mobility mass spectrometry, Molecular dynamics*

During the Krebs cycle, the fumarate is converted into malate by the addition of a molecule of water catalysed by fumarate hydratase. But in some diseases, there is a germline mutation of the fumarase gene resulting in an enzymatic deficiency and therefore an accumulation of fumarate [1]. This molecule can undergo a Michael addition with proteins that present free thiol functions (free cysteines) and this physiologically irreversible reaction is called succination (Figure 1). 2-succinocystein molecules are known to be involved in some pathologies such as diabetes or cardiomyopathies when they are overexpressed [2]. An immunoassay highlighting the reaction products of succination is available. However, no information about the spontaneity of these reactions can be deducted and their efficiency remains relatively controversial in the literature [3]. In this study, an MS-based approach was selected as a potential alternative to the current assay. Indeed, using this technique could increase the knowledge about succination by determining the reaction spontaneity and the maximal number of moieties that can be grafted into the target. The first objective was to verify the existence of spontaneous reactions of succination by MS-based approach. The spontaneity of the succination reaction has been highlighted. Indeed, some peptides/proteins with free cysteines were spontaneously succinated, such as glutathione and SUMO1. SUMO1 is used in the stabilization of some target proteins, including SERCA2, a protein involved in Ca^{2+} regulation during cardiac contraction [4]. Thus, our main objective is to evaluate by Ion Mobility Mass Spectrometry and molecular dynamics whether SUMO1 succination has an impact on its 3D structure and therefore, whether it has an impact on its function and plays a role in cardiac arrhythmia.

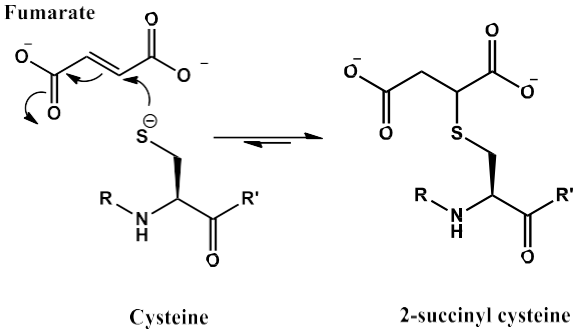

Figure 1. *Succination reaction via a Michael addition between cysteine and fumarate.*

References

1. S. C. Fletcher, M. L. Coleman; *Biochem. Soc. Trans.*, **48**, 1843–1858, (2020)
2. N. Frizzell *et al.*; *J. Biol. Chem.*, **38**, 25772–25781, (2009)
3. R. T. Casey *et al.*; *Clin. Cancer Res.*, **26**, 391–396, (2020)
4. C. Kho *et al.*; *Nature*, **477**, 601–606, (2011)

P32

Metabolomics applied to discover prognostic markers in human heart transplantation

E.C. Montatixe Fonseca,[1] M.C. Mimmi,[3] A. Corazza,[4] M. Belliato,[2] C. Pellegrini,[1] S. Pelenghi [1]

[1] Cardiac Surgery Unit 1, IRCCS San Matteo Hospital Foundation, Pavia, Italy
[2] Anesthesiology and Intensive Care Unit 2, IRCCS San Matteo Hospital Foundation, Pavia, Italy
[3] Department of Molecular Medicine, University of Pavia, Italy
[4] Department of Medical Area, University of Udine, Italy

Summary: *This study applies NMR and HPLC-MS metabolomics of in the context of human heart transplantation. Using the routinely collected endomyocardial biopsies we aim to identify metabolic markers associated with graft dysfunction or injury, both related to pre-existing conditions and to the procedural aspects of transplantation.*

Keywords: *Metabolomics, heart transplantation, NMR, HPLC-MS.*

Introduction

PGD (Primary Graft Disfunction) is one of the most significant cause of early morbidity and mortality after heart transplantation. Despite the standardized procedures and the well-defined criteria for selection of suitable grafts, the reported incidence of PGD can reach 28.2% [1]. We propose metabolomics as a tool to identify molecular markers of graft disfunction or injury, both related to pre-existing conditions and to the procedural aspects as heart preservation and transplantation.

Experimental

This study reckons on the collection of endomyocardial biopsies (EMBs) at three different time-points: immediately after organ procurement before packing for transport (**T0**), upon arrival at the hospital just before graft implantation (**T1**) and 1 week after transplantation (**T2**). The hydrophilic metabolites extracted from the biopsies will be evaluated by solution NMR following a standard procedure [2]. Metabolic profiling of the EMBs will be complemented by HPLC-MS adapting the method of Yuan M. et al. [3]: a panel of 150 metabolites will be screened with the MRM (Multiple Reaction Monitoring) experimental scheme. Due to the small size of EMBs (1-5mm diameter) the two analytical techniques will be used serially on the same extract.

Objectives

The primary aim is to determine possible correlations between altered myocardium metabolism and: initial graft condition, ischemia duration and eventual cardiac dysfunction.

Preliminary results

The metabolic extraction protocol from EMBs was optimized. The NMR analysis was completed for some T0/T1 EMBs. Notwithstanding the small dimension of the starting material, the obtained 1D-^{1}H-NMR spectra show a good signal-to-noise ratio and allow the quantification of about 20 metabolites including: amino acids (*e.g.* branched chain amino acids, Glu, Asp, Ala), carboxylic acids (*e.g.* lactate, fumarate), nucleotides (*e.g.* ATP), redox carriers (*e.g.* NAD+). The analysis via HPLC-MS is being set up.

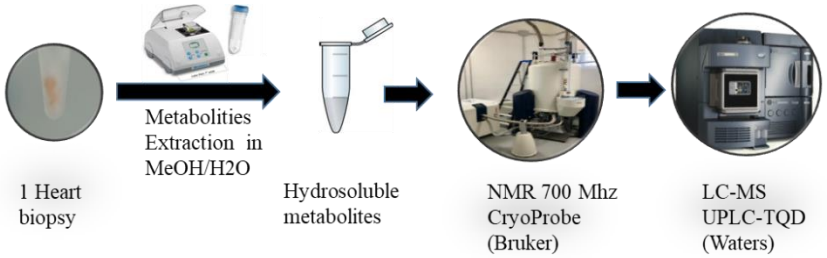

Figure 1. *Workflow of the metabolomic analysis of EMBs*

References

1. Smith, N. F. et al. *ASAIO Journal*, 68, (2022), pp 394–401
2. Beckonert, O. et al. *Nature Protocols* 2, (2007), pp 2692-2703
3. Yuan, Min, et al. *Nature Protocols* 7, (2012), pp 872-881

P33

Sterolomic profiling of human CSF and plasma to reveal altered cholesterol metabolism in Parkinson's diseases

Eylan Yutuc,[1] Manuela Pacciarini,[1] Anders Öhman,[2] Lars Forsgren,[2] Miles Trupp,[2] Yuqin Wang,[1] William J. Griffiths [1]

[1]Institute of Life Science 1, Swansea University Medical School, SA2 8PP, Swansea, United Kingdom
[2]Umea University, Umea, Sweden

Aims and Introduction

Around 10 million people worldwide suffer from Parkinson's Disease (PD), a progressive neurodegenerative disorder. To date, there is no cure for PD, but early disease identification and treatment may lead to a better quality of life. Hence, specific, and easy-detectable biomarkers for a definitive diagnosis are greatly needed. Recent findings link disordered brain cholesterol metabolism with PD. Furthermore, altered plasma and CSF levels of some oxysterols, oxidised cholesterol metabolites, have been found in PD. Of note is the oxysterol 24S-Hydroxycholesterol (24S-HC), the principal brain cholesterol elimination product. Changes in its blood or CSF concentration are believed to reflect defects in brain cholesterol turnover.
To shed a light on the contribution of cholesterol and its metabolites, to the pathogenesis of PD and, consequently, identify diagnostic/prognostic biomarkers for the disease, 100 plasma samples from baseline PD patients have been analysed through a targeted Liquid-Chromatography-Mass-Spectrometry strategy and compared with 100 healthy subjects.

Experimental and Results

A procedure for the extraction and analysis of plasma sterols incorporating derivatisation allows the detection of 22 sterol molecules, including cholesterol, oxysterols like 24S-HC and cholestenoic acids like 7αH,3O-CA (7α-hydroxy-3-oxocholest-4-en(25R)26-oic acid). Among the sterols identified, 24S-HC and 7αH,3O-CA plasma levels are significantly higher in the PD group while cholesterol is lower, with respect to non-PD. Further analysis evidences a gender difference in the brain-derived 24S-HC plasma levels, revealing a higher level of oxysterol only in PD males. A ROC analysis on the ability of 24S-HC to be a discriminating biomarker for PD shows an almost 70% chance of predicting PD when referring to 24S-HC plasma levels normalised to cholesterol.

Conclusions

Going forward, a study of longitudinal plasma from PD patients is being carried out to investigate the ability of plasma sterols to be utilised as prognostic biomarkers for disease progression.

P34

Metabolomic profiling in differential diagnosis for Parkinson's disease and atypical parkinsonisms

Erika Esposito,[1,2] Alessandro Perrone,[1,3] Chiara Cancellerini,[1] Manuela Contin,[1,4] Giovanna Calandra Buonaura,[1,4] Giovanna Lopane,[1] Jessica Fiori [1,2]

[1] IRCCS Istituto delle Scienze Neurologiche di Bologna, Bologna, Italy
[2] Dipartimento di Chimica "G. Ciamician", Università di Bologna, Bologna, Italy
[3] Dipartimento di Scienze Mediche e Chirurgiche, Università di Bologna, Bologna, Italy
[4] Dipartimento di Scienze Biomediche e Neuromotorie, Università di Bologna, Bologna, Italy

Summary: *MS based untargeted metabolomics was applied to support early differential diagnosis of patients with Parkinson disease (PD), Multiple System Atrophy (MSA) and Progressive Supranuclear Palsy (PSP). Metabolomic profile of 30 plasma samples was performed using micro liquid chromatography coupled with high-resolution mass spectrometry (microLC-HRMS).*

Keywords: *untargeted metabolomics, microLC-HRMS, Parkinson's disease*

Introduction and aim

Parkinson's disease (PD) is the second most frequent progressive neurodegenerative disease. PD development depends on an intricate combination of genetic and environmental factors [1]. The main motor symptoms of PD (tremor, rigidity, bradykinesia) can also be observed in complex neurodegenerative pathologies, namely Multiple System Atrophy (MSA) and Progressive Supranuclear Palsy (PSP), grouped as Atypical Parkinsonisms (APs).
AP prognosis, evolution, and therapeutic treatment are deeply different from PD's. Currently, PD and AP (i.e. MSA and PSP) diagnoses rely on clinical evidence, due to the lack of specific biochemical and neuroradiological markers, so an improper diagnosis could lead to ineffective therapeutic interventions.
This study aimed to identify specific biomarkers for PD and AP classification by untargeted metabolomic analysis using microLC-HRMS (Figure 1).

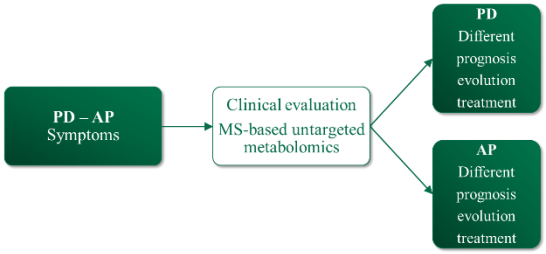

Figure 1. *Rationale of the study.*

Metabolomics workflow using microLC-HRMS

- Plasma samples (20 PD, 4 MSA, 6 PSP) were prepared via protein precipitation by adding cold acetonitrile/0,1% formic acid (v/v) to a final plasma/solvent ratio of 1:4 (v/v) [2].
- The extract was analysed in Data Independent mode (SWATH®-MS) [3], by microLC - TripleTOF 6600+ (Sciex, Concord, ON, Canada) equipped with a Luna Omega Polar C18 100x1mm 1,7 µm.
- Metabolites were identified by SCIEX OS Software using Accurate Mass Metabolite HR-MSMS Spectral Library 2.0 (Sciex, Concord, ON, Canada).
- Data were processed using MarkerView™ Software (Sciex, Concord, ON, Canada) for simultaneous feature finding, alignment, and statistical analysis to highlight metabolites of interest [4].
- Confidence in identification of metabolites of interest were further confirmed reprocessing the MS and MS/MS data with SCIEX OS (Sciex, Concord, ON, Canada).

Results and discussion

Hundreds of metabolites were confidently identified with a single run, generating a peculiar metabolic profile for each biological sample. A smaller group of patients (20 MP, 4 MSA, 6 PSP) was selected for a preliminary multivariate statistical analysis to identify disease-specific metabolic alterations (Figure 2).

Metabolites involved in tyrosine, tryptophan, purines, and fatty acids metabolism result to be discriminant for PD, MSA, and PSP (p-value < 0.05, Figure 2). Further targeted analyses on some of the discriminant metabolites may help to identify a biologically relevant subset of readily measurable markers for PD and AP differential diagnosis.

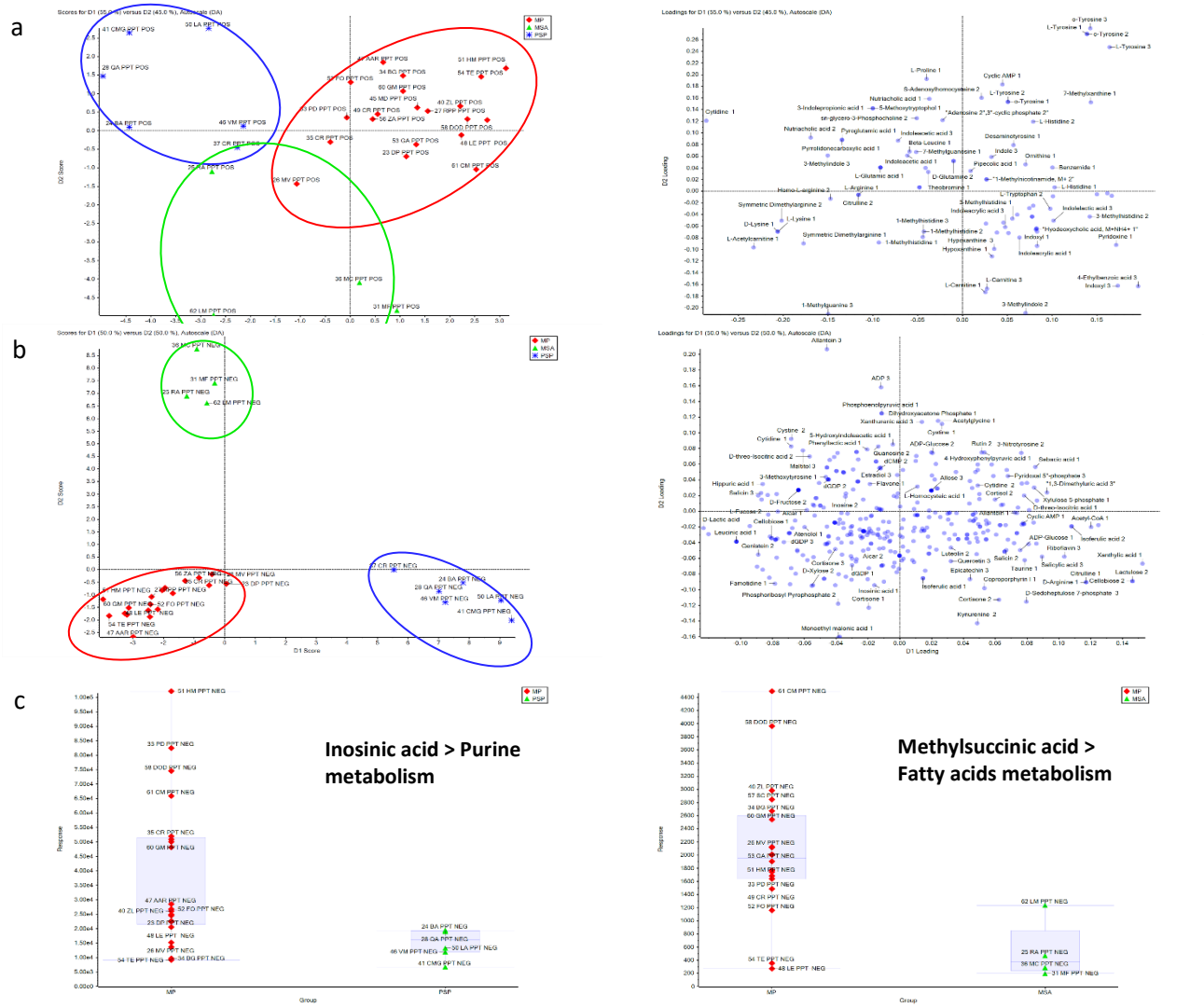

Figure 2. *PCA-DA (supervised) scores plot and loadings plot for sample analysed in positive (a) and negative polarity (b). Representative metabolites (p-value < 0,05) response for each sample group for negative polarity (c). Red squares for MP and green triangles for PSP or MSA. Box plots depict the range between the 25th and 75th percentiles of the data. The horizontal line marks the median value; capped bars indicate min and max values.*

References

1. Jankovic J.; *J Neurol Neurosurg Psychiatry.* 2008 Apr;79(4):368-76.
2. Vuckovic, D.; *Proteomic and Metabolomic Approaches to Biomarker Discovery (2nd ed.).* 2020; Pages 53-83.
3. Demianova, Z.; *Biomarkers and Omics.* 2017.
4. Gallant, V.; *Biomarkers and Omics. 2017.*

P35

Gas chromatography-mass spectrometry reveals the metabolic signature of different phenotypes of cystic fibrosis

Martina Spada, Cristina Piras, Vera P. Leoni, Antonio Noto, Luigi Atzori

Department of Biomedical Sciences, University of Cagliari

Summary: *Gas chromatography-mass spectrometry (*GC-MS) *represents a valid technique to study complex pathological conditions, such as cystic fibrosis. Thanks to its high resolution and sensitivity, GC-MS allowed this work to depict the richness of urinary metabolome and to highlight differences among patients affected by cystic fibrosis with different genotypes.*

Keywords: *Cystic fibrosis, Gas Chromatography-Mass Spectrometry, Metabolomics*

Introduction

Cystic fibrosis (CF) is an autosomal recessive disorder caused by mutations in the cystic fibrosis transmembrane conductance regulator (CFTR) gene [1]. Its product, the CFTR protein mainly acts as an ion channel, and its deficiency results in an increased density and viscosity of secretion [2]. CF shows high phenotypic variability because of the intervention of genetic and environmental factors [3]. In this context, metabolomics constitutes a useful tool to investigate pathology's complexity, providing further insights into the pathophysiology and contributing to clinical biomarkers identification. GC-MS represents one of the most widely used techniques for metabolomics studies due to its high resolution, sensitivity, reproducibility, and relatively low cost [4].

Experimental

Urine samples from 35 patients affected by CF and whit different genotypes (F508del/F508del, T338I/T338I, and F508del/T338I) were collected. An aliquot of urine was evaporated to dryness, derivatized, and diluted with hexane. Quality control samples were created by using an aliquot of all samples. Finally, samples were analyzed with GC-MS technique. Identification of metabolites was performed using the standard NIST 08 library. Chromatogram analysis was performed using MassHunter software and the resulting data were normalized by total area before undergoing statistical analysis.

Results

The supervised multivariate statistical analysis, based on the GC-MS data, allowed the separation of the samples based on the metabolomic profile. In particular, a good separation between F508del/F508del *vs* T338I/T338I genotypes, and F508del/F508del vs F508del/T338I genotypes was observed. Moreover, the comparison of the two groups T338I/T338I *vs* F508del/T338I didn't highlight significant differences. The VIP responsible for the separation were sugars (glucose, maltose, talose), organic acid (citric acid, 3-(3-Hydroxyphenyl)-3-hydroxypropionic acid and 3-Hydroxyisovaleric acid), and polyols, such as inositol isoforms. The classification obtained corresponded to the different phenotypes under investigation. So, the different metabolomic profiles are consistent with pathological conditions and clinical symptoms.

Conclusions

GC-MS analysis has proven to be a useful tool to discriminate among the different subclasses of CF, mirroring the complexity of the pathological condition. In conclusion, GC-MS represents a valid technique for better understanding physiopathological changes and identifying new clinical biomarkers.

References

1. M. C. Bierlaagh, D. Muilwijk, J. M. Beekman, C. K. van der Ent; *European Journal of Pediatrics,* (2021), 180:2731–2739.
2. M. F. Figueira, C. M. P. Ribeiro, B. Button; *Current Opinion in Pharmacology,* (2022), 65, 102248.
3. L. I. Butnariu, E. Tarcă, E. Cojocaru, C. Rusu, S. M. Moisă, M. L. Constantin, E. V. Gorduza, L. M. Trandafir; *Journal of Clinical Medicine*, (2021), 10, 5821.
4. M. Khodadadi, M. Pourfarzam; *Metabolomics*, (2020), 16, 66.

P36

Novel approach to investigate highly complex pharmaceuticals utilizing ultrahigh-resolution mass spectrometry

Ole Tiemann,[1,2] *Lukas Schwalb,*[1,3] *Christopher P. Rüger,*[1,2,4] *Martha L. Chacón-Patiño,*[4,5] *Thomas Gröger,*[3] *Ralf Zimmermann* [1,2,3]

[1] Joint Mass Spectrometry Centre (JMSC)/Chair of Analytical Chemistry, University of Rostock 18059 Rostock, Germany
[2] Department Life, Light & Matter (LL&M), University of Rostock, 18059 Rostock, Germany
[3] JMSC / Cooperation Group "Comprehensive Molecular Analytics", Helmholtz Zentrum München 85764 Neuherberg, Germany
[4] International Joint Laboratory - iC2MC: Complex Matrices Molecular Characterization, 76700 Harfleur, France
[5] Ion Cyclotron Resonance Program, National High Magnetic Field Laboratory, Florida State University, Tallahassee, FL 32310, USA

Summary: *Bituminosulfonates are promising therapeutic agents exhibiting a variety of pharmaceutical properties like antibacterial and anti-inflammatory effects However, their chemical composition remains challenging to resolve. By atmospheric pressure ionization Fourier-transform ion cyclotron resonance mass spectrometry, a molecular-level characterization revealed sub-mDa mass splits and allowed offline compound tracing throughout the manufacturing process.*

Keywords: *Pharmaceuticals, High-Resolution Mass Spectrometry, Atmospheric Pressure Ionization*

Introduction

"Non-biological complex drugs" (NBCDs) have recently gained substantial medicinal, regulatory, and economical interest. These active pharmaceutical ingredients (APIs) are neither of homo- molecular structure nor a biological compound, such as antibodies. Additionally, they "can't be isolated and fully quantitated, characterized, and/or described by physicochemical analytical means"[1]. Lately, bituminosulfonate formulations have tentatively been allocated toward NBCDs featuring broad valuable antibiotic and anti-inflammatory properties[2]. These APIs are derived from bituminous schists by dry distillation to obtain sulfur-rich shale oil. Fractionation of the crude shale oil in vacuo produces distillate precursors which, as active ingredient starting materials, are sulfonated with sulfuric acid and subsequently neutralized with sodium hydroxide solution (sodium bituminosulfonates SBS) or with ammonia (ammonium bituminosulfonates ABS). The use and efficacy as a therapeutic agent have been documented since 1882. Interestingly, a low potential for antimicrobial resistance in bacterial cells has been found, and the exact pharmaceutical mechanisms are currently being investigated[3]. While pharmaceutical effects are well documented for SBS and ABS, knowledge on the molecular composition is rather limited[5,6]. Moreover, NBCDs are reported to be highly sensitive to a robust and well-controlled manufacturing process. Thus, chemical speciation along the different processing steps is crucial for understanding transformation processes and ensuring high-quality standards. Challengingly, analytical methodologies for targeting aromatic sulfonates are seldom and rarely found in literature[4], and regulatory solutions for in-depth speciation are entirely missing.

Experimental

Fourier-transform ion cyclotron resonance mass spectrometry (FT-ICR MS) is a powerful technique to describe the isobaric complexity of highly complex matrices. Its high resolving power (> 3 000 000 @ *m/z* 400) and high mass accuracy (< root mean square error < 40 ppb) enable the calculation of sum formulas based on the exact measured masses.
Electrospray ionization (ESI) and atmospheric pressure photoionization (APPI) were utilized to cover a wide range of compounds and functionalities, leading to a detailed description of the analyzed matrices. The results and structural assumptions were validated by online derivatization multidimensional gas chromatography.

Results

We achieved a detailed chemical description of the APIs ABS and SBS[5] on a molecular level via FT-ICR MS. By utilizing complementary ionization techniques (ESI, APPI), a broader overview of the overall chemical composition of each isolated manufacturing process step was achieved. We were able to resolve the isobaric complexity resulting from various functionalities and revealing mass splits below 1 mDa. For the precursor matrices, sulfur-containing compounds were found to be the most prominent compounds. More than 50% of the total ion count (TIC) in APPI was assigned to polyaromatic sulfur heterocycles (PASHs: *e.g.*, S_1, S_2, S_3,

S4) with the sulfur atoms bound in the aromatic heterocycle, while only 6% of the TIC were identified as polyaromatic hydrocarbons (PAHs: CH). Besides PAHs and PASHs as major compounds, also trace amounts of nitrogen-containing compounds (NCCs) were found in the precursor matrices. Additionally, the respective corresponding sulfonates (*e.g.*, SO_3, S_2O_3, S_3O_3) were found in the APIs by ESI(-). Therefore, the chemical characterization enabled tracing specific compound classes throughout the process, resulting in first educt-product relation approaches. Here, PAHs and PASHs are particularly noteworthy due to their high abundances within both, precursor matrices as well as APIs. Comparing these data sets allowed first conclusions about the influence of aromaticity and degree of alkylation on the sulfonation process within the ultra-complex mixture. ESI and APPI address strongly different chemical functionalities. Hence, for tracing the manufacturing process and the resulting polarity increase of the matrix, comparing these complementary ionization techniques is crucial. As stated by Schwalb et al., for SBS resulting from light distillate precursors only sulfonated compounds were identified[5]. On the other hand, partially incomplete sulfonation was revealed for ABS produced from the middle distillate. It was striking that strongly alkylated compounds, *e.g.*, C_5-C_{36}-alkylated benzothiophenes, were found within ABS. These compounds were also found within the crude shale oil. Interestingly, the grade of alkylation found in the middle distillate was slightly lower than in ABS. Therefore, it is conceivable that during the sulfonation reaction, in addition to the intended sulfonation, side reactions also take place which generate by- products. Furthermore, steric hindrance of the alkyl chains might lead to incomplete or fully suppressed sulfonation yields in ABS. Therefore, it is possible that a better yield of the sulfonation reaction may be obtained by optimizing the reaction conditions. However, this needs to be investigated in further studies.

Conclusion

Direct infusion FT-ICR MS coupled with atmospheric pressure ionization techniques is a powerful tool to unravel the isobaric complexity of highly complex pharmaceuticals revealing molecular- level information. The high resolving power and mass accuracy enable the separation of sub-mDa mass splits. Furthermore, the offline investigation of each process step allows to trace compounds leading to the possibility of optimizing the occurring reactions. As a result, the detailed chemical information opens the possibility for routine analysis method developments as well as a deeper understanding of the underlaying biopharmaceutical mechanisms of action.

References

1. D. J. A. Crommelin, J. S. B. de Vlieger, V. Weinstein, S. Mühlebach, V. P. Shah, H. Schellekens; *The AAPS Journal*, 16 (2014), 11-14, DOI: 10.1208/s12248-013-9532-0.
2. S. Fink, A. Sethmann, U.-C. Hipler, C. Wiegand; *Eur. J. Pharm. Sci.*, 172 (2022), DOI: 10615 10.1016/j.ejps.2022.106152.
3. H. C. Korting, C. Schöllmann, W. Cholcha, L. Wolff, The Collaborative Study Group; *J Eur. Acad. Dermatol. Venereol.*, 24 (2010), 1176-1182, DOI: 10.1111/j.1468-3083.2010.03616.x.
4. Z. Feng, M. Cui, J. Liu, Y. Song, J. Q. Li; *Asian J. Chem.*, 26 (2014), 6722-6726, DOI: 10.14233/ajchem.2014.16640.
5. L. Schwalb, O. Tiemann, U. Käfer, T. Gröger, C. P. Rüger, G. Gayko, R. Zimmermann; *Anal. Bioanal. Chem.* 415 (2022), 2471-2481, DOI: 10.1007/s00216-022-04393-w.
6. J. Koch, R. Moser, J. Demel; *Archiv der Pharmazie*, 318 (1985), 198-206, DOI: 10.1002/ardp.19853180303.

P37

The role of the mass spectrometry in the discovery of new potential anticancer drugs

Francesca Meloni,[1] *Sebastiano Masuri,*[1] *Lukáš Moráň,*[2,3] *Maria Grazia Cabiddu,*[1] *Enzo Cadoni,*[1] *Josef Havel,*[4,5] *Petr Vaňhara,*[2,4] *Tiziana Pivetta* [1]

[1] Department of Chemical and Geological Sciences, University of Cagliari, Cittadella Universitaria 09042 Monserrato, Cagliari, Italy
[2]Department of Histology and Embryology, Faculty of Medicine, Masaryk University, 62500, Brno, Czech Republic
[3]Research Centre for Applied Molecular Oncology, Masaryk Memorial Cancer Institute 65653 Brno, Czech Republic
[4]Department of Chemistry, Faculty of Science, Masaryk University, 62500, Brno, Czech Republic
[5]International Clinical Research Center, St. Anne's University Hospital, 65691, Brno, Czech Republic

Summary: *A new copper(II) complex from $[Cu(phen)_2(OH_2)](ClO_4)_2$ and ursodeoxycholic acid was prepared. The new complex inhibits the lipoxygenase enzyme by allosteric modulation and shows antitumoral effect on ovarian and pancreatic cancer cells. In presence of the new complex Endoplasmic Reticulum stress regulators are overexpressed.*

Keywords: *Mass spectrometry, Cu(II)-phenantroline complexes, antitumor agents*

Introduction

Since the discovery of the cisplatin's cytotoxic properties, several metal complexes were prepared and studied for their biological activity exploiting different action mechanism [1]. Indeed, previous studies carried out in our research group have demonstrated that Cu(II) complex such as $[Cu(phen)_2(OH_2)](ClO_4)_2]$ is able to induce massive cell death in ovarian cancer cells through pro-apoptotic mechanism [2]. Several studies shown that the combination between C0 and other systems leads to novel heteroleptic complexes with good therapeutic properties against different cell lines and low side effects [3]. Ursodeoxycholic acid (UDCA) is a bile acid involved in the cholesterol catabolism and emulsification of lipid in the intestinal tract and it is also approved for the treatment of primary biliary cirrhosis and other cholestatic disorders. Combination of UDCA and conventional anticancer drugs can attenuate common side effects [4].
For this reason, we prepared a novel heteroleptic copper complex from C0 and UDCA named C0- UDCA with the aim of exploiting the biochemical characteristics of these two compounds. The studies of coordination modes, solution equilibra, antioxidant and anti-lipoxygenase properties were carried out with different experimental and theoretical approaches. The cytotoxicity against ovarian (SKOV-3) and pancreatic (PANC-1) cancer cells was studied in vitro.

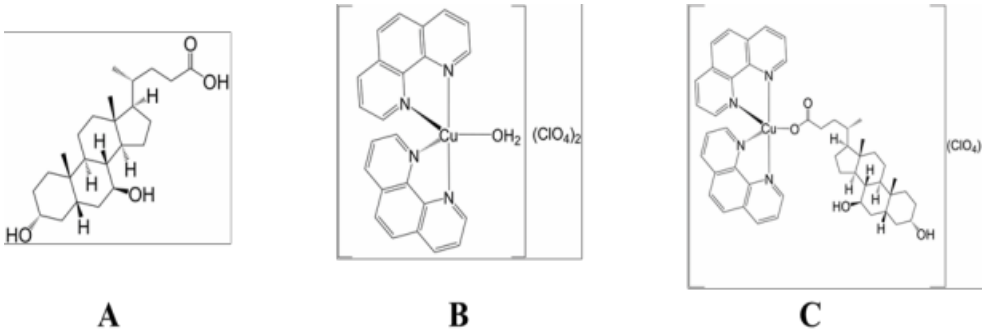

Figure 1. *A. Ursodeoxycholic acid (UDCA); B. $[Cu(phen)_2(OH_2)](ClO_4)_2$ (C0); C. $[Cu(phen)_2(UDCA- H)](ClO_4)$ (C0-UDCA)*

Results

The complex C0-UDCA was synthetized and the stoichiometry was determined by elemental analysis. In the ESI-MS spectrum of C0-UDCA a peak at 814 *m/z* was observed, corresponding to the $[Cu(phen)_2(UDCA-H)]^+$ ion, obtained from the ionization of the neutral $[Cu(phen)_2(UDCA- H)](ClO_4)$ species. High-resolution mass spectrum of C0-UDCA in the range 600-850 *m/z* was recorded to confirm the composition of the peaks at 814 *m/z* and of its fragment at 634 *m/z*. As observable, the fitting of the isotopic pattern and the matching between experimental and calculated exact masses (814.3532 u vs 814.3519 u and 634.2844 u vs 4 634.2832 u) confirmed the proposed stoichiometry.

Tandem mass experiments at different collision energies (CE) were carried out to identify the peaks containing Cu(II), phenantroline and UDCA and to have more information about the structure of new C0-UDCA.

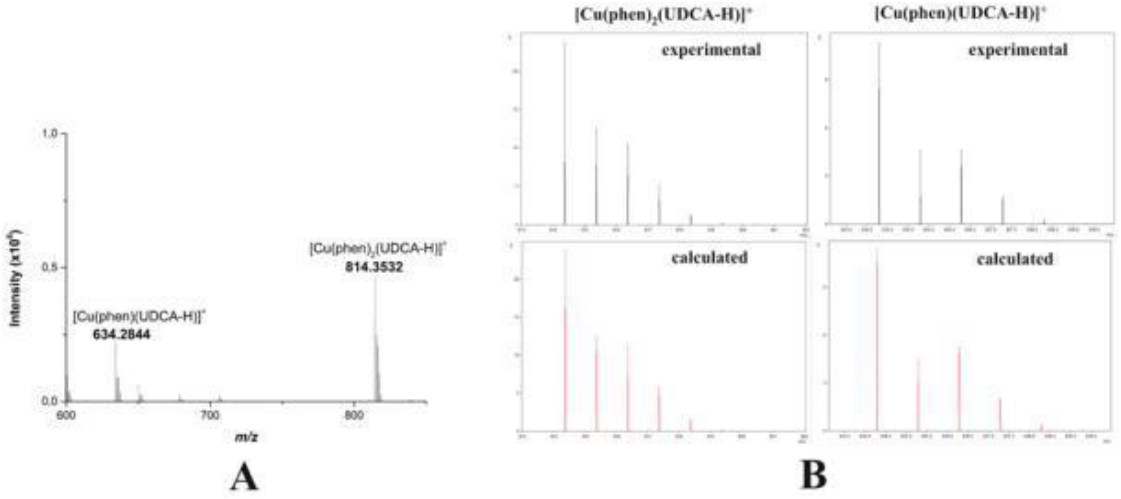

Figure 2. *High-resolution mass spectrum of C0-UDCA in the 600-850 m/z range, (B) experimental and calculated isotopic pattern for peaks at 814 and 634 m/z, (methanol: water 1:1). All the mass values are expressed as monoisotopic masses.*

The breakdown curves, obtained reporting the peak intensity vs CE, show the relative stability of the formed species: i) at 0 V the unique stable species is $[Cu(phen)_2(UDCA\text{-}H)]^+$; ii) it is necessary to apply 20 volt to completely convert $[Cu(phen)_2(UDCA\text{-}H)]^+$ in $[Cu(phen)(UDCA\text{-}H)]^+$; iii) at voltage > than 30 $[Cu(phen)(UDCA\text{-}H)]^+$ is fragmented with loss of the UDCA ligand.

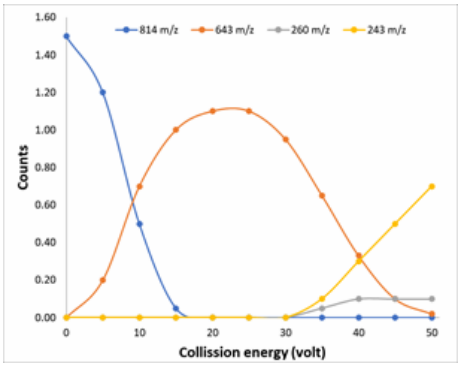

Figure 3. *High-resolution mass spectrum of C0-UDCA in the 600-850 m/z range, (B) experimental and calculated isotopic pattern for peaks at 814 and 634 m/z, (methanol:water 1:1). All the mass values are expressed as monoisotopic masses.*

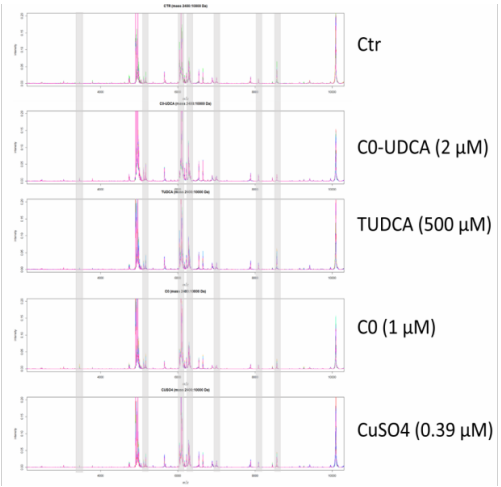

Figure 4. *Mass spectra of selected m/z regions of treated cells with the main differences in individual spectra highlighted*

The antiproliferative activity of C0-UDCA and its precursors was evaluated on SKOV-3 and PANC1- cells. A methodology of intact cell mass spectrometry, as a tool for quality cell control, bio typing and cell phenotype changes rapid identification, was introduced. Here we were also able to detect changes in the biological background of treated cells, after measuring the characteristic spectral fingerprints of individual samples [5].

Conclusions

This study shows how the chemical interaction between the $[Cu(phen)_2(OH_2)]^{2+}$ complex and the bile acid UDCA leads to the formation of the novel heteroleptic complex C0-UDCA. This complex can inhibit the cell growth and reduces cell viability of both ovarian (SKOV-3) and pancreatic (PANC-1) cancer cells at micromolar level. The combination of IC-MALDI-MS and statistical analysis allowed to distinguish between controls and cells treated with C0, UDCA and C0- UDCA to evaluate the efficacy of this compounds.

References

1. F. Trudu, F. Amato, P. Vaňhara, T. Pivetta, E.M. Peña-Méndez, J. Havel, J Appl Biomed. 13 (2015) 79–103 https://doi.org/10.1016/j.jab.2015.03.003
2. Masuri, P. Vaňhara, M.G. Cabiddu, L. Moráň, J. Havel, E. Cadoni, T. Pivetta, , Molecules. 27 (2022) 49.
3. L. Moráň, T. Pivetta, S. Masuri, K. Vašíčková, F. Walter, J. Prehn, M. Elkalaf, J. Trnka, J. Havel, P. Vaňhara, Metallomics. 11 (2019) 1481–1489 https://doi.org/10.1039/C9MT00055K
4. J.-F. Goossens, C. Bailly, , Pharmacol Ther. 203 (2019) 107396. https://doi.org/10.1016/j.pharmthera.2019.107 396.
5. P. Vaňhara, L. Kučera, L. Prokeš, L. Jurečková, E.M. Peña-Méndez, J. Havel, A. Hampl, , Stem Cells Transl Med. 7 (2018) 109–114. https://doi.org/10.1002/sctm.17- 0107.

P38

Mass-directed preparative purification of Semaglutide batches

Louisa O'Grady, Philip Gaffney, Paola De Luisi

Dr Reddy's Laboratories (EU) Ltd., Cambridge, UK

Summary: *Herein, we have used mass-directed preparative purification as a way of optimising the purity, potency and recovery of in-house synthetic Semaglutide. This ensures dimished ambiguity of the identification between the target peptide and impurities formed during synthesis and cleavage.*

Keywords: *MS, purification, Semaglutide*

Introduction

Peptides have become increasingly popular, due to the variety of their applications. Over the years, improved synthetic techniques have allowed the sythesis of increased complex samples. However, very little development has been done on preparative purification processes of peptides, causing a decline in the progress of the overall peptide workflow. HPLC-UV is the technique most commonly employed to achieve peptide purification and isolation.

Herein, we used mass-directed preparative purification as a way of optimising the purity, potency and recovery of Semaglutide as well as increasing sample throughput. This ensured dimished ambiguity of the identification between the target peptide and impurities formed during synthesis and cleavage. Mass spectrometry was used to help identify and isolate the main peptide from the contaminants for which no resolution was observed in the UV chromatogram, determining peak identity and attaining homogeneity in complex samples. Implementing two detection modes, UV and MS, allowed a more complete form of analysis, since ionisation issues as well as low UV absorbance could be observed.

Experimental

The purification of crude Semaglutide was performed on a prep HPLC system equipped with UV and MS detection. A C18 column in preparative dimensions was used. The elution was achieved in acidic conditions using a TFA buffer. The sample load was 1% with respect to the column packing.

ESI+ MS detection was employed. SIM channels were set to monitor the elution of Semaglutide and of several impurities (the main ones are listed in Table 1).

Purity analysis of the collected fractions was performed on RP-UPLC equipped with PDA detector, using a C18 column. Resolution was achieved in acidic conditions using TFA buffers.

Results

Figure 1 shows the overlay of the UV and SIM purification chromatograms for the crude sample.

The purification shown herein demonstrates increased peptide recovery since no fractionation optimisation is needed. Furthermore, reduced fraction analysis time was shown since the overall profile of the collected fractions was already known.

Overall, as shown in Table 1, one acidic purification stage afforded a final purity of 97%. Although recovery was found to only be ~67%, not all fractions were included in the calculation; instead, a total recovery of 95% was predicted and a ~60% usable (i.e. > 94% purity) yield was obtained. Furthermore, the targeted critical impurities were clearly reduced compared to the crude sample.

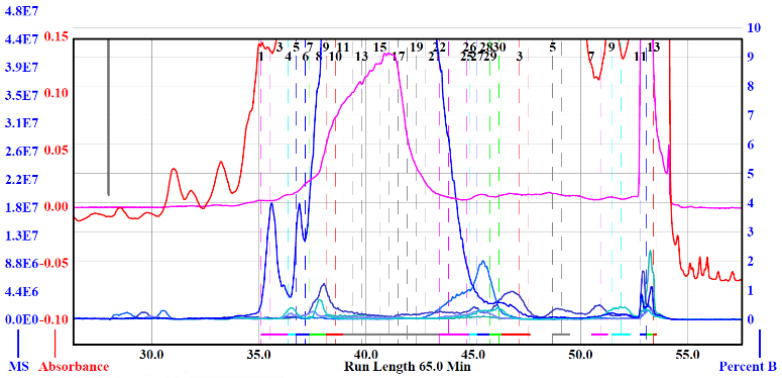

Figure 1. *Elution plot of crude sample, highlighting the UV traces (two wavelengths in red and pink) and the SIM channels (shades of blue).*

Table 1. *Purity and mass recovery results for purified fraction of crude Semaglutide.*

Fraction no.	Concent. (mg/mL)	Collected Sema (mg)	Sema Purity (%)	Impurity peak area %			
				Imp. 1	Imp. 2	Imp. 3	Imp. 4
F11	1.217	60.848	60.84	2.15	4.55	6.28	2.99
F12	5.138	262.024	96.65	0.19	0.07	0.18	0.48
F13	5.821	296.853	96.99	0.15	0.15	0.04	0.39
F14	6.189	315.627	97.71	0.13	0.17		0.35
F15	6.602	336.699	97.68	0.1	0.12		0.33
F16	6.069	309.506	94.53	0.11	0.23	0.1	0.39
F17	3.387	172.752	91.12	0.27	0.35	0.26	0.36
F18	1.716	87.522	88.68	0.29	0.26	0.21	0.27
F19	0.967	49.307	86.63	0.2			0.09
F12-F16 Combined	7.467	1642.747	97.09	0.13		0.36	0.22

Conclusions

The use of MS as well as UV detection reduced the overall purification time, with respect to both fraction analysis time and purification stages. Therefore, this will allow for the development of peptide-based projects to become more efficient. Herein, we showed a technique that delivers a final peptide sample with a high purity from a complex crude mixture. Although combining techniques has shown to be beneficial, issues have been observed regarding ionisation of main impurities. Hence, further work is required to tune the instrument, in order to improve the isolation of the predominant peptide, Semaglutide.

To optimise this further, an orthogonal stage (e.g basic purification) could be implemented to remove remaining closely eluting impurities, attaining an overall purity >97%, without affecting the recovery of Semaglutide.

P39

Investigation of the potential biotransformation of different pharmaceuticals in zebrafish embryos (*Danio rerio*), utilizing LC-QTOFMS and LC-TIMS-QTOFMS

Eleni I. Panagopoulou, Dimitrios E. Damalas, Eleni Aleiferi, Vasiliki Tzepkinli, Nikolaos S. Thomaidis

Laboratory of Analytical Chemistry, University of Athens, Panepistimiopolis Zografou, 157 71 Athens, Greece

Summary: *The aim of this study was to investigate the biotransformation capacity of ZFE exposed to different pharmaceuticals and to identify the tentative biotransformation products (bio-TPs), using LC-HRMS. Furthermore, to highlight the importance of utilizing different chromatographic techniques and Trapped Ion Mobility (TIMS) technology, for the identification of candidate bio-TPs. Overall, the results point out why biotransformation should be assessed in toxicokinetic studies.*

Keywords: *pharmaceuticals, biotransformation, LC-HRMS*

Introduction

Pharmaceuticals and their transformation products (TPs) are widely detected in the aquatic environment. Zebrafish (Danio rerio) embryo (ZFE) has emerged as a powerful alternative model- organism in ecotoxicological studies for evaluating the effects of xenobiotics in aquatic organisms [1]. Biotransformation constitutes an important factor in toxicokinetic studies, since sometimes, metabolites may exhibit higher toxicity than the parent compound. Identification of biotransformation products (bio-TPs) is a challenging task, and the lack of available reference standards makes it more difficult [1]. LC-HRMS offers a powerful approach to detect and identify these bio-TPs [2]. Despite HRMS high applicability, separation of isomeric bio-TPs is not always possible. Hydrophilic interaction liquid chromatography (HILIC) could be used as a complementary chromatographic mode for orthogonal identification of bio-TPs. Trapped Ion Mobility (TIMS) it is a very promising technology for the separation of isomers and could provide additional experimental evidence to enhance the identification confidence. The aim of this study was to investigate the biotransformation capacity of ZFE exposed to different pharmaceuticals. Also, the identification of the tentative bio-TPs, utilizing LC- HRMS. Furthermore, the importance of using two different chromatographic techniques and the added value of TIMS was investigated for the identification of bio-TPs.

Experimental

For the extraction of pharmaceuticals in ZFE samples, organic solvents were added, and a bead- beating homogenization process was followed. The ZFE extracts were analyzed by reversed phase liquid chromatography (RPLC) and HILIC, in both positive and negative ionization, by LC-ESI-QTOF. The extracts were also analysed with LC-TIMS-TOF-MS to introduce an additional dimension of separation. Target-screening approach was followed for the identification of the parent compounds, whereas the identification of tentative bio-TPs was performed through in-house developed suspect and non-target screening workflows. Collision cross section (CCS) values were used as additional experimental evidence for the identification.

Results and Conclusions

Overall, bio-TPs of Ibuprofen from both oxidative and conjugative metabolic reactions were identified and a potential metabolic pathway was proposed. The main bio-TPs of Ibuprofen presented higher intensity in comparison with the parent compound. Furthermore, the results from the two different chromatographic techniques were investigated. Reverse elution order was observed highlighting the complementarity of RPLC and HILIC. Finally, LC-TIMS-QTOFMS data provided additional evidence to support the identification of the bio-TPs of Metoprolol. In-silico biotransformation and MS/MS prediction tools can greatly facilitate suspect and non-target screening during identification process. The analytical data of this study highlight that information in two orthogonal chromatographic techniques in combination with CCS values provided additional evidence to support the identification of bio-TPs. Definitely, biotransformation should be included in future toxicokinetic studies.

References

1. Brox, S., Seiwert, B., Haase, N., Küster, E., & Reemtsma, T. *Comparative Biochemistry and Physiology Part C*: Toxicology and Pharmacology, 185–186 (2016)
2. Aceña, J., Pérez, S., Eichhorn, P., Solé, M., & Barceló, D. *Analytical and Bioanalytical Chemistry*, 409(23), 5441–5450 (2017)

P40

Antiretroviral molecules: investigating the break-down pathways

Ambar S.A. Shaikh, Kgato P. Selwe, Ed Bergstrom, Jackie Mosely, Caroline E. H. Dessent

Department of Chemistry, University of York, Heslington, York, UK

Summary: *This work aims to build upon high-quality research by investigating the photodegradation of Antiretrovirals (ARVs). Monitoring the absorption of ARVs using UV-Vis spectrophotometry, to understand how it breaks down with light (Photolysis) and also if it reacts with water (Hydrolysis). And also studying the fragmentation pattern in protonated and de-protonated modes.*

Keywords: *Antiretrovirals, Photolysis, Mass Spectrometry*

Introduction

• Emerging contaminants (ECs) are a growing concern all over the world and consist of a wide variety of chemical compounds such as pharmaceuticals, surfactants, personal care products, etc. [1].
• They have been detected in major quantities all over the environment (air, soil, and water) through analytical methods [2].
• Antiretrovirals (ARVs) are an example of pharmaceutical drugs that have been detected in the environment around the world [6].
• Antiretrovirals are used along with other medications to treat human immunodeficiency virus (HIV) infection.
• The presence of ARVs in aquatic environments may affect organisms [3] such as liver damage and overall health decline, as well as development and growth abnormalities in fish [5].

Methods

• Low-energy collision-induced dissociation (CID) was performed to investigate the ground-state thermal fragmentation characteristics of ARVs, using a Bruker Amazon (Quadrupole Ion Trap) mass spectrometer, and Higher-energy collisional dissociation (HCD) was performed by using an Orbitrap Fusion Tribrid mass spectrometer[4].
• The absorption spectra were recorded using a Thermo Genesis UV-Vis spectrophotometer using cuvettes with a 1 cm path length and approximately 3 mL volume.
• Use of 310 nm online photodissociation apparatus combined with electrospray ionization mass spectrometry detection to perform photodissociation on ARVs.

Results

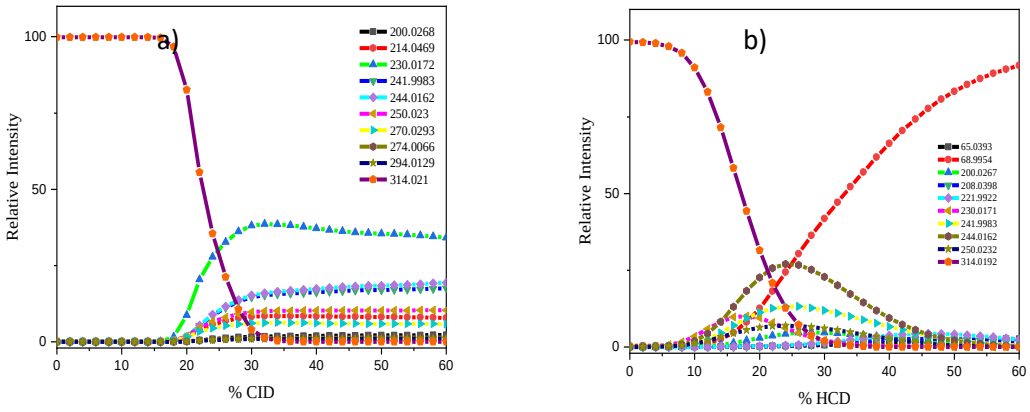

Figure 7. *(a) CID fragmentation decay curve for $[EFV - H]^-$ (m/z 314) upon CID between 0% and 60% CID energy. The curved lines included with the data points are a three-point adjacent average of such data points. (b) Parent ion dissociation curves $[EFV - H]^-$ (m/z 314, electro-sprayed in MeOH) between 0% and 60% HCD energy.*

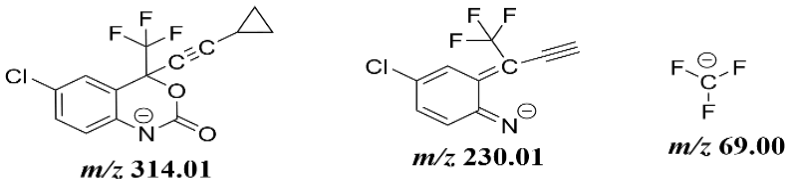

Figure 2. *Structure of parent ion, m/z 314, and the primary fragment m/z 230 and m/z 69 in CID & HCD*

Conclusions

• The fragment with *m/z* 314.02 fragmented at high CID energy to give primary fragments of *m/z* 230.01, whereas, in HCD primary fragment is *m/z* 68.99.
• The UV Spectrum obtained from the sample of ARVs showed no difference over 360 minutes
• No breakdown of ARVs through photolysis and hydrolysis.

References

1. E. Ngumba, A. Gachanja, and T. Tuhkanen, *Science of The Total Environment*, vol. 539, pp. 206–213, Jan. 2016, doi: 10.1016/J.SCITOTENV.2015.08.139.
2. K. O. K'oreje, K. Demeestere, P. de Wispelaere, L. Vergeynst, J. Dewulf, and H. van Langenhove, *Science of The Total Environment*, vol. 437, pp. 153–164, Oct. 2012, doi: 10.1016/J.SCITOTENV.2012.07.052.
3. A. F. M. M. Rahman, M. W. Attwa, and A. A. Kadi, doi: 10.26717/BJSTR.2021.38.006218.
4. N. G. K. Wong, C. Rhodes, and C. E. H. Dessent, *Molecules 2021, Vol. 26, Page 6009*, vol. 26, no. 19, p. 6009, Oct. 2021, doi: 10.3390/MOLECULES26196009.
5. L. Robson, I. E. J. Barnhoorn, and G. M. Wagenaar, "The potential effects of efavirenz on Oreochromis mossambicus after acute exposure," *Environ Toxicol Pharmacol*, vol. 56, pp. 225–232, Dec. 2017, doi: 10.1016/J.ETAP.2017.09.017.
6. H. Ramírez-Malule, D. H. Quiñones-Murillo, and D. Manotas-Duque, vol. 6, pp. 179–193, Jan. 2020, doi: 10.1016/J.EMCON.2020.05.001.

P41

Metabolism of nine synthetic opioid in zebrafish larvae using liquid chromatography mass spectrometry

Sara Pesavento, Matilde Murari, Franco Tagliaro, Federica Bortolotti, Rossella Gottardo

Unit of Forensic Medicine, Department of Diagnostics and Public Health, University of Verona, Verona, Italy

Summary: *Synthetic opioids are a major threat and a real challenge for drug policies across the world. Therefore, information about their metabolism is extremely useful. In the proposed study, zebrafish embryos were employed to identify the metabolic pathways of nine synthetic opioids by means of liquid chromatography coupled to high resolution mass spectrometry.*

Keywords: *synthetic opioids, metabolism, zebrafish larvae*

Introduction

The New Psychoactive Substances (NPS) phenomenon represents a problem of global concern, due to the lack of available information about their adverse effects and metabolism. Among them, new synthetic opioids (NSOs) are one the fastest-growing groups. Even though these compounds were originally synthetized to develop safer opioids for medical treatment, they have never been sold as pharmaceutical drugs [1]. Nevertheless, they have become extremely popular in the illicit market. Within this group, cinnamylpiperazines and 2-benzylbenzimidazoles represent two relevant subclasses [2]. Due to the obvious limitations to toxicant testing in humans, animal models are of great importance for metabolic studies. Rodents are the usual strategy for toxicological studies, but they suffer from strict and complex procedures for ethics approval. Conversely, zebrafish larvae are not included in the European animal protection legislation. Moreover, thanks to its unique features, such as easy handling and minimal requirements of drugs needed, the zebrafish model provides a valid alternative to mammal models for metabolism studies [3]. The purpose of the present evaluation was to investigate the metabolic pathways of nine members of the above-mentioned subclasses, namely AP-237, 2-methyl AP-237, isotonitazene, metonitazene, etodesnitazene, butonitazene, metodesnitazene flunitazene, and N-pyrolidino etonitazene in zebrafish larvae.

Experimental

Fifteen zebrafish larvae were exposed for 24 hours to synthetic opioids (final dose: 1 µM), and subsequently euthanized in ice. Sample preparation was performed by following the method developed by Gampfer [4]. Analyses were carried out on a Vanquish UPLC coupled with an Orbitrap Fusion™ Lumos™ Tribrid™ Mass Spectrometer (Thermo Fisher Scientific, Waltham, Massachusetts, USA). The acquisition software was Xcalibur version 3.4 (Thermo Fisher Scientifc, USA). An untargeted acquisition was performed as a screening approach, followed by a data-dependent MS/MS analysis of the most abundant peaks. Metabolite structures of the hypothetical candidate were given based on MS/MS structural assignment and accurate mass formulae prediction.

Results

As regards the two cinnamylpiperazines (AP-237 and 2-methyl AP-237), the two compounds were metabolized by zebrafish larvae only in their monohydroxylated form, whilst 2-benzylbenzimidazoles (isotonitazene, metonitazene, etodesnitazene, butonitazene, metodesnitazene flunitazene, and N-pyrolidino isotonitazene) followed different routes of metabolism. Indeed, as depicted in Figure1, the identified relevant biotrasformations were hydroxylation, N/O-dealkylation or a combination of them.

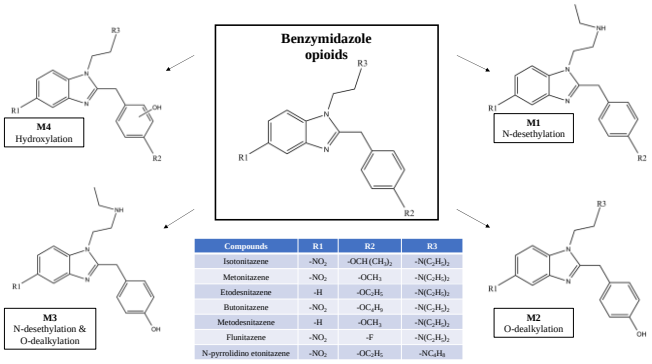

Compounds	R1	R2	R3
Isotonitazene	$-NO_2$	$-OCH(CH_3)_2$	$-N(C_2H_5)_2$
Metonitazene	$-NO_2$	$-OCH_3$	$-N(C_2H_5)_2$
Etodesnitazene	-H	$-OC_2H_5$	$-N(C_2H_5)_2$
Butonitazene	$-NO_2$	$-OC_4H_9$	$-N(C_2H_5)_2$
Metodesnitazene	-H	$-OCH_3$	$-N(C_2H_5)_2$
Flunitazene	$-NO_2$	-F	$-N(C_2H_5)_2$
N-pyrrolidino etonitazene	$-NO_2$	$-OC_2H_5$	$-NC_4H_8$

Figure 8. *Schematic metabolic pathway of benzimidazole opioids*

Additionally, Table 1 summarizes the main metabolites identified for each one of the studied compounds, along with their chemical structure, retention times and calculated exact mass of precursors and product ions.

Table 1. *List of metabolites tentatively identified in zebrafish larvae with the proposed fragmentation spectra.*

Compound Name	*Chemical formula*	*Theoretical mass (m/z)*	*Experimental mass (m/z)*	*RT (min)*	*Major fragments (m/z)*
AP-237	$C_{17}H_{24}N_2O$	273.1961	273.1965	6.8	117.0666, 155.1158 91.0515
OH-AP-237	$C_{17}H_{24}N_2O_2$	289.1911	289.1811	5.9	133.0606, 57.1291 87.0895
2-methyl AP-237	$C_{18}H_{26}N_2O$	287.2118	287.2120	7.0	117.0663, 69.1329 91.0498
OH-2-methyl AP-237	$C_{18}H_{26}N_2O_2$	303.2067	303.2057	6.0	171.1450, 33.0613 101.1026
Isotonitazene	$C_{23}H_{30}N_4O_3$	411.2391	411.2405	7.7	100.1091, 72.0785
N-desethyl isotonitazene	$C_{21}H_{26}N_4O_3$	383.2078	383.2068	7.5	72.0779, 312.1243
O-dealkyl isotonitazene (4-hydroxynitazene)	$C_{20}H_{24}N_4O_3$	369.1921	369.1929	6.4	100.1115, 133.0810 72.0877
Metonitazene	$C_{21}H_{26}N_4O_3$	383.2078	383.2097	7.1	100.1093, 72.0784 *121.0633*
N-desethyl metonitazene	$C_{19}H_{22}N_4O_3$	355.1765	355.1750	6.9	72.0785, 121.0617
O-demethyl metonitazene (4-hydroxynitazene)	$C_{20}H_{24}N_4O_3$	369.1921	369.1930	6.4	100.1094, 72.0780
Etodesnitazene	$C_{22}H_{29}N_3O$	352.2383	352.2374	6.3	100.1092, 72.0765
N-desethyl etodesnitazene	$C_{20}H_{25}N_3O$	324.2070	324.2055	5.9	253.1330, 72.0789
Butonitazene	$C_{24}H_{32}N_4O_3$	425.2547	425.2552	9.3	100.1114, 72.0802 107.0485
Hydroxy butonitazene	$C_{24}H_{32}N_4O_4$	441.2496	441.2495	7.2	100.1114, 72.0803 107.0485
Hydroxy butonitazene	$C_{24}H_{32}N_4O_4$	441.2496	441.2495	9.3	100.1116, 72.0804 107.0488
O-desbutyl butonitazene (4-hydroxynitazene)	$C_{20}H_{24}N_4O_3$	369.1921	369.1926	6.4	100.1115, 72.0803 107.0486
O-desbutyl N-desethyl butonitazene	$C_{18}H_{20}N_4O_3$	341.1608	341.1613	6.1	72.0803, 107.0485 270.0870
N-desethyl butonitazene	$C_{22}H_{28}N_4O_3$	397.2234	397.2238	9.0	72.0806, 326.1499 107.0489
Metodesnitazene	$C_{21}H_{27}N_3O$	338.2227	338.2214	5.4	100.1114, 72.0803 121.0643
O-demethyl metodesnitazene	$C_{20}H_{25}N_3O$	324.2070	324.2066	4.1	100.1116, 72.0804 86.0960
N-desethyl metodesnitazene	$C_{19}H_{23}N_3O$	310.1921	310.1921	4.9	239.1181, 72.0805 131.0601, 121.0644
Flunitazene	$C_{20}H_{23}FN_4O_2$	371.1878	371.1886	7.6	100.1116, 109.0444 72.0805
N-desethyl flunitazene	$C_{18}H_{19}FN_4O_2$	343.1565	343.1561	7.3	72.0806, 109.0444
N-pyrrolidino etonitazene	$C_{22}H_{26}N_4O_3$	395.2078	395.2081	7.9	98.0961, 107.0488 135.0801
N-pyrrolidino etonitazene reduction	$C_{22}H_{24}N_4O_3$	393.1921	393.1925	7.7	96.0804, 107.0488 135.0800
O-desethyl N-pyrrolidino etonitazene	$C_{20}H_{22}N_4O_3$	367.1765	367.1750	6.2	98.0959, 107.0485

Conclusion

In the present study, the metabolism of a panel of 9 new synthetic opioids was assessed in vivo using the zebrafish embryo as a model organism. The identified biotransformations are in line with the limited data available in scientific literature, if present. Furthermore, to the best of the authors' knowledge, in this work we reported for the first time metabolic data about butonitazene, metodesnitazene, flunitazene, and N-pyrolidino etonitazene.

References

1. United Nations Office on Drugs and Crime (UNODC). *UNODC Early Warning Advisory (EWA) on New Psychoactive Substances (NPS)* (2020).
2. Walton, S. E., Krotulski, A. J., & Logan, B. K., *Journal of Analytical Toxicology*, (2022), pp. 221–231.
3. Pesavento, S., Bilel, S., Murari, M., Gottardo, R., Arfè, R., Tirri, M., Panato, A., Tagliaro, F., & Marti, M., *Medicine, Science and the Law*, (2022), pp. 188–198.
4. Gampfer, T. M., Wagmann, L., Park, Y. M., Cannaert, A., Herrmann, J., Fischmann, S., Westphal, F., Müller, R., Stove, C. P., & Meyer, M. R., *Archives of Toxicology*, (2020), pp. 2009–2025.

P42

Nitrating activity of the hemin-$A\beta_{16}$ complex: modifications on the peptide itself

Silvia De Caro,[1,2] Simone Dell'Acqua,[1] Enrico Monzani,[1] Stefania Nicolis[1]

[1] Department of Chemistry, University of Pavia, Italy
[2] Scuola Universitaria Superiore IUSS Pavia, Italy

Summary: *This work studies the modifications undergone by the amino acid residues of the coordinated peptide themselves due to the oxidating and nitrating activity of the hemin-$A\beta_{16}$ complex, in the presence of the reactive species generated by the hemin/H_2O_2/NO_2^- system.*

Keywords: *β-amyloid peptide, heme, nitrative stress*

Introduction

β-amyloid (Aβ) peptides, deriving from the proteolysis of the amyloid precursor protein, are present in the brain and are constituted by 40-42 amino acids [1]. Aβ aggregation leads to oligomeric structures and fibrils, which are related to the onset of Alzheimer's disease [1].
Aβ can also interact with metal ions, such as copper and iron. Iron exists *in vivo* both as free ion and inside the heme group (hemin in its oxidized form). The redox activity of the latter species should be considered in pathological conditions related to neurodegenerative diseases or traumatic brain injuries, when the heme level increases.
Under oxidative stress and pathophysiological conditions related to neurodegeneration, biological nitration reactions, mainly deriving from the interaction between nitrogen monoxide, its derivatives, and reactive oxygen species (ROS), have been observed *in vivo* [2]. Protein nitration modulates the activity of enzymes involved in neurodegeneration, and it could also affect the protein aggregation properties [2].
The aim of this study is therefore to deepen the investigation of the nitration reaction promoted by the hemin-$A\beta_{16}$ complex (Figure 1) in the presence of hydrogen peroxide and nitrite [3]. We chose the $A\beta_{16}$ fragment as model of Aβ since it contains three histidines, which could provide axial coordination to iron ion, and it possesses a lower tendency to aggregate than $A\beta_{40}$ and $A\beta_{42}$ [3].

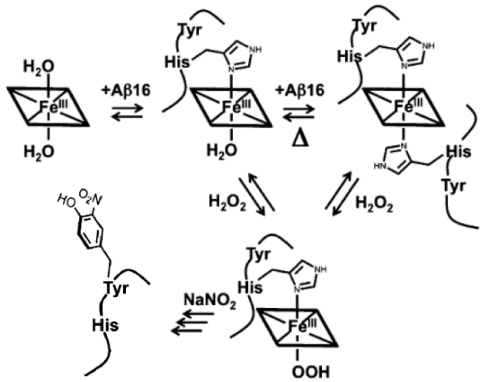

Figure 9. *Formation of the hemin-$A\beta_{16}$ complex and promotion of nitration reactions [4].*

Experimental

The samples for the peptide modifications analysis were prepared by mixing hemin (2 μM), $A\beta_{16}$ (10 μM), and, when needed, the aromatic substrate (3 or 0.3 mM) in phosphate buffer 100 mM at pH 7.4. Hydrogen peroxide and nitrite were then added in 5 aliquots of 40 μM each (mild conditions) or 4 mM H_2O_2 / 40 mM NO_2^- (harsh conditions) every 5 minutes. The samples were then incubated at 37 °C for 30 minutes before injection in the mass spectrometer. The elutions were carried out with milliQ water added with 0.1% of formic acid (solvent A) and acetonitrile added with 0.1% of formic acid (solvent B), with a flow rate of 0.2 mL/min. The solvent gradient started with 98% solvent A for 5 minutes, followed by a linear gradient from 98% to 55% solvent A in 65 minutes and to 0% solvent A in 40 minutes for the analysis of peptide and hemin modifications, respectively.

Results

It has been reported that $A\beta_{16}$ can undergo two types of modifications in the presence of ROS/RNS: oxidation due to the binding of an oxygen atom to a His residue and nitration due to the substitution of a

hydrogen atom with a nitro group on a Tyr residue. The expected sites of modifications in the $A\beta_{16}$ peptide, whose sequence is DAEFRHDSGYEVHHQK, are the tyrosine residue, Tyr_{10}, that can undergo nitration, and the histidine residues, His_6, His_{13}, and His_{14}, that can undergo oxidation. Figure 2 shows that nitration on Tyr_{10} is the principal modification, therefore it has been chosen as a marker of $A\beta_{16}$ modification for further analysis.

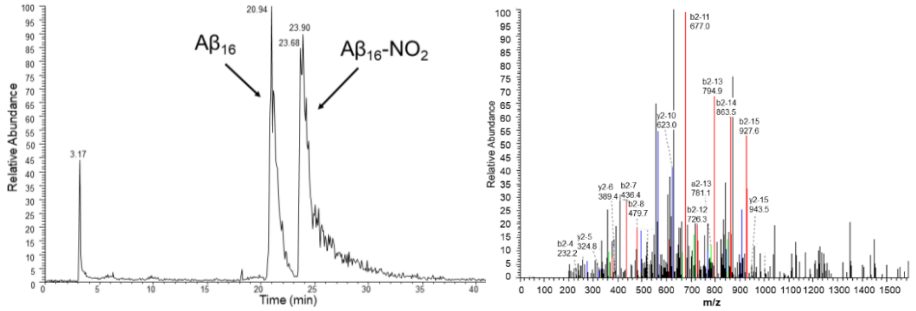

Figure 2. *HPLC chromatogram of a sample containing hemin 2 μM, $A\beta_{16}$ 10 μM, hydrogen peroxide 20 mM and nitrite 200 mM, in phosphate buffer 100 mM, pH 7.4 at 25 °C (left) and MS/MS spectrum of the peak assigned to the $A\beta_{16}$ peptide containing the nitrated Tyr_{10} residue (right).*

The time-dependent analysis of $A\beta_{16}$ nitration, both in mild (200 μM H_2O_2 / 200 μM NO_2^-) and harsh (20 mM H_2O_2 / 200 mM NO_2^-) conditions and in the presence or absence of hemin, was performed at 90 minute intervals (Figure 3). These data confirm that the presence of hemin enhances the reaction rates, doubling the nitration yield obtained after 2 hours in harsh conditions.

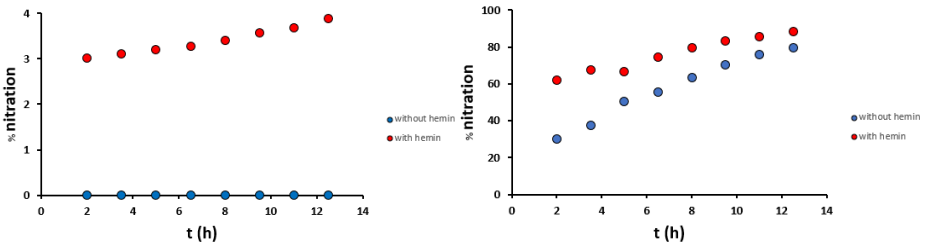

Figure 3. *Percentage nitration of the $A\beta_{16}$ peptide (10 μM) along time in mild (left) and harsh (right) conditions, in the presence (2 μM, red) and absence (blue) of hemin, in phosphate buffer 100 mM, pH 7.4 at 25 °C*

Further studies were performed adding to the reaction mixture also a phenolic/catechol substrate, to investigate its ability to protect the peptide from ROS/RNS damage. It turned out that all the substrates exhibit a protecting effect which is related to their one-electron redox potentials. Finally, the possible nitration reaction occurring on hemin was explored, but our HPLC-MS analysis show, rather than the presence of nitrated hemin, a degradation process. Probably, the hemin coordination to a small peptide like $A\beta_{16}$ is not sufficient to protect the porphyrin from degradation, differently from what previously observed with heme proteins.

Conclusions

The hemin-$A\beta_{16}$ complex exhibits a rich pseudo-peroxidase activity in the presence of H_2O_2 and NO_2^-: besides oxidation and nitration of external aromatic substrates, previously assessed with kinetic studies, it is also able to catalyze the derivatization of the bound peptide. In particular, we detected the targets (mainly Tyr_{10}) and the entities of the modifications and highlighted that external substrates and the Aβ peptide only partly protect hemin from degradation, so that intact hemin possesses a great reactivity while the reactivity of degraded hemin is lower, but not completely quenched. These results show that hemin contribution to redox reactivity in neurons should depend on the environment.

References

1. G. Chen, T. Xu, Y. Yan, Y. Zhou, Y. Jiang, K. Melcher, H.E. Xu; *Acta Pharmacol. Sin.*, 38 (2017), pp 1205-1235.
2. H. Ischiropoulos; *Arch. Biochem. Biophys*, 356 (1998), pp 1-11.
3. S. De Caro, G. De Soricelli, S. Dell'Acqua, E. Monzani, S. Nicolis; *Antioxidants*, 12 (2023), 1319.
4. G.D. Thiabaud, S. Pizzocaro, R. Garcia-Serres, J. Latour, E. Monzani, L. Casella; *Angew. Chem. Int. Ed.*, 52 (2013), pp 8041-8044.

P43

Chemical analysis and investigation of pharmacological activities of a birch bark extract from *Betula papyrifera*

Volodymyra Zuieva, Christina Bottaro, Rajendran Kaliaperumal, Matthias Bierenstiel

Memorial University of Newfoundland, 153 Park St, B1P 4W7, Sydney, NS, Canada

Birch bark has been used in cultures around the globe for medicinal purposes. However, rich indigenous knowledge of it in Atlantic Canada is at risk of being forgotten as Mi'kmaq elders pass away. One such traditional Mi'kmaq remedy is maskwiomi (maskwi = birch bark; omi = oil), an extract produced from paper birch (Betula papyrifera) in a fire pit method. This viscous extract is added to animal fats to produce a skin ointment which exhibits excellent alleviation of a variety of skin issues such as eczema, psoriasis, acne, sunburn, rashes and bug bites.

The viscous bark extract contains a complex organic matrix of over 200 compounds. Birch bark has a high concentration of triterpenes and polyphenols which have been shown to possess antioxidant and antimicrobial pharmacological activities. Most reported studies have the birch extract prepared by solvent extraction, in contrast, a torrefaction process was used to obtain the birch bark extract in this work. Our study will report the GC-MS and UPLC-MS analysis of phytochemical compounds obtained by the torrefaction process and fractions of the extract.

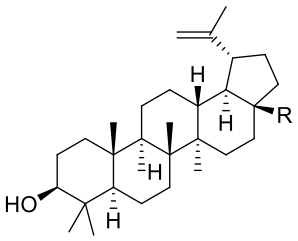

betulin (R = CH_2OH)
betulinic acid (R = COOH)

P44

Proximity-dependent Biotin Identification (BioID): a tool for screening protein- protein interactions in living cells

Pasquinna Sida, Mike Kinsella, David Scanlon

South East Technological University (SETU), X91 K0EK, Waterford, Ireland

Summary: *A detailed understanding of protein-protein interactions can aid in revealing the pathogenesis of myriad human diseases. Accordingly, the identification and characterisation of specific interactions can pave the way for the development of new therapeutics. The poster gives an overview of BioID, a powerful technique for protein interactome identification.*

Keywords: *Protein-protein interactions, Proximity-dependent biotin identification (BioID), Mass spectrometry*

Technique Overview

Protein-protein interactions (PPIs) can be considered “the molecular language of life” as they are involved in all cellular processes[1]. Human diseases such as cystic fibrosis, Alzheimer’s disease, and Huntington’s disease can be traced to abnormal PPIs[2]. These abnormal PPIs alter cellular homeostasis due to the loss of critical PPIs and/or the formation of protein complexes at the wrong location or time. To develop successful therapeutics for the treatment of these abnormal interactions a detailed understanding of the cellular system is required at the molecular level[1].

Mapping and identification of proteins, PPIs, and protein interactomes in cells is fundamental in studying protein function and biological mechanisms. For this reason, many methods have been developed to screen for PPIs. One such mass spectrometry associated method is affinity purification coupled with mass spectrometry (AP- MS). However, AP-MS has some critical limitations, primarily in detecting weaker PPIs and it exhibits difficulties in the detection of protein complexes that are localised in subcellular compartments or are inadequately soluble. Proximity-dependent biotin identification (BioID) is a mass spectrometry based technique that overcomes many of these limitations using proximity-dependent labelling (PDL)[3].

PDL involves the use of an enzyme to catalyse covalent attachment of a reactive molecule such as biotin to endogenous proteins that are in proximal distance to a bait protein. The attachment of biotin to proximal proteins enables them to be isolated and identified via mass spectrometry.

BioID employs the use of a modified biotin protein ligase to catalyse labelling of proximal proteins. BioID has been shown to identify PPIs that are difficult to detect by AP-MS. Direct comparisons with AP-MS have shown that BioID can detect a much greater quantity of interacting proteins thus demonstrating the sensitivity of the technique[4]. Recently BioID has been used to map and identify the composition of cellular compartments in human cells[5]. The technique enabled the discovery of new proteins exceeding previous techniques[5]. BioID has been applied to cancer studies[6,7], the study of proteins that are associated with Autism[8], and drug-induced PPIs in cells[9]. Recently, a range of modified biotin ligases have been developed to enhance efficiency and speed up labelling time while minimising toxicity.

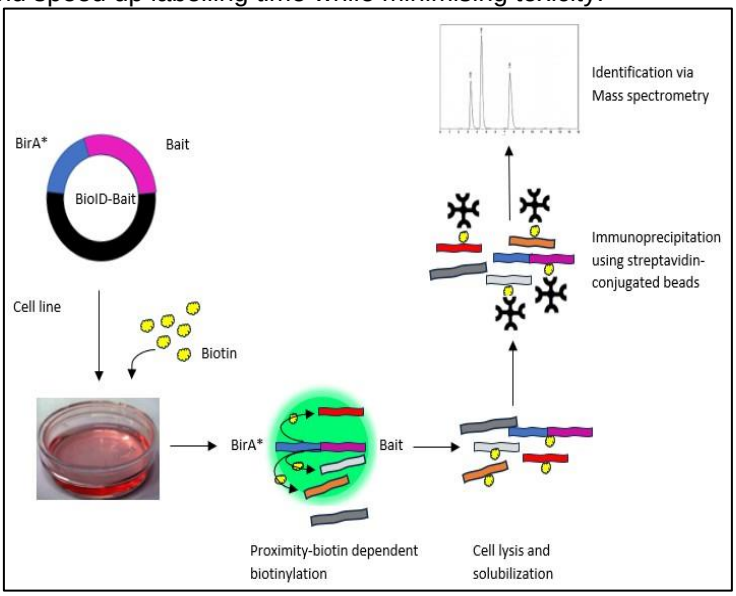

Figure 1. *Overview of BioID workflow*

References

1. Tabar, S. M., Parsania, C., Chen, H., Su, X.-D., Bailey, C. G., & Rasko, J. E. (2022). *Cell Reports Methods*, pg 100275.
2. Gonzalez , M. W., Kann, M. G. (2012). *PLoS Computational Biology*, pg e1002819.
3. Kim, D. I., & Roux, K. J. (2016). *Trends in Cell Biology*, pg 804-817.
4. Couzens A.L., Knight, J.D, Kean, M.J., Teo, G., Weiss, A., Dunham, W.H., Lin, Z.Y., Bagshaw, R.D., Sicheri F., Pawson, T., Wrana, J.L., Choi, H., Gingras, A.C. (2013). *Sci Signal,* pg rs15.
5. Christopher, G.D., Knight, J. D., Rajasekharan, A., Rathod, B., Hesketh, G.G., Abe, K.T., Youn, Ji-Y., Samavarchi-Tehrani, P., Zhang, H., Zhu, L.Y., Popiel, E., Lambert, J.P., Coyaud. É., Cheung, S.W.T., Rajendran, D., Wong, C.J., Antonicka, H., Pelletier, L., Palazzo, A.F., Shoubridge, E.A., Raught, B., Gingras, A.-C. (2021). *Nature*, pg 120-124.
6. Neville, M. C., Webb, P. G., Baumgartner, H. K., & Bitler, B. G. (2022). *Heliyon*, pg e10862.
7. Megan J. Agajanian, F. M. (2022). *Journal of Biological Chemistry*, pg 101986.
8. Murtaza, N., Cheng, A. A., Brown, C. O., Meka, D. P., Hong, S., Uy, J. A., El-Hajjar, J., Pipko, N., Unda, B.K., Schwanke, B., Xing, S., Thiruvahindrapuram, B., Engchuan, W., Trost, B., Deneault, E., Calderon de Anda, F., Doble, B.W., Ellis, J., Anagnostou, E., Bader, G.D., Scherer, S.W., Lu, Y., Singh, K. K. (2022). *Cell Reports* , pg 111678.
9. Yamanaka, S., Horiuchi, Y., Matsuoka, S., Kido, K., Nishino, K., Maeno, M., Shibata, N., Kosako, H., Sawasaki, T. (2022). *Nature Communications*, pg 183.

P45

A mass spectrometry-based multi-omics approach to explore the mechanisms of drug resistance in methicillin-resistant *Staphylococcus aureus*

Pedro C. Rosado,[1] M. Matilde Marques,[1,2] Gonçalo C. Justino [1]

[1] Centro de Química Estrutural - Institute of Molecular Sciences, Instituto Superior Técnico, Universidade de Lisboa, Av. Rovisco Pais, 1, 1049-001 Lisboa, Portugal
[2] Departamento de Engenharia Química, Instituto Superior Técnico, Universidade de Lisboa, Av. Rovisco Pais, 1, 1049-001 Lisboa, Portugal

Summary: *Exploring bacterial response to antibiotics can help elucidating antimicrobial resistance pathways and identifying new druggable targets. We used a combined mass spectrometry multi-omics approach to characterize how methicillin-resistant Staphylococcus aureus (MRSA) respond to different antibiotics, showing that integrating multi-omics data enables a comprehensive analysis of the mechanisms underlying MRSA resistance.*

Keywords: *MRSA; drug resistance; mass spectrometry.*

Introduction

Methicillin-resistant *Staphylococcus aureus* (MRSA) is a major cause of nosocomial infections, with a high mortality rate caused by multiple drug resistance. Due to the low drug availability to treat MRSA infections, there is a pressing need for innovative drugs [1]. A better understanding of antibiotic resistance mechanisms can be key in elucidating pathways for antimicrobial resistance and finding promising new targets to fight resistance[2-4]. Mass spectrometry multiple omics approach can be an asset in tackling this problem and can bring accurate and comprehensive results to understand mechanisms underlying MRSA resistance to different antibiotics and can also find promising new targets to fight antimicrobial resistance [5].

Experimental

A combined mass spectrometry approach was employed to explore the mechanism underlying the activity of ampicillin, chloramphenicol, ciprofloxacin, methicillin, and vancomycin at the lipidome, proteome and metabolome level of MRSA ATCC 43300 at 0.5× IC_{50}, IC_{50} and 2× IC_{50} concentrations.
Bacteria were seeded in Mueller-Hinton (MH) agar medium and incubated for 24 h at 37 ºC. A colony was selected for transfer to liquid MH medium and was incubated 16 h at 37 ºC at 250 rpm. An inoculum of the overnight growth was transferred to a new liquid MH medium to obtain a final optical density, measured at 640 nm (OD_{640}) of 0.02 in the presence of the selected compounds. Cells were incubated at 37 ºC for 8 h at 200 rpm and harvested to a final cell density of 1×10^9 CFU/mL. Supernatant (medium) was also collected.
Depending on the analysis, different extraction methods were applied to the cells or medium in triplicate using established approaches[4,6-7]. High-resolution mass spectrometry (HRMS) analysis was performed for each sample in triplicate using an Elute UHPLC system coupled to an Impact II QqTOF mass spectrometer with an electrospray ion source (Bruker Daltonics GmbH & Co.) (UHPLC-ESI-HRMS). Data acquisition was performed using in-house optimized methods. Metabolomics and lipidomics data were collected in both positive and negative electrospray modes coupled to RP and HILIC chromatography. Raw data were processed, analysed, and interpreted using XCMS [6]. Proteomics data analysis was performed with MaxQuant v2.1.0.0 followed by statistical analysis with Perseus v1.6.15.0 [8].

Results

Protein expression in MRSA is highly robust and greatly insensitive to the tested drugs ($p < 0.05$). Altered proteins at both the endo- and exoproteome levels are involved in DNA replication and in the PBP-dependent peptidoglycan biosynthesis pathways. ABC transporters were also found to be dysregulated. Exoproteome changes are related to quorum sensing and peptidoglycan biosynthesis, and were observed in the presence of ampicillin, ciprofloxacin, and vancomycin. At the endoproteome level, DNA repair, glycerophospholipid metabolism, and peptidoglycan biosynthesis are the main affected pathways, indicating that some of the up-regulated proteins related to transmembrane transport can be further explored as therapeutic targets. Metabolomics results evidence drug-specific and common metabolic changes across the different antibiotics, but also indicate that, except for vancomycin, all interfere with the glycan and peptidoglycan pathways, apart from a wide effect on energy production and nucleos(t)ide pathways. Interestingly, all drugs except methicillin also interfere with the molybdopterin biosynthesis, acetyl-CoA-related panthothenate and mevalonate pathways, and with folate biosynthesis. At the exometabolomic level, significant changes in arginine-dependent polyamine and pantothenate pathways are observed, together with some effect on the mevalonate pathways, which are related with cell wall biosynthesis and energy

metabolism.
Results obtained from the lipidome analysis show changes in the lipid profiles depending on the tested drug. Changes in the demethylmenaquinol-8/menaquinol-8 biosynthesis pathways were observed for ampicillin, vancomycin, and chloramphenicol, suggesting an effect in the electron transfer chain. Moreover, some changes were observed in peptidoglycan biosynthesis with ampicillin, involving the production of a specific peptidoglycan precursor, emphasizing the interference of this drug with the cell wall biosynthesis pathways.

Conclusions
In summary, the results obtained provide a comprehensive analysis of the mechanisms underlying MRSA resistance to different antibiotics, using a combined MS-omics approach (Figure 10). The characteristic changes observed can be used not only to elucidate the pathways for antimicrobial resistance to the tested drugs but can also enable finding promising new targets to overcome MRSA resistance.

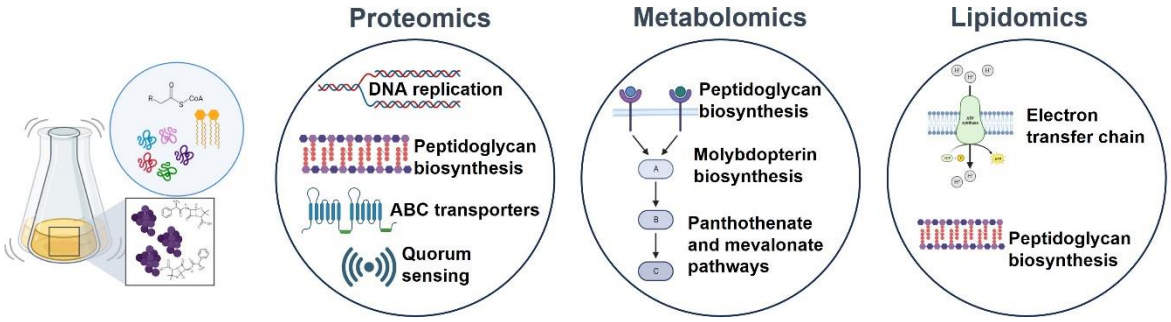

Figure 10. *Summary of the results obtained underlying MRSA resistance to different antibiotics, using a combined MS-omics approach.*

Acknowledgements
Centro de Química Estrutural is a Research Unit funded by FCT through projects UIDB/00100/2020 and UIDP/00100/2020. Institute of Molecular Sciences is an Associate Laboratory funded by FCT through project LA/P/0056/2020. The National Mass Spectrometry Network is funded through FCT (POCI-01-0145-FEDER-402-022125). PCR is an FCT-funded PhD student (UI/BD/152269/2021).

References
1. A. S. Lee, H. de Lencastre, J. Garau, J. Kluytmans, S. Malhotra-Kumar, A. Peschel and S. Harbarth; *Nat Rev Dis Primers*, (2018).
2. M. Ribeiro, S. Ceballos, P. Poeta, C. Torres and G. Igrejas; *OMICS: A Journal of Integrative Biology*, (2021), pp 711-724
3. K. Schelli, F. Zhong and J. Zhu; *Microb Biotechnol*, (2017), pp 1764-1774.
4. P. Nikolic, P. Mudgil, D. G. Harman and J. Whitehall; *Infectious Diseases*, (2022), pp 497-507.
5. D. Janiszewska, M. Szultka-Młyńska, P. Pomastowski and B. Buszewski; *Intl J Mol Sci*, (2022), pp 9601.
6. C.F. Marques, M.M. Marques and G.C. Justino; *Life Sci*, (2022).
7. C.F. Marques and G.C. Justino; *Separations* (2023).
8. C.F. Marques, P.F. Pinheiro, G.C: Justino; *STAR Protocols*, (2022).

P46

Evaluation of the best HDX-MS workflow for the analysis of Meningococcal PorB in native state

Sara Favaron,[1, 2] *Veronica Nasta,*[1] *Elisa Fasoli,*[2] *Nathalie Norais,*[1] *Lucia Eleonora Fontana* [1]

[1] GSK, Via Fiorentina 1, 53100, Siena, Italy
[2] Politecnico di Milano, Department of Chemistry, Materials and Chemical Engineering "Giulio Natta"
Piazza Leonardo da Vinci 32, 20133, Milano, Italy

Summary: *PorB, as well as other membrane proteins, can have different conformations when expressed as recombinant product or in its native environment. In order to perform reliable HDX-MS studies, various workflows were tested in order to find the best one to study PorB embedded in meningococcal detergent extracted outer membrane vesicles (dOMVs).*

Keywords: *HDX-MS, PorB, Native State*

Introduction

HDX-MS (Hydrogen-Deuterium Exchange Mass Spectrometry) is a powerful technique for investigating structural features and dynamic properties of proteins alone or in complex. In particular, it can be useful for epitope/paratope mapping studies, with important applications in drug discovery. In this context, while working with soluble recombinant proteins is relatively simple, studying membrane proteins in their native environment (e. g., embedded in outer membrane vesicles) is more challenging, since lipids cause ion suppression and loss of signal intensity during MS analysis. Many HDX-MS workflows with various delipidation steps have been investigated to study membrane proteins in their native state. This work aims at comparing different HDX-MS workflows using dOMV-embedded Meningococcal PorB as a model system. Three setups were tested: Delipidation via Size Exclusion Chromatography (SEC) coupled with online (1) and offline Digestion (2) and TCA precipitation followed by Acetone wash. (3)

Materials and Methods

MenB dOMVs were produced as previously reported. (4) Delipidation by SEC was evaluated after both online and offline pepsin digestion. On the other hand, delipidation via TCA precipitation/ Acetone wash was performed prior to online digestion of the sample. In all cases, delipidated peptides were trapped on a VanGuard column for desalting, separated over an Acquity UPLC coulmn and analyzed with a hybrid electrospray ionization quadrupole time-of-flight (ESI-Q-TOF) mass spectrometer (Synapt G2-Si, Waters). Peptide identification was carried out by tandem mass spectrometry in MS^E mode and data were processed using Protein Lynx Global Server 3.01 (Waters). DynamX V 3.0 (Waters) was the software used for peptide analysis.

Results

The three workflows were evaluated based on the number of identified peptides, % of protein sequence coverage and redundancy. The results of the analysis are reported in Table 1.

Table 1*. Schematic comparison of the coverage maps obtained with the three techniques*

HDX-MS Workflow	Peptides Number	Protein Coverage	Redundancy
1. Online Digestion + SEC	51	84.3%	3.78
2. Offline Digestion + SEC	43	78.8%	2.81
3. TCA Precipitation/Acetone Wash	127	94.5%	5.96

Conclusions

The TCA Precipitation/Acetone wash workflow was identified as the most efficient to study dOMV-embedded MenB PorB. It will be used to investigate conformation and dynamics of the protein in its native state and in its recombinant form as well as in epitope mapping studies.

References

1. V. Calvaresi, A. Redsted et al., *Analytical Chemistry* (2021)
2. L. Tsiatsiani, M. Akeroyd et al., *Analytical Chemistry* (2017)
3. D. Donnarumma, C. Maestri et al., *Journal of Proteome Research*, (2018)
4. I. Claassen, J. Meylis et al, *Vaccine*, (1996)

P47

Mass spectrometry's role in the study of correlation between oxidative stress, OSAS and obesity

Chiara Maccari,[1] Michele Miragoli,[1,2] Rosario I. Statello,[1] Agnese Martini,[3] Roberta Andreoli [1,2]

[1] Department of Medicine and Surgery, University of Parma, Parma, Italy
[2] CERT, Center of Excellence for Toxicological Research, University of Parma, Italy
[3] INAIL, the National Institute for Insurance against Accidents at Work, Department of Medicine, Epidemiology, Workplace and Environmental Hygiene, Rome, Italy

Summary: *Oxidative stress, inflammation and metabolic dysregulation are involved in the pathogenesis of more common diseases, like obesity and obstructive sleep apnea syndrome, that can have a major impact on public health. In this study we want to investigate the association between urinary biomarkers oxidative stress and these pathologies.*
Keywords: *Mass spectrometry; Oxidative stress; Obesity*

Introduction

Oxidative stress is involved in various diseases and leads to changes in macromolecules whose nature is both structural and functional. In the case of oxidative damage and proteins, an enhancement in the methyl-transferase activity was observed, resulting in an increase in methylated states of the amino acid L-arginine, namely DiMetilArginine Asymmetric (ADMA) and Symmetric (SDMA), and a decrease of NO. In case of oxidative stress and nucleic acids, a lot of different products on DNA or RNA bases were identified such as 8-hydroxy-2'deoxyguanosine (8dGuo), one of the most studied biomarkers of oxidative stress [1]. In particular this study take in exam the correlation between oxidative stress and diseases such as Obstructive Sleep Apnea Syndrome (OSAS) and obesity.
OSAS is a chronic disease which has serious economic and social implications, often under-diagnosed (cases not diagnosed in the population are 40-70%) and therefore not treated.
Instrumental diagnosis of OSAS is based on the identification of episodes of apnea and hypopnea per hour of sleep through cardio-respiratory monitoring. However, the therapeutic diagnostic path of care must start from the formulation of the clinical suspicion that should be formulated by general practitioners, Competent doctors, medical specialists and dentists through accurate medical history and research of sentinel signs/symptoms.
There is evidence that untreated OSAS may contribute to the pathophysiological mechanisms underlying the origin and/or development of hypertension, cardiac ischemia, myocardial infarction, congestive heart failure, and stroke. Of the different possible consequences of OSAS in patients, the most widely recognized may be the development of systemic hypertension.
Obesity has a similar symptomatology and causes similar damages as OSAS. Moreover, Obesity is a risk factor for OSAS development.
This study aims to investigate the relationship between OSAS, obesity and oxidative stress, through the quantification of urinary ADMA, SDMA and oxidated forms of guanine excreted in free forms in urine (8dGuo, 8Gua, and 8Guo) with LC-MS/MS, comparing them with gravity of OSAS and BMI. Knowing these relationships could allow us to better understand the mechanisms and interactions between these pathologies and oxidative stress.
This study was funded by BRIC-INAIL 2018 ID: 04 SLeeP@SA Project - Occupational health and prevention of the obstructive sleep apnea: a silent epidemic (www.sleeposas.it)".

Experimental

We recruited 164 subjects, divided into: **a.** patients with OSAS **b.** control healthy subjects.
a. 43 subjects (24 males and 19 females, with a variable BMI) were recruited from an hospital in Rome, they were asked to collect medical history and extemporary urine for the analysis of biomarkers. **b.** 121 healthy subjects, 64 males and 57 females, with variable BMI were selected to cover all the weight range (underweight, normal-weight, overweight and obese).
LC-MS/MS determinations were carried out on a API4000 triple quadrupole mass spectrometer (Sciex), equipped with a TurboIonSprayTM interface. Chromatography was performed on an Atlantis dC18 column using variable proportions of 10 mM aqueous formic acid and methanol with 5% AcCN at a flow-rate of 0.20 ml/min to quantify ADMA and SDMA. The same column but with different mobile phases (variable proportions of 10 mM aqueous formic pH 3.75 acid and methanol) was used to quantify the biomarkers of oxidative stress on nucleic acids. Quantitative analysis was performed by method of standard additions in matrix using a labelled internal standard for each analyte.

Results

We observed that the ADMA and SDMA concentrations increased with the gravity of the OSAS disease (AHI) and the BMI, suggesting an activation of the PRMT enzymes and an inhibition of the NOs synthetases (Figure 1).

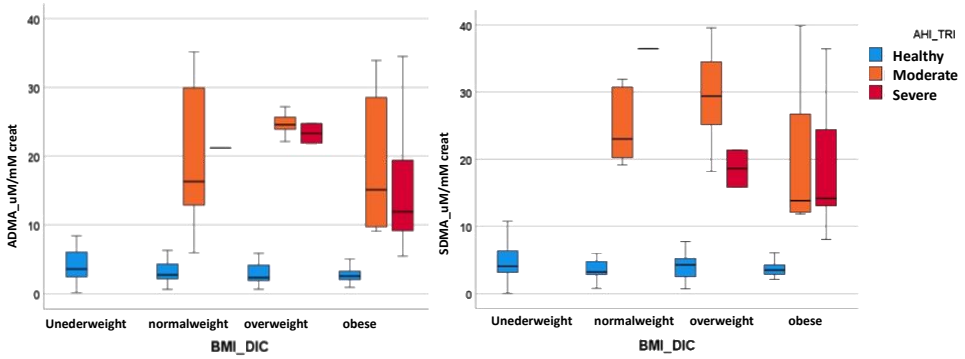

Figure 1. *Box plot of ADMA (uM/mM creat) in relationship with AHI and BMI*

Correlations between BMI, AHI and urinary concentrations of biomarkers of oxidative damage to guanine and dimethyl forms of arginine expressed as a function of creatinine were evaluated and confirmed.
The analysis of the data, in term of nucleic acid damage, indicates that BMI influences the urinary concentration of oxidative stress biomarkers, 8dGuo particularly (Figure 2).

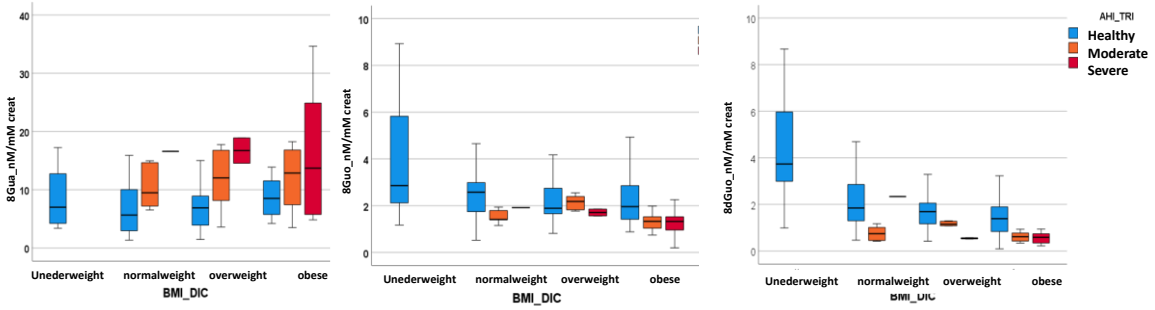

Figure 2. *Box plot of 8Gua, 8Guo and 8dGuo (nM/mM creat) in relationship with AHI and BMI.*

A negative trend was observed between BMI and 8dGuo or 8Guo. Moreover, there is a positive correlation between BMI and 8Gua, ADMA and SDMA. The levels of 8dGuo reflect the proportion of oxidative damage to DNA that has been repaired without the activation of specific pathways, differently from 8Gua which is generated by hOGG1 activity [2]. This trend could be explained by assuming a partial reduction in the efficiency of non-specific repair systems of nucleic acids when an increase in oxidative damage is observed. Same trend is observed also for 8Guo that represents the share of damage suffered by RNA and eliminated. Also for RNA no specific repair mechanisms are known, until now. The same trends were observed even if the subjects were stratified by OSAS gravity.
Although the number of the subjects involved in this study is limited, we confirmed a positive correlation between 8Guo and 8dGuo and between the dimethyl forms of arginine ADMA and SDMA.
For the first time, a positive correlation with 8Gua and a negative correlation with 8OHdG was observed for ADMA and SDMA.

Conclusions

Urinary concentrations of biomarkers of oxidative stress are affected by weight and severity of OSAS pathology. There is an increase in excretion of 8Gua, ADMA and SDMA concentrations in urine samples of subjects affected by OSAS compared to those detected in samples of healthy subjects.
The correlations expose are intriguing but should be the subject of further investigation with an increased number of cases.

References

1. Jordan W., Cohrs S., Degner D., Meier A., Rodenbeck A., Mayer G., Pilz J., Ru ̈ther E., Kornhuber J., and Bleich S., Evaluation of oxidative stress measurements in obstructive sleep apnea syndrome, 2006, J Neural Transm, 113: 239–254, DOI 10.1007/s00702-005-0316-2
2. Kang I.G, Jung J.H., and Kim S.T., The Effect of Obstructive Sleep Apnea on DNA Damage and Oxidative Stress, 2014, Clin Exp Otorhinolaryngol., 6(2): 68–72, doi: 10.3342/ceo.2013.6.2.68

P48

Laser settings' optimization for single cell MALDI-TOF MS imaging of human CD19+ lymphocytes

Ivana Marković,[1,2] Željko Debeljak,[1,2] Bojana Bošnjak,[2,3] Dario Mandić [1,2]

[1] Clinical Institute of Laboratory Diagnostics, University Hospital Centre Osijek, Osijek, Croatia
[2] Faculty of Medicine Osijek, JJ Strossmayer University of Osijek, Osijek, Croatia
[3] Clinical Institute of Transfusion Medicine, University Hospital Centre Osijek, Osijek, Croatia

Summary: *Different laser settings affect the lateral resolution of MALDI-TOF MSI of single B lymphocytes. Better differentiation of the metabolome of B lymphocytes and its surroundings is achieved with a laser diameter of 10 µm.*

Keywords: *single cell MALDI TOF MSI, lateral resolution, laser diameter*

Introduction

High lateral resolution MALDI-TOF imaging is mandatory for conducting single cell analysis and understanding cell metabolism. The aim of this study was to evaluate the impact of different laser settings on the true lateral resolution of MALDI TOF IMS analysis of human B lymphocytes.

Experimental

CD19+, mostly B, lymphocytes (cell size 8-10µm) taken from a healthy blood donor were isolated on an ITO slide and covered with a CHCA matrix using an iMLayer sublimation device (Shimadzu, Kyoto, Japan). After matrix recrystallization, 40 B lymphocytes were selected using light microscope integrated in the iMScope TRIO MALDI-TOF IMS instrument (Shimadzu, Kyoto, Japan). Cells and their surroundings (medium) mass spectra were recorded using the following settings: D0 (5 µm laser diameter, x and y pitch size 6.5x5.5 µm, 80 nJ laser energy, 20 Hz frequency, 20 shots per pixel) and D1 (10 µm laser diameter, x and y pitch size 11x9 µm, 95 nJ laser energy, 20 Hz frequency, 20 shots per pixel) in mass ranges 300-600 Da and 600-950 Da (10 cells per setting and mass range). Differences of MSI signal intensities between cells and medium were assessed as regions of interest (ROI) and were calculated by t-test implemented in IMAEREVEAL v1.1 software (Shimadzu, Kyoto Japan). Principal component analysis (PCA) was used for dimensionality reduction. $P < 0.05$ and 2-fold change signal intensities between cell and medium ROI were considered significant.

Results

As a result of different laser settings, average number of pixels per cell ROI for D0 conditions was 3 in contrast to D1, where average number of pixels was 1. This is in accordance with the number of peaks per ROI which is summarized in Table 1. There was a significant difference in peak count per cell ROI between D0 and D1 settings in both mass ranges (both $P < 0.001$).

Table 1. *Median [interquartile range] of peak count per ROI in B lymphocytes and count of statistically significant signal intensities between B lymphocyte and medium*

	Median [IQR]		**Count (%) of statistically significant signal intensities**	
	300-600 Da	**600-950 Da**	**300-600 Da**	**600-950 Da**
D0	1174 [1029-1471]	1628 [1530-2130]	132 (11.2 %)	218 (13.4%)
D1	264 [204-338]	188 [162-221]	153 (57.9%)	78 (41.5%)

Regardless the smaller total peak count per cell ROI, D1 settings had higher count and percentage of peaks whose intensity was significantly different between cells and medium (Table 1).
PCA analysis showed different results for D0 and D1 settings in metabolic differentiation of B lymphocytes and theirs medium: while in D1 settings ROI populations are fully separated, that is not the case in D0 settings (Figure 1A-D). The variance is best explained for D1 settings in mass range 300-600 Da (PC1 vs. PC2 87.5%) (Figure 1C). B lymphocyte population (blue dots) is scattered due to the physiological heterogeneity of B lymphocytes' metabolome.
Figure 2 shows optical image and overlapped MS image of one B lymphocyte and its surroundings.

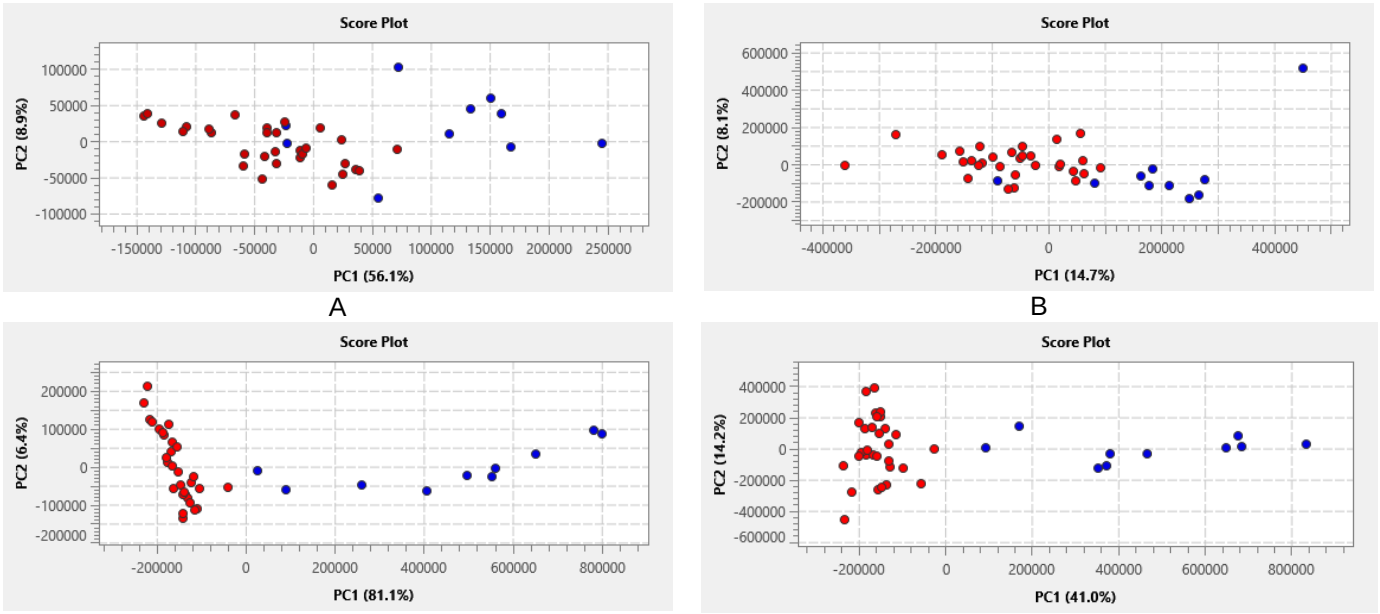

Figure 1. *PCA analysis of B lymphocytes and medium m/z signals. A) D0 300-600 Da, B) D0 600-950 Da, C) D1 300-600Da, D) D1 600-950 Da*

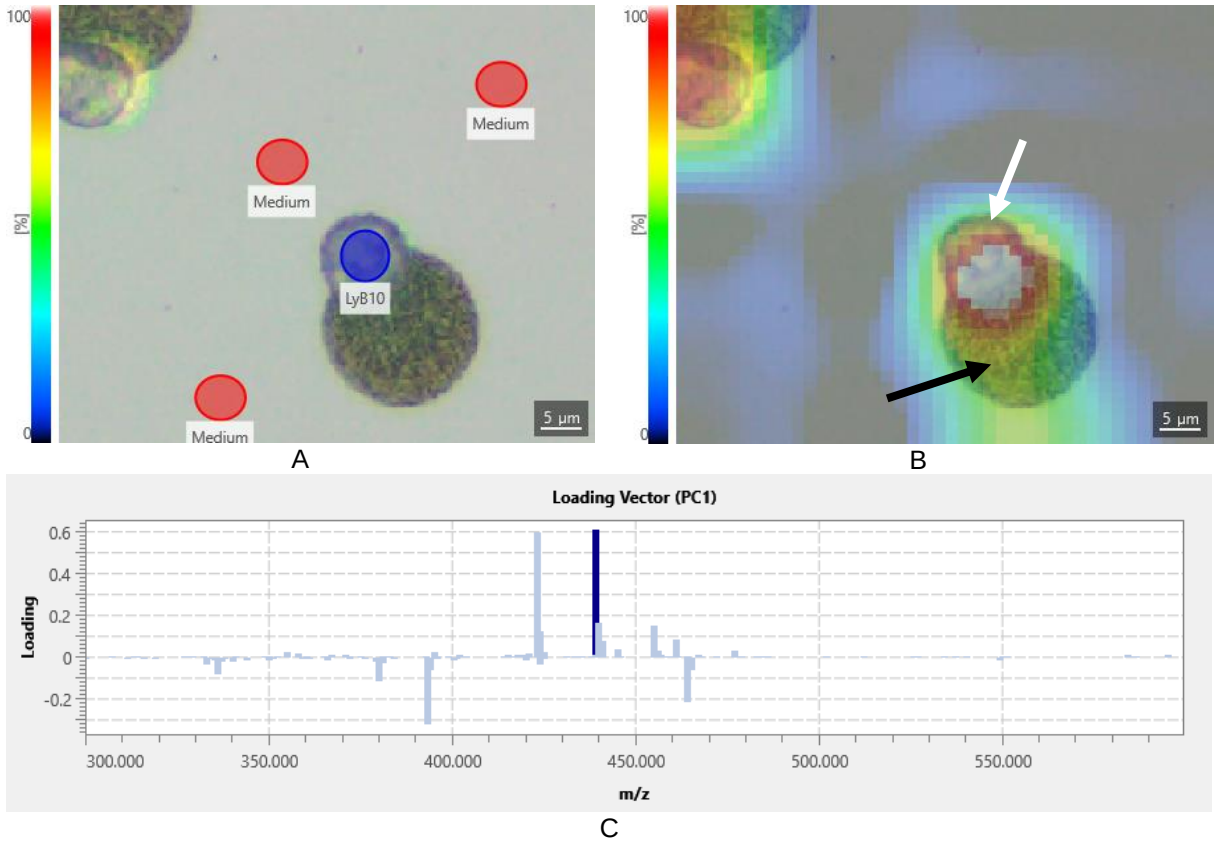

Figure 2. *Spatial distribution of m/z 439.02 Da. A) optical image of B lymphocyte with ROIs on cell and its surroundings (medium), B) MS image of m/z 439.02 Da overlapped over the optical image. It is visible that the highest signal intensity is on cell nucleus (white arrow), but some is on spilled cytoplasm (black arrow; the cell ruptured due to exposure to vacuum in the sublimation device), C) Image of PC1 loading vector showing the influence of m/z 439.02Da on variance explanation in PCA analysis.*

Conclusion

Different laser diameter has an impact on the true MALDI-TOF MSI lateral resolution. The current D1 settings can well differentiate the metabolic footprint of CD19+ B lymphocytes from their surrounding and it is suitable for the single cell analysis.

P49

BeatBox and iST for streamlined FFPE tissue processing: A xylene-free, robust, and high-throughput sample preparation for proteomic analysis

Jasmin Johansson, Katharina Limm, Silvia Würtenberger, Marcello Stein, Nils A. Kulak, Katrin Hartinger

PreOmics GmbH, Planegg/Martinsried, Germany

Summary: *We developed a fast and robust FFPE workflow for LC-MS analysis using the BeatBox tissue homogenizer and optimized iST sample preparation. This workflow eliminates the need for xylene-based deparaffinization and allows processing of up to 96 samples in parallel. It enables thorough proteomic analysis, thereby outperforming traditional sonication-based approaches.*

Keywords: *FFPE, sample preparation, BeatBox*

Introduction

Formalin-fixed, paraffin-embedded (FFPE) tissues are an invaluable resource for retrospective clinical studies to investigate molecular mechanisms or discover novel biomarkers.
However, formalin fixation makes FFPE sample preparation for proteomic analysis extremely challenging and harsh conditions must be applied to reverse cross-linking and extract proteins efficiently. In addition, paraffin interferes with liquid chromatography-mass spectrometry (LC-MS) analysis, so most protocols require an upstream xylene-based deparaffinization step, which is time-consuming, toxic, and carries the risk of sample loss.
To address these challenges, an optimized workflow combining the BeatBox tissue homogenizer and the iST kit for proteomic sample preparation has been developed. It eliminates the need for xylene-based deparaffinization and allows efficient and robust processing of 96 samples in parallel from FFPE tissue to clean peptides in one working day.

Method

Snap-frozen mouse organs (1-2 mg tissue pieces) and matching FFPE samples (10 µm curls) were processed in 96-well format using BeatBox homogenization coupled to iST sample preparation. For FFPE samples, an optimized workflow was established: FFPE curls were homogenized for 10 minutes with high-power mode in the BeatBox, followed by an one-hour incubation at 80-95°C, 1000rpm to de-crosslink, extract, reduce and alkylate proteins in one step. After cooling to room temperature, the samples were transferred to fresh plasticware while the solidified paraffin remained in the primary plasticware. Applying the iST sample preparation protocol, tryptic digestion was followed by an optimized peptide clean-up with an additional washing step designed to effectively remove last traces of paraffin. Peptides were analyzed on a nano-LC coupled to a timsTOF mass spectrometer in DIA mode.

Results

A step-by-step benchmark of this innovative workflow against a conventional xylene-based deparaffinization and sonication workflow was performed using mouse heart muscle, kidney and liver.
The same mouse tissues were preserved either fresh frozen or in FFPE format to evaluate the performance of the two tissue preservation techniques for proteomic analysis.
For FFPE tissues, BeatBox outperformed sonication for both xylene-based and xylene-free methods revealing >10% increase in protein IDs for all tissue types (Figure 1).

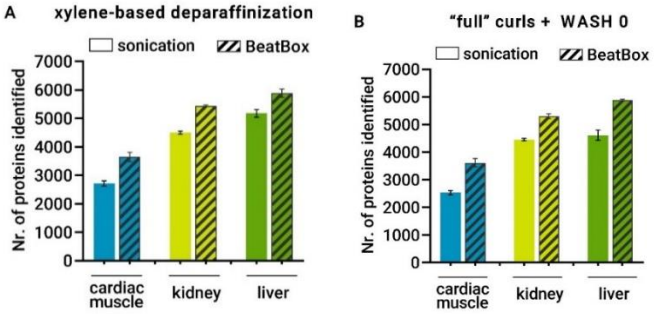

Figure 11. *Comparison of protein identifications after BeatBox and sonication-based FFPE workflows. FFPE tissue samples from mouse cardiac muscle, kidney, and liver were homogenized in triplicate either using the BeatBox or a standard sonication device. Samples were prepared using the iST technology and then analyzed via LC-MS. FFPE samples were either deparaffinized using xylene (A) or used as "full" curls treated with an optimized iST purification using WASH 0 buffer (B). Error bars represent the standard deviation.*

Comparing proteins extracted from fresh frozen and FFPE tissues, both treated with the BeatBox + iST workflow without xylene, yielded a high overlap of up to 87% of shared proteins and a similar dynamic range. In conclusion, the PreOmics´ BeatBox-iST workflow for FFPE tissues enables thorough proteomic analyses, while being easy-to-use and eliminating the need for xylene-based deparaffinization, which makes it suitable for large-scale retrospective studies.

P50

Improved detection of tryptic peptides from tissue sections using Desorption electrospray ionisation mass spectrometry imaging (DESI-MSI)

Heather Bottomley,[1] Jonathan Phillips,[1] Philippa Hart [2]

[1] University of Exeter, Stocker Road, Exeter, EX4 4PY, UK
[2] Medicines Discovery Catapult, Alderley Park, Block 35, Mereside, Macclesfield SK10 4ZF, UK

Summary: *Enhanced detection of many tryptic peptides has been acquired using DESI-MS imaging, with the addition of proteomic target list confirmation. These images are at a higher spatial resolution than the tryptic peptide images previously obtained using DESI-MSI in tissue sections.*

Keywords: *DESI imaging, Tryptic peptides, Tissue sections.*

Introduction

DESI-MSI is an ambient ionisation technique used frequently for the detection of lipids [1], small molecules [2], and drug targets [3]. Previously, DESI had only limited use for the detection of proteins and peptides in tissue [4], due to the setup and needs around deconvolution of data resulting in a small number of species being detected at lower spatial resolution. We know that there are differences in the ions detected using DESI and matrix-assisted laser desorption/ionization (MALDI) for other molecules, so we sought to identify whether this extends to proteomic species. Here, we present the use of DESI for the detection of large numbers of tryptic peptides from mouse and rat brain tissue sections, with enhanced spatial resolution when compared to previous DESI-MSI studies.

Experimental

The images were obtained with DESI using a Waters pre-commercial heated inlet (approx. 450°C) to the mass spectrometer (Waters, Synapt G2-si). Further, ion mobility separation was applied in a traveling wave ion guide with nitrogen gas to resolve spectral overlap of peptide ions and improve the detection of multiply charged species. Other DESI optimisation included the sprayer nozzle position and respective source geometries. The images acquired had a resolution of 100 µm for the rat brain sections and 50 µm for the mouse brain sections. The tryptic peptides observed were filtered against LC-MS generated (Thermo Exploris 240) proteomic target lists for consecutive sections of both the mouse and rat brain sections, allowing tentative protein assignment for each peptide ion image.

Results

Tryptic peptides were detected with DESI at precise locations in the mouse and rat brain tissue sections. These peptides were assigned protein IDs using a proteomic target list, generated from LC-MS of homogenised tissue. This allows for further interpretation of peptide function, which is of great importance when considering possible application areas of the method (e.g. biomarker discovery/monitoring). Large numbers of peptides and corresponding proteins were detected for both tissues using DESI. Therefore, the benefit of using DESI to find a greater number of tryptic peptide ions has been demonstrated, due to the improved detection of multiply charged species.

Those peptides detected through DESI that showed precise localisation were compared to the same peptides found using matrix-assisted laser desorption/ionization (MALDI). This indicates that DESI could corroborate those tryptic peptides found in MALDI or could be used as an alternative to MALDI where needed. Some spatially localised peptides ions were observed in DESI that were not found in the MALDI replicates; these were typically multiply charged peptides with a low mass to charge ratio. Further investigation is required to fully understand how many more proteins this allows to be identified, or how much these additional ions bolster protein ID from MS imaging experiments. To allow this comparison, MALDI acquisition was conducted using consecutive tissue sections and the same conditions as for DESI (with the obvious addition of a chemical matrix for ionisation).

Conclusions

Improved detection of tryptic peptides in tissue using DESI-MSI at higher spatial resolution than shown previously, has been achieved. These peptides were tentatively assigned with the addition of a proteomic target list. DESI-MSI can be used alongside MALDI-MSI for tryptic peptide confirmation, allowing drug targets to be detected in the tissue with greater certainty. The benefit of using DESI-MSI to find a greater number of localised tryptic peptide ions has been demonstrated, due to the improved detection of multiply charged species.

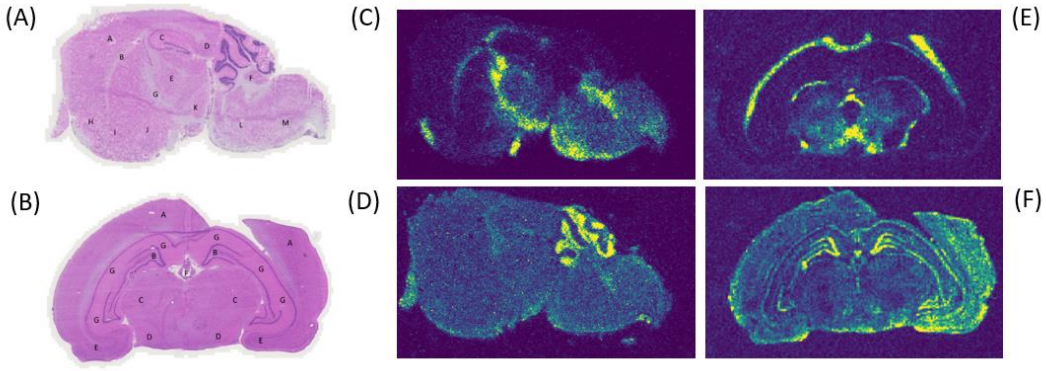

Figure 12. *H&E stain of a consecutive section of (A) mouse brain and (B) rat brain after DESI-MSI. For the mouse brain, A - Cerebral cortex, B - Corpus callosum, C – Hippocampus, D – Midbrain, E – Thalamus, F – Cerebellum, G – Fornix, H - Anterior Olfactory nucleus, I - Ventral Striatum, J - Basal Forebrain, K – Hypothalamus, L – Pons, M – Medulla. For the rat brain, A - Parietal Cortex, B – Hippocampal Dentate Gyrus, C – Thalamus, D – Hypothalamus, E - Amygdaloid Nucleus, F - Habenular Nucleus, G - Cornu Ammonis. Examples of DESI-MSI generated images, showing the precise localisation of corresponding proteins for tryptic peptides from mouse brain sections. These proteins include: (C) ATP synthase subunit alpha, 517.9128 m/z ± 54.9 ppm and (D) Pyruvate dehydrogenase E1 component subunit alpha, 494.7287 m/z ± 84.2 ppm. Examples of DESI-MSI generated images that show the precise localisation of corresponding proteins for tryptic peptides from a rat brain sections. These proteins include: (E) Glutamate receptor ionotropic kainate 1, 566.2651 m/z ± 5 ppm and (F) Atrial natriuretic peptide receptor 1, 459.2229 m/z ± 48.2 ppm.*

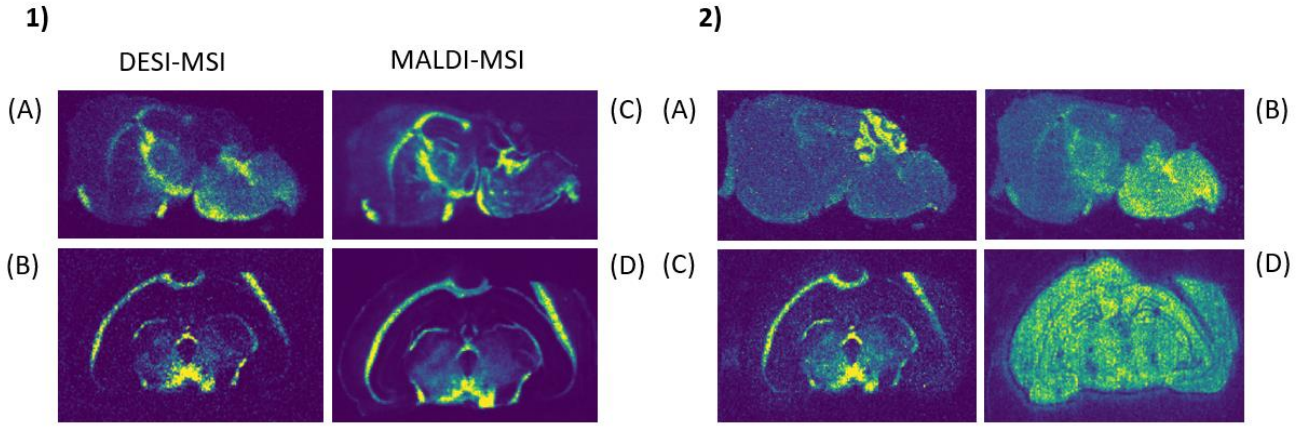

Figure 2. *1) DESI-MSI compared to MALDI-MSI for corresponding proteins from tryptic peptides in these example images obtained from mouse brain sections and the rat brain sections. Including a mouse brain section with tryptic peptide ATP synthase subunit alpha for both images (A) 517.9128 m/z ± 54.9 ppm and (C) 1553.738 m/z ± 32.4 ppm. A rat brain section with Gamma-enolase for both images (B) 550.7667 m/z ± 79.6 ppm and (D) 1099.519 m/z ± 0.156 Da. 2) DESI-MSI can identify corresponding proteins for the tryptic peptides that have not been detected using MALDI-MSI in the mouse brain for these replicates. These include, (A) Rap1 GTPase-GDP dissociation simulator 1, 483.7967 m/z ± 44 ppm and (B) Neural cell adhesion molecule, 1670.3024 m/z ± 216.3 ppm. DESI-MSI can identify peptides that have not been detected using MALDI-MSI in the rat brain for these replicates. These include, (C) Gamma-aminobutyric acid receptor subunit beta, 726.3945 m/z ± 96.8 ppm and (D) Serine protease inhibitor A3K, 842.4849 m/z ± 98.3 ppm.*

References

1 J. M. Wiseman, D. R. Ifa, Q. Song, and R. G. Cooks, *Angew. Chemie - Int. Ed.*, vol. 45, no. 43, pp. 7188–7192, 2006, doi: 10.1002/anie.200602449.
2 N. B. Holm, M. Deryabina, C. B. Knudsen, and C. Janfelt, *Anal. Bioanal. Chem.*, vol. 414, no. 24, pp. 7167–7177, 2022, doi: 10.1007/s00216-022-04269-z.
3 L. Lamont *et al.*, *Anal. Chem.*, vol. 90, no. 22, pp. 13229–13235, 2018, doi: 10.1021/acs.analchem.8b03857.
4 M. W. Towers, T. Karancsi, E. A. Jones, S. D. Pringle, and E. Claude, *J. Am. Soc. Mass Spectrom.*, vol. 29, no. 12, pp. 2456–2466, 2018, doi: 10.1007/s13361-018-2049-0.

P51

MS fingerprinting of cyclic modified peptides and proteins with chloromethyl acryl reagents

Maria J. S. A. Silva,[1,3] Lujuan Xu,[1,2] Pedro M. P. Gois,[3] Seah Ling Kuan,[1,2] Tanja Weil [1,2]

[1] Max-Planck Institute for Polymer Research, Ackermannweg 10, 55128 Mainz, Germany
[2] Institute of Inorganic Chemistry I, Ulm University Albert-Einstein-Allee 11, 89081 Ulm, Germany
[3] Research Institute for Medicines (iMed.ULisboa), Faculty of Pharmacy, Universidade de Lisboa 1649-003 Lisbon, Portugal

Summary: *Site-selective modification of peptides and proteins enables the design of new well-defined hybrids useful for advanced bioimaging or targeted therapies. Mass spectrometry tools are essential to investigate the selective modification of peptides/proteins at single disulfide bridge by new bioconjugation reagents like chloromethyl acryl, and structural confirmation of synthesized bioconjugates.*

Keywords: *Trypsin digestion, LC-MS/MS analysis, cross-linked bioconjugates*

Introduction

Somatostatin (SST) and lysozyme are two biomolecules with solvent-accessible disulfide bridges that were efficiently modified by the bifunctional 2-chloromethyl acrylates equipped with a PEG-Tz crosslink.[1] The site-selectivity of these new bioconjugation handles were further confirmed based on LC-MS/MS studies for MS fingerprinting of the afforded conjugates.

Experimental

Purified conjugates were digested with trypsin in ammonium carbonate with 1:20 (*w/w*), activated trypsin/protein at 37ºC for 2-20h. If necessary the digestion was quenched with formic acid. Samples for LC-MS analysis were diluted 4 times in ammonium acetate solution (20 mM, pH 7.0).

Liquid chromatography–mass spectrometry (LC-MS) measurements were conducted using a Dionex Ultimate 3000 UHPLC+ system equipped with a Multiple-Wavelength detector, an imChem Surf C18 TriF 100 Å 3 µm 100 x 2.1mm column connected to Thermo Scientific Q Exactive hybrid quadrupole-Orbitrap mass spectrometer (Thermo ScientificTM Q ExactiveTM Plus). Tryptic peptides were separated with a 0.2 mL/min and mixture of water with 0.1% formic acid (buffer A) acetonitrile with 0.1% formic acid (buffer B), with a gradient from 3 to 95 %B over 90 min, at a flow rate of 0.2 mL/min. The exact mass spectrometer was operated in the positive ion mode with alternating MS scans of the precursor ions and AIF (all ion fragmentation) scans in which the peptides were fragmented by SID (Surface-Induced Dissociation) of 50 eV. Both scan types were performed with 70000 resolution (at *m/z* 200) with each scan taking 0.05 s, and the maximum fill time was set to 1 s as well. The *m/z* range for the MS scans was selected between 300–1600, and the *m/z* range for AIF scans was chosen between 150–1600. The target value for the MS scans was 10^6 ions, and the target value for the AIF scans was 3 x 10^6 ions. Skyline software[2] was used to generate the list of Lysozyme digestion fragments from *in silico* trypsin digestion. The simulation of protein digestion also considered zero missed cleavages, no Methionine oxidation and all Cys in reduced form. All generated fragments were combined and added PEG-Tz crosslink as a structural modification variable on Cys residues. For the analysis, the transition list was used to check Extracted Ion chromatogram (EIC) within a 6 ppm range for all possible fragments that included precursor charges of 1 to 6, within 300-1600 *m/z* range.

Results

As illustrated in Figure 1A, a 2h trypsin digestion of SST-PEG-Tz generated Fragment 1 with the PEG-Tz cross-linker attached. Both peaks *m/z* 440.1918 $[M+3H]^{3+}$ and 659.7853 $[M+2H]^{2+}$ were detected in the LC-MS analysis, validating the proposed structure for the double modified SST peptide. The site of modification was further investigated with MS/MS fragmentation using SID 50 eV. The b and y ions detected are displayed in Figure 1B and C.

On the other hand, lysozyme is a larger substrate that required extended trypsin digestion (20h). To validate the site-selectivity of PEG-Tz crosslink for C6 and C127 of Lysozyme C (P00698), all possible S-S rebridging positions were considered.

Among the four disulfide bridges of lysozyme, only one was selectively modified by the chloromotheyl-PEG-Tz cross-linker. The C6-C127 is the most solvent-accessible and probably the bioconjugation site. Indeed, only the tryptic fragment with cross-linked C6 to C127 was detected by LC-MS, confirming the proposed structure. Additional MS/MS fragmentation further validated that the reagent selectively modified the Cys residues present on this detected fragment.

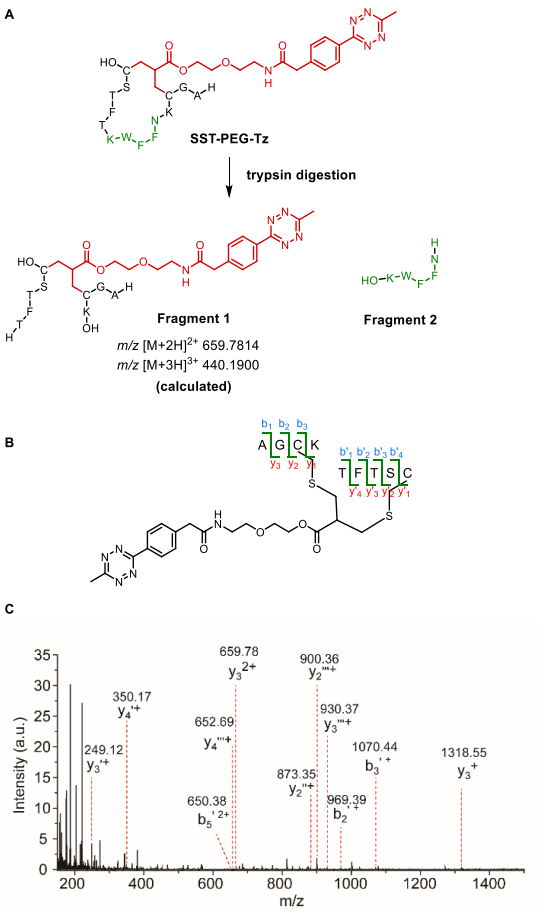

Figure 14. *A) Tryptic fragments of SST-PEG-Tz; B) expected b and y ions from AIF; C) Full spectrum of fragment 1 using SID 50 eV.*

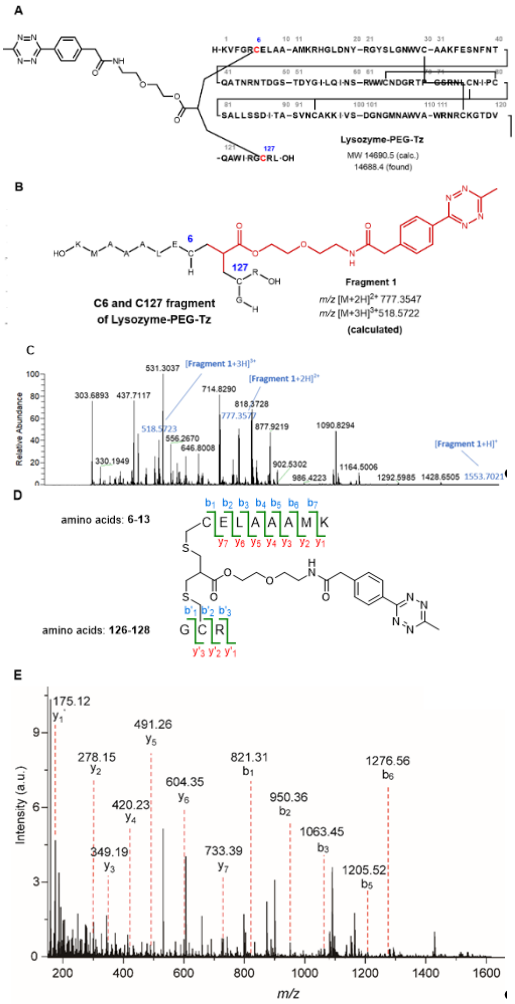

Figure 13. *A) Structure of Lysozyme-PEG-Tz; B) Detected tryptic fragment C6 and C127; C) Full spectrum of detected fragment, ions found are highlighted in blue; D) expected b and y ions from AIF; E) Full spectrum of fragment 1 using SID 50 eV.*

Conclusion

LC-MS/MS studies were crucial to validate the proposed peptide and protein conjugates. Based on these results, the chloromethyl acrylates are efficient reagents for disulfide rebridging, through highly specific two consecutive thiol-Michael additions.

References

1. L. Xu, M. J. S. A. Silva, P. M. P. Gois, S. L. Kuan, T. Weil, *Chem. Sci.* 2021, 12, 13321-13330.
2. B. MacLean, D. M. Tomazela, N. Shulman, M. Chambers, G. L. Finney, B. Frewen, R. Kern, D. L. Tabb, D. C. Liebler, M. J. MacCoss, *Bioinformatics* 2010, 26, 966-968.

P52

Derivatization-targeted analysis of amino compounds: from neutral loss scan to dynamic multiple reaction monitoring mode

Larissa Silva Maciel,[1] *Arianna Marengo,*[2] *Michaela Hříbková,*[1,3] *Koit Herodes* [1]

[1] Institute of Chemistry, University of Tartu, Tartu, Estonia
[2] Dipartimento di Scienza e Tecnologia del Farmaco, Università di Torino, Torino, Italy
[3] Department of Pharmaceutical Chemistry and Pharmaceutical Analysis, Charles University Hradec Králové, Czech Republic

Summary: *Derivatization-targeted analysis is an approach employed for the identification of compounds, narrowing down the number of possibilities. A sample is submitted to derivatization with diethyl ethoxymethylenemalonate enabling the detection of amino compounds by neutral loss scan mode, due to the loss of a neutral ethanol fragment from the derivatives' parent ion by LC-MS/MS.*

Keywords: *derivatization, diethyl ethoxymethylenemalonate, neutral loss scan mode.*

Introduction

The field of metabolomics is dedicated to the identification and quantification of metabolites in biological samples [1]. One of the widely used techniques for metabolite identification is liquid chromatography-tandem mass spectrometry (LC- MS/MS), since it is sensitive and provides information about the molecular weight and functional group of compounds. Currently, there is no available technique selective and sensitive enough to cover the wide range of diversity of metabolites, complicating the process of their identification. A way to narrow down the number of compound possibilities is through derivatization, where a moiety is introduced in the analyte of interest by a chemical reaction. Diethyl ethoxymethylenemalonate (DEEMM) was chosen as the derivatization reagent for amines since the reaction is carried out in a straightforward manner and because of the constant fragmentation pattern of the DEEMM-derivatives: the loss of a neutral fragment (46, ethanol molecule) from the parent ion. This follows to employ neutral loss scan (NLS) mode, allowing the detection of all the compounds that lose a specific neutral fragment upon fragmentation, in an approach called derivatization-targeted analysis. For example, 33 amino compounds were detected and semi-quantified in the extracts of five Cardueae species in NLS. Compounds identified at level 1, i.e. by the injection of a reference standard, can be quantified by multiple reaction monitoring (MRM) mode since it is more sensitive. This complementary step was applied to agricultural by-products and bee products.

Results and conclusion

The first part of the work was dedicated to making the NLS chromatographic profile cleaner, since several compounds, such as the excess of DEEMM and its hydrolysis product, interfered with the detection of amines. The best approach was adding a quenching reagent after 2 h, namely hydroxylamine, due to its solubility in the reaction media and its short retention time [2]. The method was applied to five cardueae species, four *Carduus* and three *Ptilostemon casabonae* (L.) Greuter samples from different locations and overall, 33 amino compounds were detected and semi-quantified in NLS. Statistically analyses (e.g. PCA, PLS-DA) revealed that the samples can be discriminated at the genus level [3]. The same approach has been employed for agricultural by- products and bee products, with an additional step of quantification of the detected amines in MRM mode. In conclusion, the derivatization-targeted analysis of amino compounds approach is useful for a variety of samples studied for different purposes.

References

1. J.R. Idle, F.J. Gonzalez, *Cell Metab*. 6 (2007) 348–351. https://doi.org/10.1016/j.cmet.2007.10.005.
2. L.S. Maciel, A. Marengo, P. Rubiolo, I. Leito, K. Herodes, *J. Chromatogr. A*. 1656 (2021) 462555. https://doi.org/10.1016/j.chroma.2021.462555.
3. A. Marengo, L.S. Maciel, C. Cagliero, P. Rubiolo, K. Herodes, *Plants*. 12 (2023). https://doi.org/10.3390/plants12020319.

P53

A spatial multi-omics investigation into spinal cord remodeling in mouse mutant strains with altered myelin basic protein abundance

Rachel Pryce,[1] *Hooman Bagheri*,[2] *Alan C. Peterson*,[2] *Pierre Chaurand* [1]

[1] Department of Chemistry, Université de Montréal, Montreal, Quebec, Canada
[2] Department of Neurology and Neurosurgery, McGill University, Montreal, Quebec, Canada

Summary: *Myelin basic protein (MBP) is the basic structural protein of myelin and changes in abundance of MBP can be monitored by mass spectrometry imaging techniques. This allows the detection and characterization of region-specific changes. Lipidomic changes were monitored in parallel and showed significate restructuring of the spinal cord.*

Keywords: *Mass spectrometry imaging, Myelin basic protein, Lipidomics*

Introduction

Myelin basic protein (MBP) is responsible for connecting the lipid layers of the myelin sheath [1]. It is believed to be a limiting factor in the production of myelin. The inability to properly construct myelin greatly decreases the efficiency of nerve conduction and occurs in several neurodegenerative diseases, such as multiple sclerosis [2]. It is hypothesized that MBP dysregulation may be an important factor in the genesis of these diseases, prompting the production of mouse models that are genetic mutants for the *Mbp* gene`s enhancer region. These mutants produce between 160-8% of wild-type *Mbp* mRNA, which results in major reconstruction of the mouse spinal cord [2]. The shiver mouse which is not expressing the *Mbp* gene was also investigated.

Methods

Five tissue microarrays (TMA) were prepared using dissected spinal cord cervical regions at post-natal day 90 (P90). Embedding was performed in 1.5% carboxymethyl cellulose. Each TMA contains a spinal cord from each genotype. All TMAs were analyzed in triplicate. TMAs were cut at 12 µm thickness using a cryostat.

The relative abundance and distribution of MBP were measured within the spinal cord using mass spectrometry imaging (MSI) to differentiate between the grey and white matter. Sections were first digested overnight with trypsin before analysis by MALDI MSI using spray deposited alpha-cyano-4-hydroxy cinnamic acid (CHCA) as a matrix [3]. A reporter MBP tryptic peptide was used to measure relative MBP abundance within the white matter across the mutant cohort.

After determining that the genetic changes greatly affected the abundance of MBP, other potential molecular changes were considered. As cholesterol makes up 44% of the lipid component of myelin, it was monitored using silver-assisted LDI MSI [4]. Changes in phospholipid abundance were also investigated using dual polarity MALDI MSI using 1,5-diaminonapthelene (1,5-DAN) as matrix [5].

MSI was performed at 50 µm (MBP, Cholesterol) or 75 µm (phospholipids) spatial resolution using a ultrafleXtreme MALDI-TOF MS (Bruker Daltonics) in reflectron geometry. Data analysis was performed using flexImaging v4.1 (Bruker Daltonics) and the R package Cardinal (v3.2).

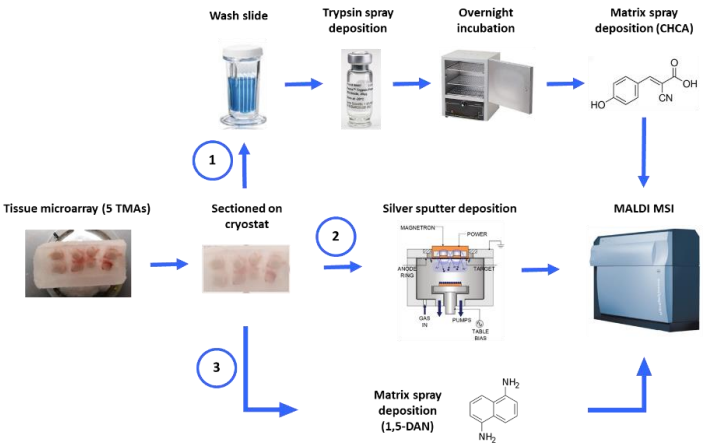

Figure 1. *Methodology used for the monitoring of 1) MBP peptides, 2) cholesterol and 3) phospholipids by MSI.*

Results

In 90-day old mice, levels of MBP were shown to range from 120-8% of the wild-type, corresponding to a range from 122-25% Mbp mRNA in these mice. A strong correlation was therefore seen between the amount of Mbp mRNA and the amount of MBP detected (Figure 2).

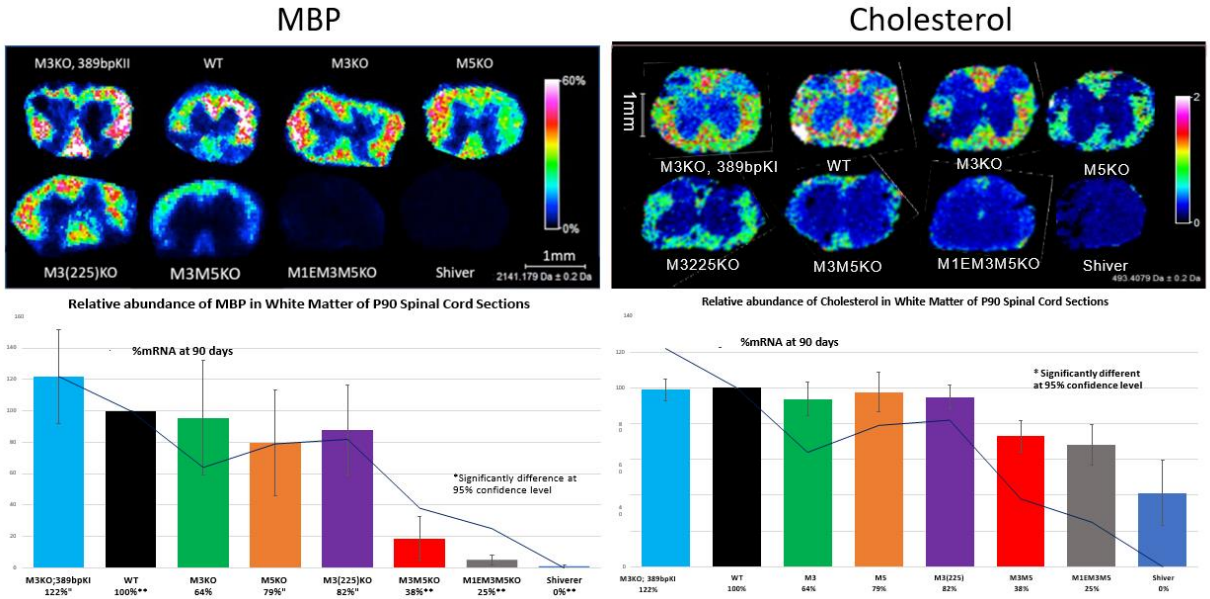

Figure 2. *Top: P90 distribution of MBP and cholesterol in mouse spinal cord measured by MALDI and AgLDI MSI, respectively. Bottom, P90 relative white matter MBP and cholesterol amounts with respect to wild type (WT) for all mutant and Shiver mice. The solid black trace indicates Mbp mRNA expression levels.*

Cholesterol levels remained stable for the single mutation knockouts (122-64 % Mbp mRNA) but reduced significantly in the double (38% *Mbp* mRNA) and triple (25% *Mbp* mRNA) knockouts (by 27 and 32% respectively), falling to about 40% of WT cholesterol levels in the white matter of the shiver mouse (0% *Mbp* mRNA) (Figure 2). Interestingly, a slight increase in cholesterol levels was observed in the grey matter of the triple-knockout mouse and the shiver negative control.

For phospholipids, significant changes were detected in both the white and grey matter with decreasing Mbp mRNA expression (Figure 3). For example, PC(36:3) increased 6-fold in the white matter, whereas PA(44:9) decreased to about 10% of the wild-type levels in the white matter. Interestingly, PE(P-40:6), which is localized to the grey matter, increased 3-fold. Overall, about 80 lipid species showed distinctive variation trends with decreasing *Mbp* mRNA expression, many of which are statistically significant.

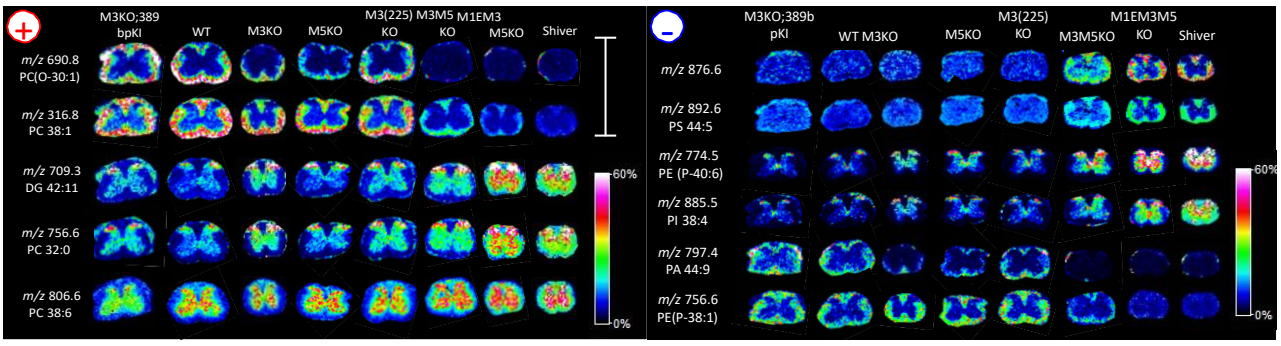

Figure 3. *P90 distribution of selected phospholipids in mouse spinal cord measured by dual polarity MALDI MSI.*

The sum of these results demonstrates that at P90, alterations in MBP abundance leads to the extensive remodeling of both the spinal cord white and grey matter. These results may also shed valuable insights in the onset and development of demyelination neurologic disorders.

References

1. Podbielska et al., *Int. J. Mol. Sci*. 22(14), 2020, 7319
2. Bagheri, et al. *PLoS Genet*. 16(8) 2020.
3. Clemis, et al. Anal. Chem. 84, 2012, 3514-3522
4. Dufresne et al., *Anal Chem*, 85, 2013, 3318-3324
5. Thomas et al., *Anal. Chem*., 84, 2012, 2048-2054

P54

Finding the molecules transported by SLCs: machine learning supported targeted metabolomics

Christoph Bueschl,[1] Iciar Serrano,[1] Juan Sanchez,[1]Daniela Reil,[1] Kristaps Klavins,[1] J. Thomas Hannich,[1] Sabrina Lindinger,[1] Abigail Jarret,[1] Tabea Wiedmer,[1] Giulio Superti-Furga [1,2]

[1] CeMM Research Center for Molecular Medicine of the Austrian Academy of Sciences, Vienna, Austria
[2] Center for Physiology and Pharmacology, Medical University of Vienna, Vienna, Austria

Summary: *A method for discovering compounds delivered by certain SLCs is presented here. It is a targeted metabolomics approach comprised of approximately 200 well-known substances that are examined using high-performance LC-QQQ-MS equipment and custom-tailored quantification software to power WP2 of the RESOLUTE project.*

Keywords: Mass spectrometry, Big Data, Bioanalysis

Introduction

The innovative medicines initiative funded RESOLUTE consortium is a public-private partnership systematically investigating the solute carrier family. Solute carrier transporters (SLCs) are an understudied but therapeutically relevant protein family with 446 members. SLCs regulate metabolism directly by controlling metabolite transport across membranes at the cell surface and between sub-cellular compartments. We use targeted metabolomics to study metabolism in a systematic family-wide manner and relate metabolic phenotypes to SLC function. The goal is to address SLCs individually and using a guilt-by-association principle.

Methods

We have developed a high-through-put workflow to grow inducible SLC overexpressing cell lines, extract metabolites and quantify them in a reproducible manner.
We use an ion-pairing, reversed phase chromatographic separation coupled to triple quadrupole dynamic MRM mass spectrometry to allow absolute quantification of 200 metabolites of which around 140 can robustly be detected in our cellular systems representing more than 50 metabolic pathways.

Results and conclusion

After manually integrating already more than 300'000 chromatographic peaks, we are using machine learning to automatize peak picking and peak integration. Data is visualized using an in-house data pipeline. Metabolite changes in response to over-expression of specific SLCs are used to identify primary substrates directly or to deorphanize SLCs based on similarity to SLCs with known substrates. Targeted metabolomics data is eventually integrated with proteomics and transcriptomics data to further deepen the understanding of SLC biology and function**.**

References

1. Superti-Furga G, Lackner D, Wiedmer T, Ingles-Prieto A, Barbosa B, Girardi E, Goldmann U, Gürtl B, Klavins K, Klimek C, Lindinger S, Liñeiro-Retes E, Müller AC, Onstein S, Redinger G, Reil D, Sedlyarov V, Wolf G, Crawford M, Everley R, Hepworth D, Liu S, Noell S, Piotrowski M, Stanton R, Zhang H, Corallino S, Faedo A, Insidioso M, Maresca G, Redaelli L, Sassone F, Scarabottolo L, Stucchi M, Tarroni P, Tremolada S, Batoulis H, Becker A, Bender E, Chang YN, Ehrmann A, Müller-Fahrnow A, Pütter V, Zindel D, Hamilton B, Lenter M, Santacruz D, Viollet C, Whitehurst C, Johnsson K, Leippe P, Baumgarten B, Chang L, Ibig Y, Pfeifer M, Reinhardt J, Schönbett J, Selzer P, Seuwen K, Bettembourg C, Biton B, Czech J, de Foucauld H, Didier M, Licher T, Mikol V, Pommereau A, Puech F, Yaligara V, Edwards A, Bongers BJ, Heitman LH, IJzerman AP, Sijben HJ, van Westen GJP, Grixti J, Kell DB, Mughal F, Swainston N, Wright-Muelas M, Bohstedt T, Burgess-Brown N, Carpenter L, Dürr K, Hansen J, Scacioc A, Banci G, Colas C, Digles D, Ecker G, Füzi B, Gamsjäger V, Grandits M, Martini R, Troger F, Altermatt P, Doucerain C, Dürrenberger F, Manolova V, Steck AL, Sundström H, Wilhelm M, Steppan CM. The RESOLUTE consortium: unlocking SLC transporters for drug discovery. Nat Rev Drug Discov. 2020 Jul;19(7):429-430. doi: 10.1038/d41573-020-00056-6. PMID: 32265506.
2. Bueschl C, Doppler M, Varga E, Seidl B, Flasch M, Warth B, Zanghellini J. PeakBot: machine-learning-based chromatographic peak picking. Bioinformatics. 2022 Jun 27;38(13):3422-3428. doi: 10.1093/bioinformatics/btac344. PMID: 35604083; PMCID: PMC9237678.

P55

Exploring the cellular actions of chelerythrine employing an untargeted mass spectrometry proteomics approach

Artem Petrosian, Pedro F. Pinheiro, Gonçalo C. Justino

Centro de Química Estrutural - Institute of Molecular Sciences, Instituto Superior Técnico, Universidade de Lisboa, 1049-001 Lisboa, Portugal

Summary: *Chelerythrine is a natural alkaloid that exhibits a strong anti-proliferative effect on Jurkat, LNCap, and MM.1S. At a proteome level, while the effect on MM.1S is system-wide effect characterized by increased protein expression, in Jurkat cells is centred around the cytoskeleton and chromatin subcellular structures.*

Keywords: *Chelerythrine, proteomics, cell response.*

Introduction

In 2020, an estimated 4 million people were diagnosed with cancer, and 1.9 million deaths were reported.[1] Despite all the advances in treatment and the increased survival rate in past decades, cancer still remains one of the leading causes of death worldwide.

Chelerythrine is a well-known membrane-permeable alkaloid which selectively inhibits protein kinase C and has served as the base for many potential new cancer-targeting drugs. While it displays a potent activity against cancer cell lines, inducing apoptosis and delaying tumour growth, a complete overview of chelerythrine action is yet to be achieved.[2]

Experimental

In this study, we tested the anticancer activity of chelerythrine on model T-cell leukemia (Jurkat), metastatic prostate cancer (LNCap), and IgAl-over-expressing B lymphoblast cell line from multiple myeloma (MM.1S) cell lines. Cytotoxicity values for each cell line were determined using the resazurin reduction assay in 96-well plates.

Jurkat and MM.1S cells were then exposed to chelerythrine at correspondent EC_{10} and EC_{50} concentrations for 48 h, and cells were harvested for an untargeted proteomics protocol. Briefly, cells were flash-frozen in liquid nitrogen and lysed by freeze-thaw cycles. A filter-assisted sample preparation (FASP) protocol was employed to process the SDS-solubilized lysed cells, where cysteine alkylation and tryptic digestion were carried out on 30 kDa MWCO ultra-filtration regenerated cellulose centrifugal filters.[3] Tryptic digests were analysed on a Impact II QqTOF (Bruker) interfaced through an ESI source to an Elute UPLC system, employing a routine chromatographic separation on a XB-C18 column (Phenomenex) using gradient mixtures of 0.1 % formic acid-acidified water and acetonitrile as mobile phase.[4] Data were processed with MaxQuant [5] for peptide and protein identification (employing a fixed Cys carbamidomethylation and variable Met oxidation, N-terminal acetylation, and Ser/Thr/Tyr phosphorylation modifications); statistical analysis was performed on Perseus,[6] and enrichment and functional analysis were carried out with Strings.[7]

Results

Chelerythrine exhibits an anti-cancer effect with EC_{50} values lower than 20 µM for the tested cell lines, which is comparable to some anticancer drugs (Figure 1).

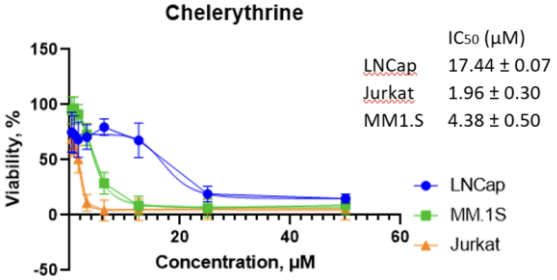

Figure. 15. *Dose-response curves and IC_{50} values of chelerythrine for LNCap, Jurkat and MM.1S cell lines.*

At a proteome level, MM.1S cells response to chelerythrine at either the EC_{50} (Figure 2) and EC_{10} encompasses changes in proteins predominantly involved in ribosomal and endoplasmic reticulum protein processing, specifically telomerase assembly, protein localization regulation, and chaperone-assisted refolding (Figure 2).

Up-regulated proteins include 6 members of the heat shock protein family (HSP90AB1, HSP90B1 HSPA5, HSPA8, HSPA9, HSPD1), implying a role for this alkaloid in the cellular response to specific stress stimuli. 40S and 60S are also widely up-regulated (Figure 3) in agreement with the overall up-regulation of protein production. Altogether, results indicate that chelerythrine leads to an overall increase of protein production, in agreement with its pleiotropic effects in many signalling pathways described in the literature.[8]

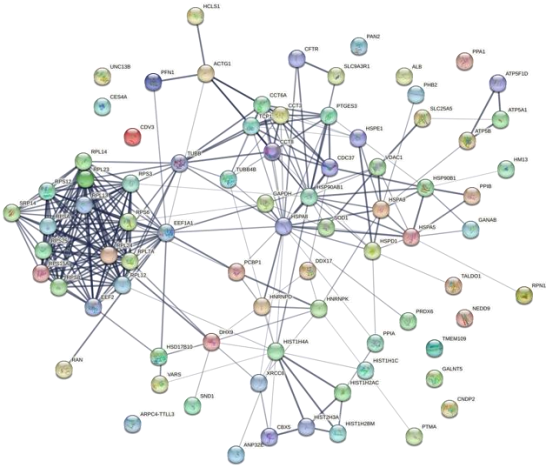

Figure 2. *Physical protein subnetworks derived from the significantly ($p < 0.05$) dysregulated proteins identified in chelerythrine-exposed MM.1S cells at EC_{50} concentration.*

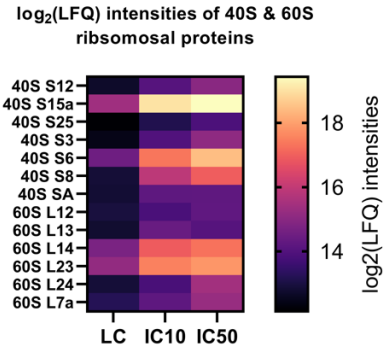

Figure 3. *Up-regulation of the 40S and 60S ribosomal proteins identified upon MM.1S exposure to chelerythrine at EC_{50} concentration.*

In Jurkat cells, chelerythrine induced the dysregulation of proteins that are annotated predominantly as structural constituents of chromatin and of the cytoskeleton (Figure 4), including tubulin and actins.

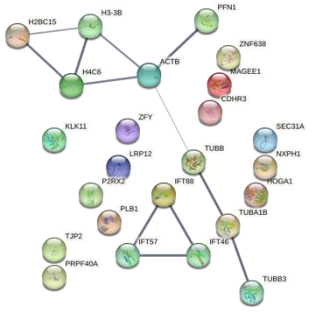

Figure 4. *Physical protein subnetworks derived from the significantly ($p < 0.05$) dysregulated proteins identified in chelerythrine-exposed Jurkat cells at EC_{50} concentration.*

As most of dysregulated proteins are involved in cytoskeleton and chromatin organization, chelerythrine is expected to play an important role in cell cycle and division control, culminating in the observed decreased viability of chelerythrine-exposed Jurkat cells observed previously (Figure 1).

Conclusions

Taken together, results indicate that while chelerythrine displays an overall anti-proliferative effect on the

assayed cell lines, the mechanisms underlying that effect appear to be distinct. While in Jurkat cells alterations are centred around the cytoskeleton and chromatin cellular components, in MM.1S protein expression is widely increased. The mechanisms through which this results in MM.1S cell death are currently being studied to better understand the effect of this alkaloid in the regulation of multiple cell pathways.

References

1. ECIS - European Cancer Information System. Available at: https://ecis.jrc.ec.europa.eu (Last accessed on 2 April 2023).
2. X.M. Chen, M. Zhang, P.L. Fan, Y.H. Qin, H.W. Zhao; *Oncology Letters*, 11 (2016), pp 3917-3924.
3. J.R. Wiśniewski JR; *Methods in Molecular Biology*, 1841 (2018), pp 3-10.
4. C.F. Marques, M.M. Marques, G.C. Justino; *Life Sciences*, 310 (2022), pp. 121056.
5. S. Tyanova, T. Temu, J. Cox; *Nature Protocols*, 11(2016), pp. 2301-2319.
6. S. Tyanova, T. Temu, P. Sinitcyn, A. Carlson, M.Y. Hein, T. Geiger, M. Mann, J. Cox; *Nature Methods*, 13 (2016), pp. 731-740.
7. D. Szklarczyk, R. Kirsch, M. Koutrouli, K. Nastou, F. Mehryary, R. Hachilif, A.L. Gable, T. Fang, N.T. Doncheva, S. Pyysalo, P. Bork, L.J. Jensen, C. von Mering C. *Nucleic Acids Research*, 51 (2023) pp. D638-D646.
8. J. Vacek, B. Papoušková, P. Kosina, A. Galandáková; *Journal of Chromatography B,* 941 (2013), pp. 17-24

P56

Determination of peptide peak purity by molecular feature extraction using accurate mass LC-MS

Gregory Kelly, Peter Smith, John Malone, Philip Nicholl

Almac Group Limited, 20 Seagoe Industrial Estate, BT63 5QD, Craigavon, Ireland

Summary: *Peak purity is an essential technique to ensure the quality, safety and efficacy of manufactured Active Pharmaceutical Ingredients (APIs) in the pharmaceutical industry. At Almac, the use of Molecular Feature Extraction (MFE) has become an established GMP assured procedure for the identification of co-eluting impurities, particularly in peptide products.*

Keywords: *Peak Purity, Molecular Feature Extraction, Peptides.*

Introduction

With the recent emergence of Covid-19 pandemic, the growing importance of biologics-based medicines has never been more prevalent. When compared to small molecule drugs, peptides are more specific, potent and selective to receptors found on the target cell's surface (Figure 1).[1]

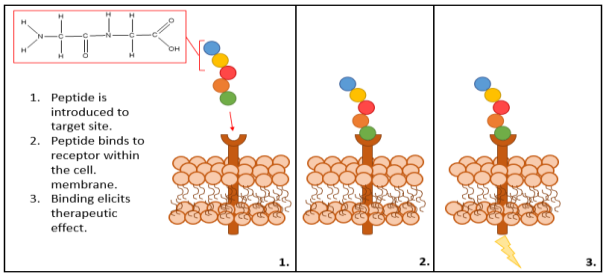

Figure 1. *Therapeutic peptide mechanism of action from introduction to elicitation of effect in target site.*

As modern medicine starts to move away from traditional small molecule based drugs and towards the clinic use of biopharmaceuticals such as peptides, regulatory authorities must catch up. Historical quality control and stability indicating methods such as peak purity by 3D-UV are no longer satisfactory or specific when dealing with biologics due to their spectral complexity and behaviour, therefore new quality control avenues must be explored. One prudent solution to impurity profiling is the introduction of peak purity by Molecular feature extraction (MFE). This case study presents the use of MFE algorithm to determine peptide peak purity during a section of a drug development campaign. Specifically, this study focuses on stages from predevelopment through to development of a stability indicating method and release a pre-process validation batch of oncological biopharmaceutical peptide.

Technique

The use of accurate mass instrumentation such as Quadrupole Time of Flight (Q-TOF) Mass Spectrometry, represent key instrumentation for quantification and impurity identification in peptide materials.[2] Employing the MFE algorithm, created by Agilent Technologies, facilitates 'compound' finding within a peak of interest. Once selected the algorithm will extract individual molecular features (known as sample compounds) regardless of chromatographic complexity or compound resolution. Once extracted the algorithm assesses all extracted molecular features to identify covariates based on accuracy of mass measurements (charge state envelope, isotopic distribution, adducts or clustering) and group those ions that are related. Within this context covariance describes abundance peaks that share peak start, peak maxima, peak profile and end of peak. The algorithm can then assign multiple ion species of the same neutral molecule to a singular compound – this is referred to as a Feature. This assignment occurs due to the software recognising multiply charged states or adduct formation. Therefore, the algorithm can assess a peak to determine the presence of potential individual compounds.[3] An operator can then study the output to determine if these peaks are related to the peak of interest – if not, they can be determined as co-eluting within that peak (Figure 2).

Its predecessor, peak purity by 3D ultraviolet spectroscopy (3D-UV), is commonly used for small molecule analyses, but is not capable of sufficiently determining peak purity of peptide and biologic products due to spectral similarities. Conversely, the MFE algorithm generates a vast quantity of more detailed information and, alongside expert interpretation allows analysis of much larger APIs and structurally similar impurities. Without the use of MFE for this Almac Peptide, it would not have been possible to identify the severely low levels of potential co-eluting impurities observed.

A

Cpd	File	RT	m/z	Mass	Vol	Vol %
4	Peptide X T=12 Months Stability Sample	22.XXX	105X.XXX	316X.XXXX	133880	0.29
5	Peptide X T=12 Months Stability Sample	22.XXX	104X.XXX	313X.XXXX	576771	1.24
6	Peptide X T=12 Months Stability Sample	22.XXX	185X.XXX	924X.XXXX	241139	0.52
8	Peptide X T=12 Months Stability Sample	22.XXX	154X.XXX	308X.XXXX	798509	1.72
9	Peptide X T=12 Months Stability Sample	22.XXX	157X.XXX	621X.XXXX	385306	0.83
14	Peptide X T=12 Months Stability Sample	22.XXX	102X.XXX	308X.XXXX	40403996	86.88
16	Peptide X T=12 Months Stability Sample	22.XXX	156X.XXX	311X.XXXX	102363	0.22
17	Peptide X T=12 Months Stability Sample	22.XXX	155X.XXX	622X.XXXX	178283	0.38
18	Peptide X T=12 Months Stability Sample	22.XXX	103X.XXX	310X.XXXX	1443055	3.1
19	Peptide X T=12 Months Stability Sample	22.XXX	104X.XXX	312X.XXXX	411553	0.88
20	Peptide X T=12 Months Stability Sample	22.XXX	156X.XXX	306X.XXXX	154496	0.33
21	Peptide X T=12 Months Stability Sample	22.XXX	106X.XXX	317X.XXXX	393784	0.85
25	Peptide X T=12 Months Stability Sample	23.XXX	105X.XXX	316X.XXXX	284015	0.61
26	Peptide X T=12 Months Stability Sample	23.XXX	105X.XXX	314X.XXXX	238277	0.51
28	Peptide X T=12 Months Stability Sample	23.XXX	104X.XXX	313X.XXXX	164945	0.35

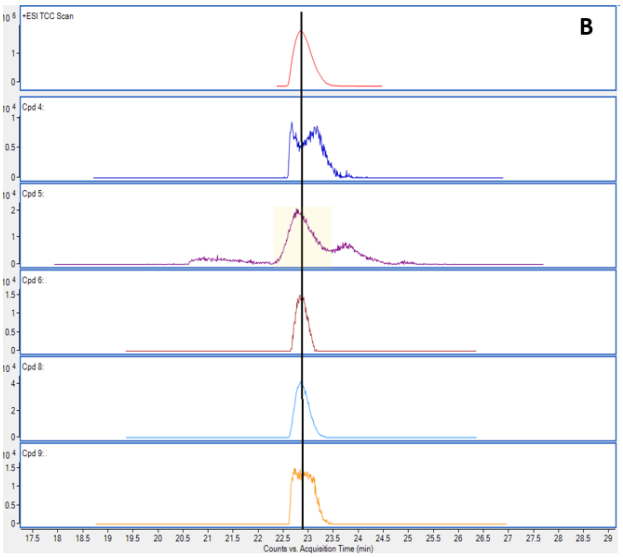

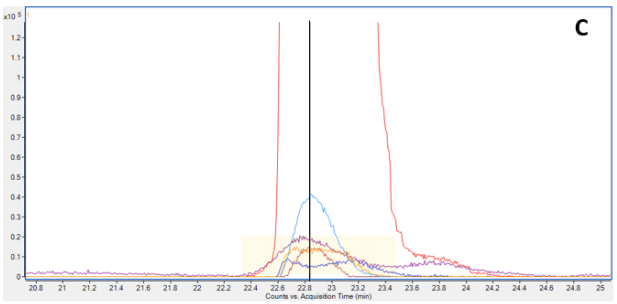

Figure 2. *Peak purity assessment of Almac Peptide stability sample by MFE. Panel A is the compound table pertaining to main Peptide API peak. Co-eluting impurity has been highlighted to emphasise the compound's retention time, m/z, mass, volume and % vol. Panel B portrays a stacked plot of Extracted Ion chromatograms derived from below the main Peptide API peak by MFE. With the API spectral peak on top, a black line shows the peak maxima of the main API peak. Compound 5 (highlighted) does not line up with the peak maxima and is considered co-eluting. This is confirmed by panel C which shows an overlay of the peaks shown in panel B.*

Conclusions

This data depicts the successful use of the MFE algorithm's involvement as an investigative tool in the identification of an unknown co-eluting impurity found within a stability study by LC-MS. MFE successfully allowed for the release of a batch of Peptide X and its subsequent stability indicating method.

References

1. J. Lau, M. Dunn. *Bioorganic & Medicinal Chemistry*, 2018, **26**, 2700-2709.
2. D. Pokar, A. Sahu, P. Sengupta, *Journal of Analytical Science and Technology*, 2020, **11**, 1-13.
3. M. Li, R.D. Josephs, A. Daireaux, T. Choteau, S. Westwood, G. Martos., R. I. Wielgosz, H. Li. *Analytical and Bioanalytical Chemistry*, 2021, **413**, 1861-1870.

AUTHOR INDEX

ISBN 9788890738890